DISSERTATION

THE ROLE OF LIN28 IN THE MOLECULAR REGULATION OF PLACENTA DEVELOPMENT AND FUNCTION

Submitted by

Jill L. Seabrook

Department of Biomedical Sciences

In partial fulfillment of the requirements

For the degree of Doctor of Philosophy

Colorado State University

Fort Collins, Colorado

Spring 2013

Doctoral Committee:

Advisor: Quinton A. Winger

Colin M. Clay
Gerrit J. Bouma
Jennifer G. DeLuca

ABSTRACT

THE ROLE OF LIN28 IN THE MOLECULAR REGULATION OF PLACENTA DEVELOPMENT AND FUNCTION

Proper regulation of trophoblast proliferation, differentiation and function are critical for placenta development and function. Placenta establishment and development originates and depends upon trophoblast stem cells differentiation into specialized trophoblast sub-types. Disruption to temporal or molecular programs regulating the differentiation of trophoblast stem cells can result in insufficient sub-lineage trophoblast populations, and ultimately in compromised invasion or utero-placental vascular remodeling, poor metabolic exchange and/or abnormal endocrine function. In the human, trophoblast dysfunction is thought to be an underlying cause to the development of increased intervillus blood pressure, perfusion velocity and the development of global hypertension and inflammation associated with placental dysfunction and disease.

LIN28, an RNA binding protein, has been well characterized as a potent post-transcriptional regulator of differentiation in embryonic stem cells and other progenitor cell populations, and has been used in conjunction with SOX2, OCT4, MYC and NANOG to induce somatic cells to dedifferentiate into iPSC. LIN28 has been described to have two distinct regulatory mechanisms for maintaining pluripotency: inhibition of *let-7* miRNA maturation, and direct post-transcriptional regulation of target mRNA. The mammalian genome consists of two *LIN28* homologs, *LIN28A* and *LIN28B*. Recent

studies have suggested that LIN28A and LIN28B function to inhibit *let-7* miRNA maturation through two distinct mechanisms. While there is a high degree of homology in structure and function, LIN28A is localized and functions in the cytoplasm, whereas LIN28B is thought to localize and function in the nucleus. Whether LIN28A and LIN28B have compensatory or overlapping function, or whether homolog dominance is cell type or developmentally determined, have yet to be fully elucidated. Estimates using in silico databases identify over five thousand putative mRNA targets for *let-7* miRNAs. Despite much study in embryonic stem cells, to date, little is known about the function of LIN28 in the placenta.

Preliminary microarray data comparing proliferative primary mouse trophoblast stem cells (mTS) with differentiated mouse trophoblast giant cells (mTGC), demonstrated a significant decrease in *Lin28a* and increased levels of *let-7* miRNA. These preliminary data provided compelling evidence that *Lin28a* had a regulatory role during trophoblast differentiation, and that regulation was through a *let-7* miRNA mediated pathway.

The first aim of this study was to confirm the microarray data, and determine if LIN28A had a regulatory role in the differentiation of trophoblast cells. We assessed LIN28A *in vitro* using mTS and the immortalized first-trimester human trophoblast cell line, ACH-3P. We observed that LIN28A decreased and *let-7* miRNA increased when mTS were induced to differentiate into mTGCs upon the removal of FGF4, heparin and conditioned

medium. Similarly, we observed that LIN28A decreased in ACH-3P cells induced to syncytialize with forskolin treatment.

The second aim of this research was to assess LIN28 *in vivo.* Given the difficulty in obtaining human placenta tissue, we used the mouse as a model. We examined serial sections of embryonic day 11.5 mouse placenta and observed abundant LIN28A in the chorioallantoic interface and labyrinth layer, with little LIN28A in spongiotrophoblast or differentiated trophoblast giant cells (mTGC).

The third aim was to determine the effect of *LIN28A* deficiency on trophoblast differentiation and function. To do this, mTS and ACH-3P cells were infected with an shRNA sequence designed to target either mouse *Lin28a*, or human *LIN28A* for degradation. While loss of *Lin28a* in mTS did not result in phenotypic or morphological change when maintained under proliferative conditions, *LIN28A* knockdown in human ACH-3P cells resulted in increased spontaneous syncytialization, and increased levels of syncytiotrophoblast markers: hCG, *LGALS13* and *ERVW-1* mRNA. Additionally, targeted degradation of *LIN28A* mRNA in ACH-3P resulted in increased responsiveness to forskolin-induced differentiation.

Together these data suggest that LIN28A has a functional role in regulating trophoblast differentiation and function. These data also suggest that loss of *LIN28A* in human

trophoblast is sufficient to induce differentiation, but that in the mouse, LIN28A likely acts in concert with other factors to inhibit trophoblast differentiation.

Late in the study, we had the opportunity to assess LIN28 in first-trimester, term and IUGR term placenta human tissue. We wanted to repeat aims one and two using this tissue to determine if our observations in the mouse were conserved in the human, and that our observations using ACH-3P cells were consistent with primary human tissue. We found that LIN28B was more abundantly expressed in primary term placenta tissue, than LIN28A. Concomitantly, a collaborative study with Dr. Anthony's lab found that *Lin28b* was more abundantly expressed, compared to *Lin28a,* in elongated sheep conceptuses. Together, these data suggest that LIN28 regulation of trophoblast differentiation may vary among species, and that the mouse may not be the best model for understanding LIN28 regulation in the human placenta.

ACKNOWLEDGMENTS

When we become more fully aware that our success is due in large measure to the loyalty, helpfulness, and encouragement we have received from others, our desire grows to pass on similar gifts. Gratitude spurs us on to prove ourselves worthy of what others have done for us.

-Wilferd A. Peterson (1900-1995)

Dr. Winger Thank you for seeing my potential for achievement. You encouraged me to think independently and take personal initiative. You also supported my attendance at many different conferences and workshops, which provided some outstanding opportunities for making connections, learning new material and stretching my boundaries.

Dr. Anthony I can't thank you enough for all of your support and guidance, both in the lab and with my career development. You always held me to a higher standard, which encouraged me to think, to ask questions, and to stay focused. I am thankful to have had the opportunity to work in your lab and participate as contributing member- from discussing journal articles, to learning new lab techniques, to wrangling sheep.

Dr. Clay Thank you for welcoming me into your lab and treating me as a member of the team. Your lab provided a constructive, professional and often fun environment in which to work and learn. I am also grateful to have had the ability to speak frankly, and to rely on you for sound guidance and advice.

Drs. DeLuca & Bouma I am grateful to you both for your time, guidance and constructive suggestions. Your input provided me with new perspectives that broadened my outlook and approach to science. Thank you.

Jeremy Cantlon Your genuine love of science, your enduring spirit of inquiry and your wit was often my esprit de corps. You inspired me to think and then to laugh, which continually renewed my optimism, focus and determination. It was your patience and humor that frequently made the science fun- thank you!

Lindsey, Jen & K.C. Thank you for your help, dedication and camaraderie in the lab. Thank you most of all for making me laugh!

Rick & Donya None of my accomplishments would be possible without your continual support, encouragement and understanding. You two are what really matter to me. Thank you for filling my heart.

TABLE OF CONTENTS

LIST OF FIGURES

CHAPTER II

CHAPTER III

CHAPTER IV

CHAPTER I: INTRODUCTION

Population statistics collected by the United Nations Population Fund and The Preeclampsia Foundation estimate that over 500,000 women die worldwide each year from pregnancy-related causes, and that 13-15% of those deaths are due to complications of the pregnancy disorder preeclampsia (PE). In the U.S., the rate is higher, with 18% of maternal deaths caused by PE. Additionally, according to the New England Journal of Medicine, PE is the primary reasons for early induction of labor, and accounts for 15% of premature births. Prematurity and fetal growth restriction are the leading causes of perinatal morbidity and mortality. While the incidence of intrauterine growth restriction (IUGR) varies with population demographics, IUGR is estimated to affect 5% of pregnancies, approximately 30 million babies per year.

PE is characterized clinically by the development of maternal proteinuria and hypertension after the 20^{th} week of gestation. If left untreated, PE can deteriorate in eclampsia, which is characterized by the development of multiple organ failure, stroke, seizures, and in the worst cases, maternal and/or fetal death. IUGR is clinically characterized as a failure of the fetus to reach its genetic growth potential due to pathological inhibition. There is some variability in diagnosing IUGR babies. Some practitioners classify babies with a birth weight that is two standard deviations below the median for gestational age when compared to their population-matched peers as IUGR,

while others diagnose babies with birth weights below the 3rd or 5th percentile of weight for gestational age.

The acute health implications for these diseases include, total fetal loss, growth restricted neonates, the development of maternal hypertension and preterm delivery, with preterm delivery alone estimated to have an economic impact of $26 billion annual per year. In addition to acute health complications, epidemiological studies have reported long-term health implications for women and children who experience pregnancies complicated by placental disease. Clinical and epidemiological studies of IUGR pregnancies suggest these children have an increased risk of obesity, cardiovascular disease, hypertension, and type-2 diabetes later in life. A study by Bellamy et al. [1] reported that women with a history of preeclampsia are twice as likely to develop cardiovascular diseases between 5 – 15 years after pregnancy. However, it is not known whether placenta dysfunction is the direct cause for the increased risk of cardiovascular disease, or whether the stress of pregnancy exacerbates a pre-existing sub-clinical cardiovascular condition. These data do suggest that women with pregnancy complications should be proactively monitored for the onset of disease, and that suboptimal cardiovascular function may be predictive of pregnancy complications.

While the underlying etiology of PE and IUGR are not known, poor placenta establishment and/or placenta dysfunction are thought to be the predominant contributors, and are the focus of many research efforts. Assessments of placental

tissue taken from PE and IUGR pregnancies are associated with lower cytotrophoblast fusion indices, fewer nuclei per syncytiotrophoblast and a higher rate of syncytiotrophoblast apoptosis and shedding. Doppler flow velocimetry data suggests IUGR pregnancies have increased uterine artery Doppler resistance indices. PE is a disease that almost exclusively affects humans, exceptions being rare reports in the patas monkey (*Erythrocebus patas*) and the guinea pig (*Cavia porcellus*), however no other mammal experiences PE to the degree observed in humans. Some researchers suggest PE is a maladaptive consequence associated with the high invasiveness of the human placenta. Many suggest that PE and IUGR develop when extravillous trophoblast cells fail to adequately invade and remodel maternal uterine vasculature. Poor maternal vascular remodeling prevents placental blood flow from increasing to accommodate increasing fetal demand, resulting in increased intervillous blood flow velocity, perfusion ischemia, reperfusion injury, and excessive syncytiotrophoblast shedding.

Ultimately, proper placenta function relies upon timely and robust differentiation of villous progenitor cytotrophoblast into functional syncytiotrophoblast and extravillous trophoblast subtypes. Consequently, deregulation of trophoblast proliferation, differentiation and/or function is likely to be a key contributor to the development of placental dysfunction and disease. Therefore, understanding the molecular mechanisms regulating trophoblast proliferation, differentiation and function is important for understanding, diagnosing, and ultimately treating placental disease. Progress in our

understanding of placenta development and disease not only will contribute to an improvement in pregnancy outcome, but also will contribute to improving the long-term health of individuals from pregnancies complicated by placental disease.

CHAPTER II: REVIEW OF LITERATURE

CULTURAL PERSPECTIVES

The word for placenta has different meanings in different languages, which provides insight into a culture's perspective on pregnancy and birth. In English the word placenta is derived from the Greek word *plakoenta,* which literally means 'flat cake,' likely inspired by the discoid shape of the human placenta. In Tahitian the placenta is called *pufenua*, meaning 'heart of land' [2], and in the Southeast Asian Hmong, the word for placenta means 'jacket', and in both cultures the placenta has lifelong spiritual significance for the family [3, 4]. The Japanese word for placenta is *ye* or *yena*, meaning 'elder brother', and is used extensively in Japanese myths to explain the origins of some of the 6,852 islands that make up the Japanese archipelago [5].

> *"The two Deities were united and became husband and wife. First of all, the islands of Ahaji and Aha being considered the placenta, they produced the island of Oho-yamato no Toyo-aki-tsu-shima, next the island Iyo, next the island of Tsukushi, next, as twins, the islands of Oki and Sado, next the island of Koshi, next Oho-shima, and next Kojima."* [5]

In many cultures the placenta receives ceremonial handling, including burial and placentophagy, and is often regarded as the infant's twin with an important role in ensuring the spiritual health of the infant, the mother and the community [3]. In contrast,

western medicine and much of modern western culture have historically regarded the term placenta as an anatomical curiosity or as human waste [3]. However, the pre-term placenta is regarded as an important tissue for research and clinical inquiry, as well as a useful source for gestational diagnostic information [6, 7].

PLACENTAE FORM & FUNCTION

The placenta is a complex organ that transiently exists to facilitate vital metabolic exchange and endocrine signaling between mother and fetus during pregnancy. While vivaparity relies on the placenta to facilitate the close proximity of the maternal and fetal circulatory systems in order to facilitate metabolic exchange, significant evolutionary placental diversity among eutherian mammals demonstrates that this can be achieved by many different mechanisms. Placentas vary in size, shape, mode of attachment, and degree of maternal vascular invasion and remodeling. Such diversity has likely developed to accommodate species variation in gestational duration, litter size, environmental conditions, and offspring size and maturation at birth.

COMPARATIVE PLACENTATION

There are various approaches for grouping and classifying placentae, however the system of classification developed by Benirschke et al. [8] designated five features important for placenta morphological classification: 1) placental shape, 2) fetomaternal interface, 3) fetomaternal interdigitation, 4) fetomaternal blood flow interrelations, 5) neonatal-placenta weight ratio.

Placenta shapes

Placenta shapes include diffuse, cotyledonary, zonary, discoid and bidiscoid. The diffuse placenta is characterized by fetomaternal interface covering the entire chorioallantoic surface. Domestic species with a diffuse placenta include the horse and pig. In contrast, the cotyledonary placenta interfaces with the uterine epithelium in multiple distinct areas on the uterine epithelium called caruncles; together the fetal cotyledon and maternal caruncle form multiple interfacing units called placentomes. Domestic ruminant species such as cattle, sheep and goats have cotyledonary placentas. The third placenta shape is the discoid placenta. Rather than many small distinct areas of interface, the discoid placenta has a single roun area (in the case of the bidiscoidal placenta, two areas) interfacing with the uterine epithelium. The discoid placenta is found in a diverse number of species including most rodents (hamsters, mice, rats, guinea pigs and beavers), rabbits and hares, armadillos and sloths, as well as many primates, including humans. Interestingly, Leonardo da Vinci's sketch *Studies of the Foetus in the Womb* drawn in the early sixteenth century (c. 1513) depicts a human fetus with a cotyledonary placenta (Figure 1). Despite having succeeded a detailed investigation of the placenta in the cow (Figure 2), this suggests that the distinction between the cotyledonary and discoid placenta types may not have been fully recognized at the time [9, 10]. Finally, the zonary placenta forms a circumferential belt of interdigitation around the fetus, and is found in domesticated dogs and cats, as well as elephants and manatees.

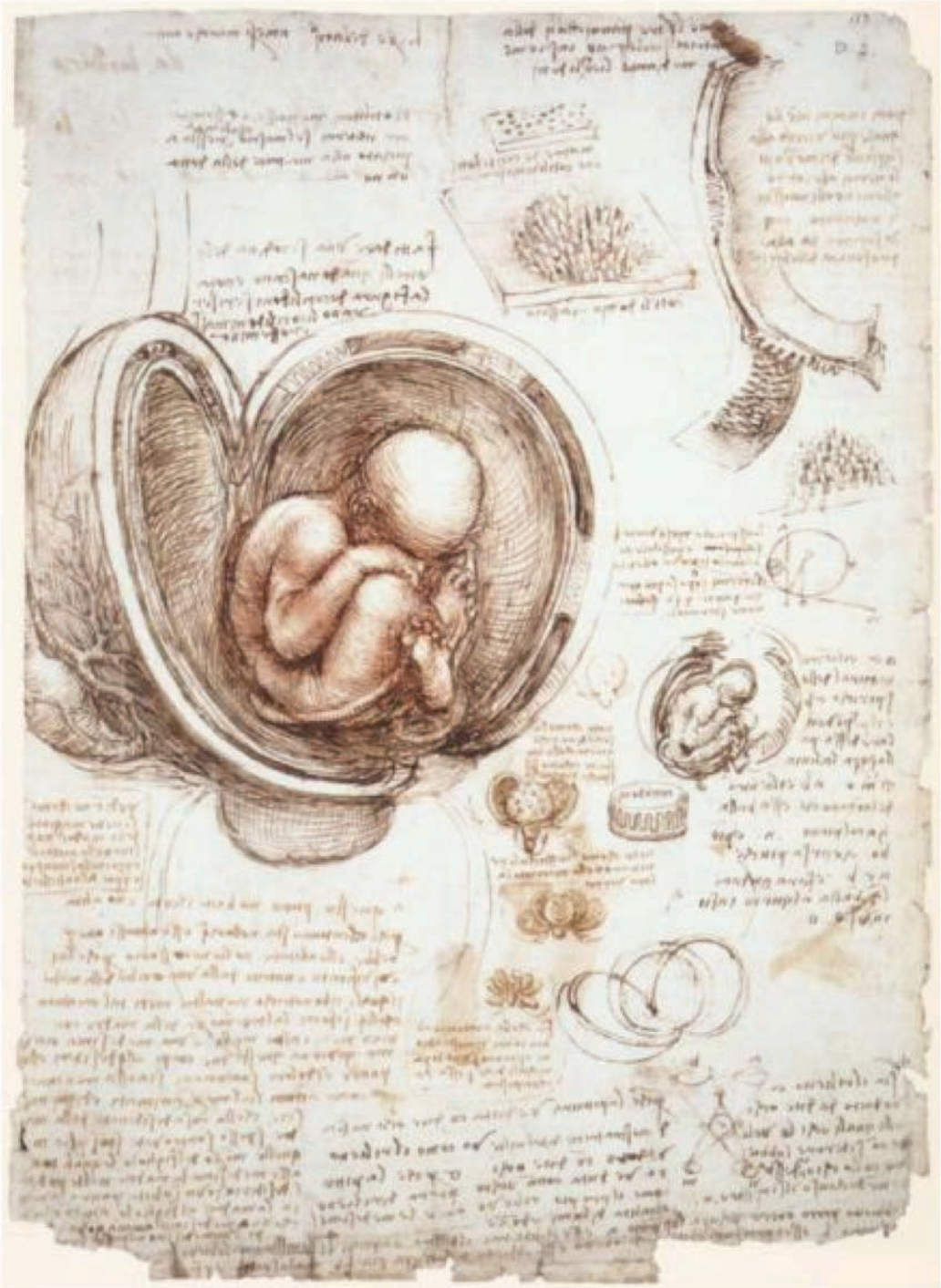

Figure 1. Leonardo da Vinci's, Studies of the Feotus in the Womb.

Drawn in the early 16th century (c. 1513). Currently housed at the Royal Collection, Windsor Castle, London, UK. This image is in the public domain, which permits unrestricted copy, distribution and display.

Figure 2. Leonardo da Vinci's, Uterus of a Pregnant Cow.

Drawn in the early 16th century (c. 1508). Currently housed at the Royal Collection, Windsor Castle, London, UK. This image is in the public domain, which permits unrestricted copy, distribution and display.

Fetomaternal interface

The Grosser method of placenta classification, groups placenta based on the number of tissue layers separating maternal and fetal circulatory systems at the fetomaternal interface, and identifies four distinguishable groups: 1) epitheliochorial placenta, 2) syndesmochorial placenta, 3) endotheliochorial placenta, 4) hemochorial placenta, which can be further sub-grouped in to hemotrichorial, hemodichorial and hemomonochorial placenta [8, 11]. In the epitheliochorial placenta the fetal chorion interfaces an intact uterine epithelium resulting in six tissue layers between fetal and maternal circulation: maternal endothelium, maternal connective tissue, uterine epithelium, fetal trophoblast, fetal connective tissue and fetal endothelium. In ruminant species, syncytialization of trophoblast or epithelial cells, or trophoblast-epithelial hybrid syncytialization, occurs at the fetomaternal interface, giving rise to endocrinologically active binucleate cells [8, 12] of the syndesmochorial placenta. The endotheliochorial placenta is characterized by additional breakdown of the fetomaternal barrier, removing maternal connective tissue and leaving maternal endothelium to directly abut fetal trophoblast. The hemochorial placenta results when fetal trophoblast erodes the endometrial endothelium resulting in direct interaction between the fetal trophoblast epithelium and maternal blood. The hemochorial placenta can be further sub-divided into groups characterized by the number of trophoblast epithelial layers present [8, 13].

Fetomaternal interdigitation

The placenta interface is the site for metabolic exchange between the mother and fetus. Maximizing the metabolic exchange efficiency can be achieved by increasing surface area, either through occupying large areas of uterine epithelium, minimizing tissue barriers at the fetomaternal interface, or by maximizing interdigitation at the fetomaternal interface. Therefore an important component of placenta classification is the type of interdigitation at the fetomaternal interface. There are five distinct types of interdigitation starting with folded, and progressing in conformational complexity, to lamellar, trabecular, villous and labyrinthine [8, 11]. The pig placenta has shallow folded interdigitations, which protrude minimally from the chorion. Laminar interdigitation is similar to the folded type, but projections extend farther from the chorionic plate; this interdigitation is found in domestic cats and other carnivores. The next level of complexity can be seen in trabecular interdigitation, which secondary branches are incorporated into the folded structure. The human placenta has villous interdigitation, which is characterized by many three dimensional villi tree-like structures, each possessing a high degree of complex branching. These villi protrude into the intrauterine space through which maternal blood flows. Finally, there is the labyrinthine interdigitation found in rodents, which consists of a tortuous sponge-like network of tunnels and chambers suffused with maternal blood [8, 11].

Fetomaternal blood flow interrelations

Metabolic exchange efficiency across the fetomaternal interface is an important characteristic for understanding placenta form and function. The vascular arrangement of capillaries and the direction of blood flow at the fetomaternal interface directly influence gas and nutrient exchange capacity and efficiency of the placenta. Three blood flow interrelations have been defined in mammals: 1) crosscurrent, 2) multivillous, 3) countercurrent. The crosscurrent blood flow interrelation observed in carnivores and in the lower primates, is an arrangement where the vessels and blood flow direction are at ninety-degree angles, and represents the least efficient of the mammalian systems. The multivillous flow exchange characteristic of human and ruminant placentae is the next most efficient, with villi-embedded vessels submerged essentially within a large maternal vessel or cistern. Lastly, the countercurrent exchange, a highly efficient system characterized by parallel vessel arrangement and counter-directional blood flow [8, 11].

Neonatal-placenta weight ratio

The weight ratio between fetus and placenta, is often used as a marker for determining the efficiency of fetomaternal blood exchange, with less efficient blood flow arrangements, such as in swine (9:1), having poorer weight ratios at birth when compared to animals with more efficient exchange systems, such as rodents (20:1) [8]. Additionally, suboptimal fetal-placental weight ratios may be a clinical indicator for diagnosing infants of compromised pregnancies [14].

EXPERIMENTAL MODELS

Given the inaccessibility of human placenta tissue, and the inability to experimentally modify human embryos, much of our understanding regarding placenta development is derived from experiments in other mammals, including rodents, sheep and non-human primates, or from the utilization of *in vitro* technologies such as cell lines.

ANIMAL MODELS

Given the high degree of variability in placentation between species, animal models often function to provide insight on specific aspects of human placenta physiology.

Mouse

The advantages to using the mouse include its small size, frequent cyclicity, short gestational period and a hemochorial placenta. Additionally, transgenic technologies make it possible to utilize transgenic mouse lines for specific gene inquiries. However, basic structural differences such as the comparatively shallow trophoblast invasion and labyrinthine exchange interface are marked disadvantages for modeling human placenta invasion, vascular remodeling or the diseases associated with theses processes such as intrauterine growth restriction (IUGR) and preeclampsia (PE) [15, 16]. Additionally, the mouse and human placentae have distinct endocrine profiles, varying greatly in regards to role of progesterone, as well as the complete lack of human chorionic gonadotropin (hCG) in the mouse [16, 17]. Finally, the short gestational period of the mouse (21 days) results in multiple altricial young, whereas the comparatively

long human gestation, which results in a single more fully developed offspring, requires the human placenta to function for 265 days.

Sheep

The advantages to using sheep include a relatively long gestational period (145 days) resulting in one or two fully developed offspring. Sheep are easy to handle and their pregnancy will withstand invasive procedures allowing for extensive inquiry into fetal physiological development [18, 19]. Consequently, sheep have been used extensively as a model for IUGR [20, 21]. The most notable disadvantage to using sheep is its epitheliochorial, cotyledonary placenta, which demonstrates little to no trophoblast invasion. Additionally, sheep are expensive, require specialized facilities, and undergo seasonal cyclicity.

Non-human primates

Old world monkeys (*Cercopithecidae*) such as baboons and macaques have invasive hemochorial villous placenta, with similar intravillous circulation, trophoblast invasion and spiral artery remodeling, and similar fetomaternal interface characteristics as characterized in the human [22, 23]. Given the physiological similarities, old world monkeys have been valuable models for modeling human implantation, gestational diseases such as PE, and artificial reproductive technologies (ART) [24-26]. The primary drawbacks to using non-human primates include the cost to maintain research colonies, as well as the ethical concerns and empathetic public perspective the public has towards primates.

IN VITRO MODELS

In addition to animal models, cell lines have been developed to study trophoblast development and function *in vitro*. In the mouse, isolated primary trophoblast cells can be maintained in culture indefinitely when supplemented with FGF4, heparin and fibroblast conditioned medium [27]. However, a correlative set of growth factors has not yet been identified for maintaining primary human trophoblast cells in culture. Consequently, different immortalization techniques have been used to create human trophoblast cell lines for *in vitro* experiments. In 1968 Pattillo and Gey established the BeWo trophoblast cell line from choriocarcinoma [28]. Pattillo and Gey reported that the BeWo cell line maintained the morphology of the cytotrophoblast, and functional hCG hormone synthesis [28]. In 2007, Hiden et al. created the ACH-3P cell line by fusing primary first trimester trophoblast cells with the choriocarcinoma cell line AC1-1 [29]. The resulting ACH-3P cells synthesized hCG, were HLA-G positive (an extravillous trophoblast cell marker), and showed fusion and invasion characteristics, suggesting they were a potential *in vitro* model for cytotrophoblast, extravillous trophoblast and syncytiotrophoblast lineages [29]. An obvious drawback to using choriocarcinoma as an immortalization mechanism is the possibility of introducing undesirable tumorogenic characteristics to the cell line making data interpretation problematic. An alternative approach taken by Graham et al. (1993) involved transfecting first-trimester human trophoblast cells with simian virus 40 large T antigen, to create the HTR-8/SVneo human trophoblast cell line [30]. The resulting HTR-8/SVneo cells maintained morphology and invasion characteristics of parental trophoblast cell line, and

transfection resulted in the ability to synthesize hCG [30]. However, reported drawbacks to using SV40-mediated transformation include abnormal trophoblast invasion characteristics such as hyperinvasiveness and non-responsiveness to anti-proliferative and anti-invasion TGF-beta signaling [31]. Additionally, miRNA expression profiling experiments suggest that HTR-8/SVneo cells have a miRNA fingerprint distinct from choriocarcinoma trophoblast cell lines and primary trophoblast cells [32]. Specifically, many of the miRNAs that differed in HTR-8/SVneo cells were those from the primate-specific chromosome 19 miRNA cluster (C19MC), a genomic region on chromosome 19 that is epigenetically regulated in the human placenta [33]. Most recently, Straszewski-Chavez et al. (2009) infected first trimester trophoblast cells with human telomerase reverse transcriptase (hTERT), creating the Swan 71 human trophoblast cell line [34]. The resulting Swan 71 cells were HLA-G positive, produced very low levels of hCG, and exhibited the ability to invade, suggesting the Swan 71 cell line was a potential *in vitro* model for the intravillous cytotrophoblast or extravillous trophoblast cell lineages [34].

No *in vitro* cell culture model is a perfect surrogate for modeling the complexity of the human placenta. However, given the inaccessibility to human placenta tissue and the experimental limitations for isolated primary human trophoblast cells, careful use of appropriate cell models remains a useful research approach.

PLACENTA DEVELOPMENT IN THE HUMAN

Like all eutherian mammals, the major function of the human placenta is to provide an exchange interface between the mother and fetus to facilitate fetal growth and development while preserving maternal health. The human placenta is characterized as having a discoidal shape, hemomonochorial interface, and a multivillous fetomaternal blood flow relationship [8]. The human placenta is highly invasive compared to other species, mediating extensive uterine spiral artery remodeling to increase the volume of blood available for metabolic exchange between mother and fetus.

DECIDUALIZATION

The human placenta is unique from many others in its high degree of trophoblast invasion into the decidua and the inner myometrium, which contributes to extensive remodeling of the uterine vasculature [35-37]. This deep placentation results in higher blood flow to the placental bed and uterine arteries, which supports increased metabolic transfer across the complex villus structure [38]. The purpose of this adaptation has been proposed to be for supporting increased fetal demands and a longer gestational period which simple diffusion cannot support [8]. However, unregulated trophoblast invasion and uterine vascular remodeling would lead to uterine damage and potentially fatal hemorrhaging during pregnancy. In order to allow for deep trophoblast invasion required necessary for pregnancy while protecting maternal health, the human has developed the adaptation of decidualization [35, 37]. An added advantage of decidualization is that because the majority of remodeling occurs in the decidual tissue,

the uterine vasculature and hemodynamics are returned to normal in the postpartum, non-gravid uterus [35, 37].

Decidualization is a process by which mid-luteal mesenchymal cells in the uterine stroma are converted into converted from fibroblast-like cells, into secretory epithelial-like decidual cells [39, 40]. The decidualization process is mediated by ovarian hormones progesterone, estradiol and relaxin regardless of fertilization or subsequent pregnancy [39, 41]. The resulting decidual cells are characterized by an alteration in structural constituents, such as collagen IV, as well as an altered biochemical profile [42]. Decidual cells have increased expression of hormones (prolactin, coricotropin releasing hormone, insulin like growth factor-binding protein-I), cytokines (IL-6 and IL-8), growth factors, matrix metalloproteases (MMPs) and tissue inhibitors of MMPs (TIMPs), and tumor suppressor tetraspanin CD82 (KAI-I), many acting to regulate trophoblast invasion [35, 39, 43-45]. In addition to serving as a substrate for trophoblast invasion, the decidua protects the early embryo from maternal immune rejection, and produces a mélange of lipids and proteins which provide nutrients to the early embryo until the placenta is established [42, 45, 46]. Ultimately, the decidua acts as a physical and biochemical substrate conducive for trophoblast invasion and embryo development, as well as barrier to prevent excessive trophoblast invasion and maternal harm.

ORIGINS OF THE TROPHECTODERM

Given the inaccessibility of human placenta tissue, animal models are used as surrogates for understanding the stages of human placenta development and function.

Despite notable differences, the mouse and the many transgenic and knockout mouse technologies have been used for studying the human placenta [47-50].

In the fertilized mammalian embryo, early cleavage events result in the formation of individual blastomeres [51]. Between the 8- and 16-cell stage asymmetric cellular division results in two distinct cell populations, and the inner blastomeres which will differentiate into the inner cell mass (ICM) and later the three embryonic germ layers, and the outer blastomeres which will differentiate into the trophectoderm (TE) [51]. The TE blastomeres are characterized by apical-basal polarity, intracellular junctions and ion transporters, which facilitate the formation of a fluid-filled blastocoele cavity at the 32-cell stage [49, 52-54].

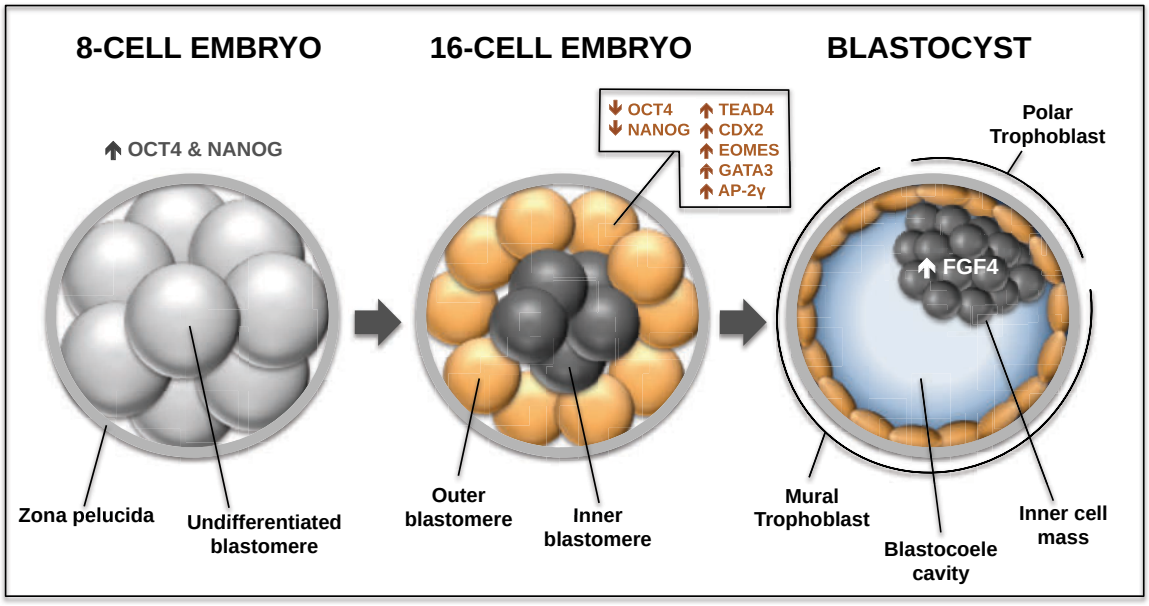

Figure 3. Initial differentiation events in the early embryo.

Undifferentiated blastomeres differentiate into two distinct blastomeres subtypes and ultimately into the inner cell mass (ICM) cells that will make up the embryo proper and the trophectoderm (TE) that will form the placenta.

In the mouse, TE differentiation from the ICM is marked by decreased expression of the transcription factor OCT4, and high levels of transcription factors TEAD4, CDX2, EOMES, GATA3 and AP-2γ [47, 55]. *Cdx2* and *Eomes* transcription factor expression is regulated by paracrine signaling of embryonic fibroblast growth factor 4 (FGF4) from the ICM through the FGF receptor-2 (FGFR2) expressed in the TE [27, 56]. *Fgf4* expression, as well as *Cdx2* and *Eomes* expression, is driven by NODAL, a member of the transforming growth factor β-related (TGF-β) protein family [57]. TEAD4 is likely upstream of CDX2, as forced *Tead4* expression in mouse ESC initiates CDX2 and differentiation down TE lineage [58]. The role for GATA3 is not as clear; while overexpression results in CDX2-independent TE differentiation, *Gata3* knockout does not adversely affect TE development possibly due to overlap with GATA2, EOMES and AP-2γ [59-61]. The paracrine signaling originating from the ICM creates two microenvironments and two TE populations, the proliferative polar TE in direct contact with the ICM, and the peripheral mural TE [51, 62]. The polar TE continues to proliferate and serve as a precursor stem cell niche from which all subsequent trophoblast sub-lineages arise [54]. While the polar TE continues to proliferate, in the mouse the mural TE enters a state of endoreduplication characterized by continued DNA replication but cessation of cell division, resulting in a primary trophoblast giant cell population that will mediate implantation and invasion [51, 62, 63]. In contrast to the mouse, human TE does not endoreduplicate, but forms multinucleated syncytium by cell fusion which will modulate implantation and invasion in the human [8].

The human embryo is thought to follow a similar molecular developmental program as the mouse, however to date, the direct assessment of TE differentiation using human embryos has not been feasible due to ethical restrictions. Attempts to isolate human and non-human primate primary trophoblast cells have included isolating trophoblast outgrowths, as well as artificially downregulating *OCT4,* and/or overexpressing *CDX2* in embryonic stem (ES) cells, but a method for maintaining human a self-renewing trophoblast population has yet to be reliably established [64-67]. Studies using non-human primate blastocysts show that overall *OCT4* expression patterns in the human blastocyst are similar to the mouse with some notable differences [64]. In the mouse, downregulation of *OCT4* is required before the TE differentiation events are permitted to proceed, whereas in the primate the initial TE differentiation events begin before full downregulation of *OCT4* [64]. In both the mouse and primate, hatched blastocysts express OCT4 only in the ICM [64]. *CDX2* expression in the human is similar to the mouse as confirmed using trophoblast cells isolated from non-human primate blastocyst outgrowths, trophoblast cells isolated from embryoid bodies, and a microarray of TE from surplus preimplantation IVF embryos [64, 68, 69]. *EOMES* expression during differentiation of TE in the human is less clear. Recent data from microarray analyses of surplus human IVF embryos has identified numerous potential regulatory factors and signaling cascades in human TE, including NOTCH, WNT mitogen-activated protein kinase, TGF-β, integrin-mediated cell adhesion, epigenetics, steroidogenesis, phosphatidylinositol 3-kinase, and apoptosis [69, 70].

It is important to note that microarray data from surplus IVF embryos have been collected from subfertile women undergoing fertility treatment. While these data suggest there are fundamental differences in molecular regulation and timing of mouse and human TE differentiation pathways, additional studies are needed to confirm these findings.

TROPHECTODERM DIFFERENTIATION AND THE ROLE OF TROPHOBLAST CELLS IN PLACENTA DEVELOPMENT

While the initial differentiation events establish the TE as a distinct cell population from the ICM, the resulting TE must give rise to all subsequent trophoblast sub-lineages necessary for proper placenta development.

In the human, the TE gives rise to the proliferative cytotrophoblast progenitors, which in turn give rise to the other trophoblast sub-lineages [8]. During implantation and invasion, the polar trophoblast cells start to proliferate and the outer TE layer in contact with the maternal epithelium start to fuse forming the primary syncytiotrophoblast (ST) which is responsible for initial invasion at implantation [8]. While the syncytiotrophoblast lose proliferative potential with fusion, the underlying cytotrophoblast (CT) cells continue to proliferate and will maintain ST renewal and function through continuous CT-ST fusion [8]. The primary syncytiotrophoblast layer thickens and forms many finger-like projections that invade the endometrium. Vacuoles form and expand within the syncytiotrophoblast projections creating a system of lacunae and trabeculae that will eventually form the intervillous space and placental villi which will be bathed with

maternal blood [8]. The proliferative cytotrophoblast, that make up the primary chorionic plate, begin to invade the syncytiotrophoblast trabeculae until they reach the peripheral tips of the trabeculae (referred to as the trophoblastic shell) at the syncytiotrophoblast-endometrial interface [8]. At the trophoblastic shell, the cytotrophoblast cells proliferate to form a pool of progenitors from which extravillous trophoblast cells will differentiate and invade the endometrium [8, 22, 71]. Like the syncytiotrophoblast cells, extravillous trophoblast cells lose their proliferative capacity when they migrate away from the trophoblastic shell. However, the invasion of the extravillous trophoblast cells is distinct from the initial invasion of the syncytiotrophoblast. Extravillous trophoblast do not fuse, but individually invade the maternal decidua, endometrium and myometrium, to remodel the maternal uterine arteries from high-resistance, low-flow vessels into low-resistance, high-flow vessels [8].

Trophoblast invasion

A healthy pregnancy is characterized by profound vascular adaptations [72]. Blood flow through the non-pregnant uterus accounts for less than 1% of total cardiac output [35]. Pregnancy increases blood flow to the uterine arteries 1000% [72]. In order to support such a dramatic increase in blood flow without concomitant increase in the number of uterine arteries, existing arteries must significantly increase in diameter. Poiseuille's law of fluid dynamics, which states that fluid flow through a cylinder changes proportionally with the radius to the fourth power, is often cited to demonstrate the significant contribution spiral artery remodeling provides toward the increased hemodynamic capacity of the pregnant uterus [35, 73]. The extravillous trophoblast cells invade by

interstitial and endovascular pathways, replace the endovascular smooth muscle and vascular endothelium of uterine spiral arteries resulting in significantly dilated vessels with decreased vasomotor control [8, 74, 75].

The first phase of extravillous trophoblast invasion is passive, in that the extravillous trophoblast are pushed away from the trophoblastic shell by continued cytotrophoblast proliferation, before acquiring invasive phenotype [8]. Invasion, is in part, facilitated by proteinase lytic degradation of maternal extracellular matrix by the extravillous trophoblast, but is also facilitated by complex endocrine signaling between extravillous trophoblast and the uterus. Numerous proteases, cytokines and hormones have been implicated in the regulation of extravillous trophoblast invasion, including factors such as matrix metalloproteinases (MMPs), the tissue inhibitors of MMPS (TIMPs), endothelial isoform of nitric oxide synthase (eNOS), as well as angiogenic factors such as vascular endothelial growth factor (VEGF), placena growth factor (PlGF), and angiopoiein-2 (Ang-2) [8, 76, 77]. Additionally, proliferation of the cytotrophoblast progenitor cells at the trophoblastic shell, and invasion of the extravillous trophoblast are both regulated by oxygen tension [78-80]. During the first-trimester there is a steep oxygen gradient between the trophoblast cells along the trophoblastic shell (18mm Hg) and intervillous space, and maternal intraarterial blood (95-100 mm Hg) [8, 81]. Several studies by Genbacev et al. [78, 79] demonstrated that hypoxic conditions (2% O_2) increased trophoblast proliferation and invasion *in vitro*. Additionally, endovascular extravillous trophoblast form multicellular plugs that occlude the arterial lumen resulting in prolonged

period of low intervillous oxygen tension supporting a prolonged period of trophoblast invasion [8, 82]. Between 10-17 weeks of gestation, the extravillous trophoblast plugs are no longer observed, intervillous blood flow increases, and intervillous oxygen rises concomitantly [83].

Trophoblast syncytialization

Syncytial fusion is the dissolution of the plasma membrane that separates adjoining cells of the same lineage resulting in a specialized, multinucleated tissue known as syncytium. While membrane fusion is a widespread biological event integral to endocytosis and exocytosis, fertilization and viral infection, fusion events resulting in multinucleated syncytium are unique to specialized tissues such as placental syncytiotrophoblast and myoblast [84-86]. In the human placenta, proliferative trophoblast progenitors programmed to undergo syncytial fusion create and maintain the syncytiotrophoblast, which will initiate invasion at implantation and function as the villous epithelial maternal-fetal interface throughout pregnancy. In ruminant species such as sheep and cows, syncytialization of trophoblast or epithelial cells, or trophoblast-epithelial hybrid syncytialization, occurs at the fetomaternal interface, giving rise to endocrinologically active binucleate cells [8, 12]. In 2002 Potgens, et al. distinguished two distinct types of syncytial fusion in the human: primary trophoblast fusion occurring peri-implantation, and secondary trophoblast fusion beginning around day 11 and continuing until termination of pregnancy. Primary trophoblast fusion involves basolateral fusion of adjoining polar trophoblast cells, which are in contact with uterine epithelium at the leading edge of the implanting blastocyst and creates the

syncytiotrophoblast responsible for initial implantation and invasion necessary for pregnancy establishment [84, 87, 88]. Secondary trophoblast fusion involves the continual incorporation of the underlying cytotrophoblast into existing syncytiotrophoblast tissue at the surface of the chorionic villus. The continual cyto-syncytial fusion in the placental villus maintains the structural and functional integrity of the fetomaternal interface as the placenta grows, and is balanced by rapid syncytiotrophoblast turnover, with aged syncytial nuclei forming knot-like clusters and sloughing into maternal blood [88].

Membrane fusion requires coordination between fusogenic proteins and membrane destabilization, which will ultimately result in the dissolution of the plasma membrane, reorganization of cytoskeleton components, and integration of cytoplasmic contents of two adjoining cells. Additionally, intertrophoblast fusion is integrated with trophoblast differentiation to syncytiotrophoblast; differentiation is characterized by an exit from the cell cycle, reduction in DNA transcription, and transitioning to endocrine, immunologic and metabolic functionality. There is some debate whether syncytial fusion is triggered by initiation of the apoptosis cascade, or whether it is the result of specific differentiation events independent of apoptosis [88, 89]. In either case, strict regulation of syncytial fusion must be maintained to ensure adequate syncytiotrophoblast function while preventing depletion of the pool of cytotrophoblast precursors.

Human endogenous retrovirus (HERV) sequences represent approximately 5 - 8% of the human genome with three distinct human HERVs actively expressed in the human reproductive tract and placenta: HERV-W, HERV-FRD and ERV-3. HERVs containing the *env* gene sequence encode for a complete envelope glycoprotein (Env) comprised of surface and transmembrane subunits, and a synthetic peptide; the Env protein structure has functional potential for recognizing target cells, initiating fusion and suppressing immune response [90].

Expression of HERV-W *env* leads to the production of the fusogenic protein syncytin-1 described by Blond et al. (1999) and named by Mi et al. (2000). Syncytin-1 is abundantly expressed in the placenta and has been identified in both syncytiotrophoblast and cytotrophoblast. Syncytin-1 has been demonstrated to mediate trophoblast cell fusion through its interaction with sodium-dependent neutral amino acid transporter B^0 to form the placental syncytium [87, 90, 91]. Additionally, syncytin-1 may safeguard the placenta against exogenous retroviral infection through receptor blocking [90]. The HERV-FRD *env* gene encodes for HERV-FRD Env, also called syncytin-2, which is structurally and functionally similar to syncytin-1. Despite similarities, experiments by Blaise et al. (2003) demonstrated that syncytin-2 mediates fusion through a different receptor, and contains an immunosuppressive domain, which may be important for ensuring successful fetal allograft [92]. The third HERV expressed in placental syncytiotrophoblast is ERV-3; transcribed from a single copy on chromosome 7 [90, 93]. Notably, the ERV-3 *env* has a high incidence of polymorphism in populations

of European descent; a stop codon in the transmembrane region truncates the protein and prevents plasma membrane anchoring, making fusogenic properties unlikely. The presence of the polymorphism in ERV-3 has not been correlated to pregnancy complications suggesting there is compensative redundancy [90, 93]. Experiments have demonstrated that ERV-3 *env* increases during forskolin-induced differentiation *in vitro*, with ERV-3 *env* expression increasing concomitant with chorionic gonadotropin production suggesting ERV-3 may contribute to the regulation of trophoblast differentiation and hormone production [90, 91, 93].

The action of fusion proteins such as HERVs may be required but are not sufficient to induce fusion alone. Zhou, et al. (2011) chronicled cell fusion as a 5-step process, rather than as an event; necessary steps sited included: priming, chemotaxis, membrane adhesion, membrane fusion and post-fusion resetting [94]. For most physiological conditions cell fusion is undesirable. Regulated conditional priming is required, and involves mobilizing the necessary fusion proteins and adhesion molecules, altering plasma membrane structure and removing inhibitory regulation [94]. Plasma membrane structure modification is required, and redistribution of negatively charged phospholipids such as phosphatidylserine (PS) to the external plasma membrane leaflet is necessary for fusion to proceed [94-96]. Studies have attributed the efflux of PS to the action of protein kinase A [97] and ATP-dependent ABC class floppases [98]. Huppertz et al. (2006) suggested that externalization of PS was required to guide proper orientation of fusogenic proteins upon insertion into the plasma

membrane [85, 96]. The fusion peptide sequence at the N-terminus of transmembrane subunit of HERV *env* contains a sequence that encodes for a hydrophobic α-helix secondary structure that assumes an oblique orientation when inserted into the plasma membrane [86, 99, 100]. The oblique orientation contributes to the disruption of phospholipid continuity and promotes structural changes in the plasma membrane, which lead to the formation of fusion pores and contributes to the induction of membrane fusion [85, 86, 101].

In the hemochorial human placenta, the syncytiotrophoblast serves as the metabolic interface between the fetus and mother, and is vital for regulating nutrient and gas transport between maternal and fetal circulations, providing endocrine signaling necessary for maternal recognition and adaptation, as well as modulating immune suppression necessary for protecting the fetal allograft. During the normal course of pregnancy, aged apoptotic syncytial nuclei are extruded into maternal circulation in what are called syncytial knots, and during the third trimester up to three grams of syncytial tissue can shed into maternal circulation per day [102]. The rate of shedding is in part regulated by the rate of fusion of underlying cytotrophoblast to the syncytial layer. The underlying cytotrophoblast regulates the apoptotic cascade in part by paracrine signaling, but also through the rate of fusion; because transcription levels are lower in syncytiotrophoblast, continual cytotrophoblast fusion is required to provide mRNA, protein and organelles necessary for continued cellular function [102]. Aberrant syncytial formation or renewal due to excessive syncytial shedding or insufficient cytotrophoblast

fusion, or disease states leading to syncytial damage, could compromise syncytiotrophoblast function and fetomaternal interface integrity, and contribute to the development of pregnancy-related disease.

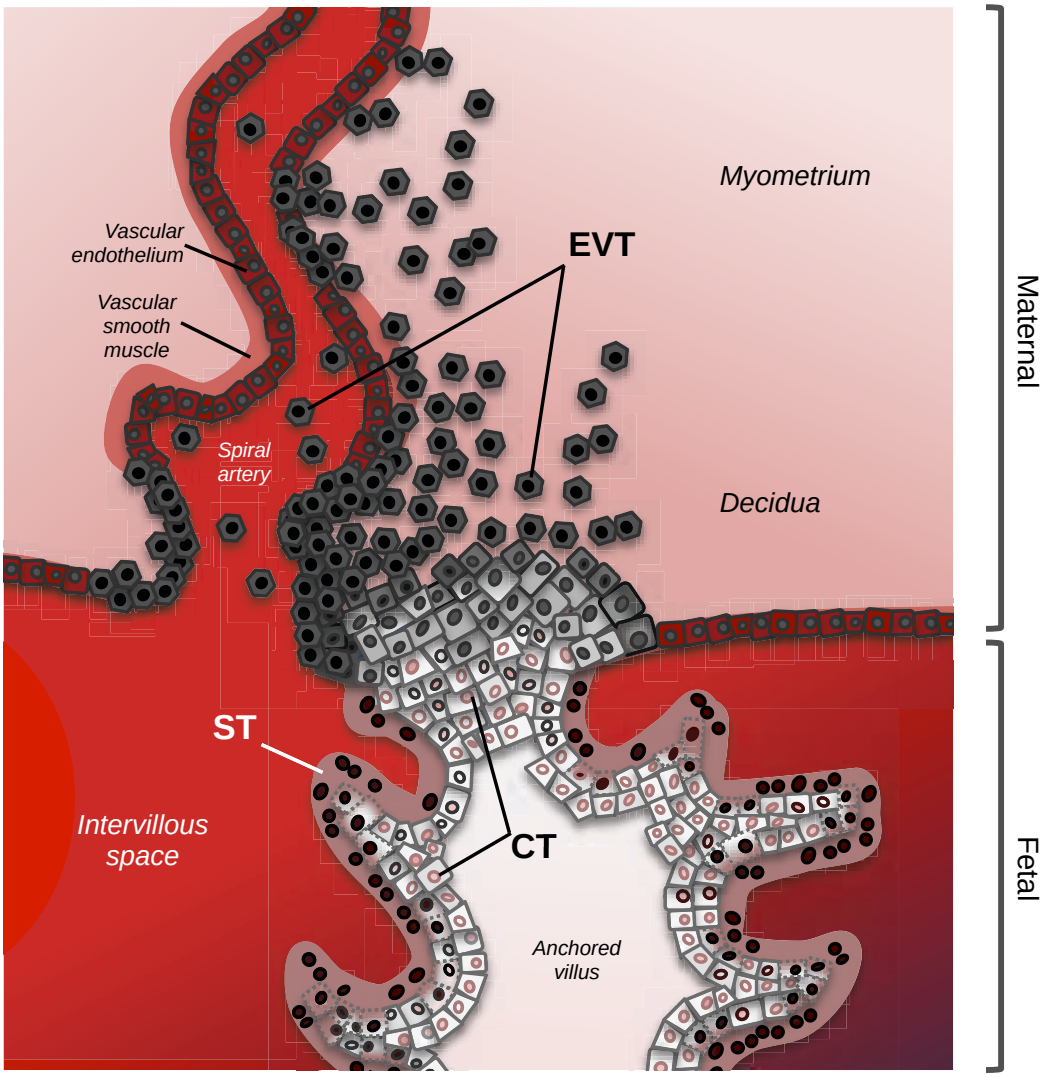

Figure 4. Trophoblast sub-lineages of the placenta villus (human).

Extravillous trophoblast cells (EVT); syncytiotrophoblast cells (ST); cytotrophoblast cells (CT).

PLACENTAL HORMONES

The placenta is an endocrine organ, producing hormones as well as responding to fetal and maternal endocrine signaling in order to dynamically regulate metabolic efficiency and oxygen availability and ultimately fetal development throughout pregnancy [103].

The syncytiotrophoblast layer of the human placenta is the main site of hormone production and secretion, producing a number of hormones including progesterone, estrogens, human placental lactogen (hPL) and human chorionic gonadotropin (hCG) [104, 105]. The corpus luteum (CL) is the primary source of progesterone until the seventh or eighth week of pregnancy after which the placenta becomes the main source [106]. Progesterone plays an important role in the maintenance of pregnancy by repressing uterine contractility until the onset of parturition [107]. Estrogen has been shown to support the production of progesterone by facilitating syncytiotrophoblast uptake of LDL, and stimulating the fetal adrenal gland to produce steroid precursors [108]. Additionally, estrogen regulates fetal cortisol production late in gestation [108]. Human placental lactogen is detectable by the sixth or seventh week of pregnancy and increases through the second trimester before plateauing in the third trimester [109]. hPL acts to stimulate insulin-like growth factor (IGF) production in the mother, increasing glucose and amino acid availability for the fetus. Additionally, hPL directly regulates fetal growth and development by stimulating the production of IGF, insulin and adrenocortical hormone production in the fetus [110].

Human chorionic gonadotropin (hCG)

Human chorionic gonadotropin (hCG) is a primate-specific glycoprotein hormone belonging to a family of hormones, which includes luteinizing hormone (LH), thyroid stimulating hormone (TSH), and follicle stimulating hormone (FSH). These hormones consist of two protein subunits joined by disulfide bonds, a unique beta-subunit, which confers biological specificity and a common alpha-subunit shared by all family members [111, 112]. While the common alpha-subunit is encoded by a single gene on chromosome 6 (6q14-q21) [113], the hCG beta-subunit is encoded by a cluster of six *CGB* genes residing on chromosome 19 (19q13.32) [114-116]. The *CGB* genes are adjacent in contiguous and inverted repeats close in proximity to the gene encoding for LH beta-subunit (*LHB)*, which is considered to be the evolutionarily ancestor [117]. It has been proposed that *CGB* arose from a gene duplication of *LHB* followed by two frame shift mutations resulting in an elongation of the open reading frame (ORF) into the *LHB* 3′ untranslated region, and 24 additional codons [116].

hCG and LH share a high degree of homology, however the hCG beta-subunit (CGB) has a higher carbohydrate content and 30 additional amino acids at its carboxy-terminus which include a proline-rich side chains resulting in a prolonged half-life [116, 118, 119]. In addition to extending the half-life, the CGB carboxy-terminal peptide acts as a routing signal for an alternate secretory pathway [120]. While LH is secreted basolaterally from gonadotrope storage granules upon GnRH signaling, hCG is constitutively secreted from the apical membrane of syncytiotrophoblast cells into maternal circulation [116, 120, 121]. Additionally, alternate N- and O-glycosylation of the same CGB core, coupled

with alternate subunit combination results in five distinct hCG molecules with distinct functions: regular hCG, sulfated hCG, hyperglycosylated hCG (HhCG), free-beta hCG and hyperglycosylated free-beta hCG [122].

Despite differences in structure, hCG and LH bind the same G-protein-coupled receptor (LHCGR) [111]. Ligand binding causes an increase in adenylyl cyclase activity mediated by intracellular, membrane-associated G-proteins resulting increase in cyclic adenosine monophosphate (cAMP) and steroid biogenesis [123]. During the luteal phase of the menstrual cycle, LH binds and stimulates the maintenance of the CL [124]. In the absence of pregnancy, the CL will undergo spontaneous regression. In the case of pregnancy, the pre-implantation blastocyst begins secreting hCG six to nine days after fertilization, which binds to LHCGR on the CL, prevents CL regression and maintains production and secretion of estrogens, relaxin, progestins and inhibin hormones necessary for maintaining pregnancy [125, 126]. hCG is secreted predominately by the syncytiotrophoblast, and is often used as a marker of cell fusion and syncytial differentiation [127, 128]. Maternal serum concentrations of hCG increase rapidly after implantation and increasing placental syncytial mass, before plateauing at a level maintained for the remainder of pregnancy [129, 130]. After the seventh week of pregnancy, the CL regresses and progesterone production is assumed by the placenta (luteo-placental shift) negating the need for continued hCG-mediated CL maintenance [126]. In addition to supporting progesterone production, hCG also promotes implantation [131], uterine angiogenesis [132], as well as maternal immunotolerance

[133] and male fetal sexual differentiation [134, 135]. Finally, abnormal hCG secretion has been used as a diagnostic marker for trisomy 18 (Edward's syndrome) [136], and trisomy 21 (Down's syndrome) [137], as well as trophoblastic tumors [138, 139].

LIN28

Background

LIN28 is an RNA-binding protein that was first characterized by Ambros and Horvitz (1984) as a member of a family of cell lineage-determining proteins critical for the regulation of heterochronic developmental timing in the nematode, *Caenorhabdtis elegans* (*c. elegans*) [140]. Heterochronic gene expression regulates critical developmental events by determining somatic cell fate according to a particular developmental stage. Disruptions or mutations that alter heterochronic gene expression result in either delayed or precocious cell lineage development, ultimately disrupting the normal developmental patterns. Naturally occurring *Lin28* mutant *c. elegans* larva observed by Ambros and Horvitz had precocious development and partial hermaphroditic transformation during sexual development [140, 141]. Later, Moss et al. [142] found that proper *c. elegans* larval development required high levels of LIN28 during the first stage, followed by strict down-regulation of LIN28 upon completion of the first stage. They found that insufficient first-stage LIN28 expression resulted in the omission of the second stage events and precocious progression to third stage cell differentiation events. Moss et al. demonstrated that the down-regulation of LIN28 at the end of the first stage was equally important for development, as maintenance of

expression beyond the first stage caused aberrant protraction of second stage events, and ultimately stunted development [142].

LIN28 is highly conserved, as demonstrated by Moss and Tang (2003) who identified *Lin28* homologues in *Drosophila, Ciona, Xenopus,* mouse, and human [141]. Additionally, they demonstrated that the murine *Lin28* orthologue exhibited similar temporal expression patterns during embryonic development, suggesting LIN28 has a critical role during mammalian embryonic development. They found that Lin28 protein was highly expressed in 9.5 – 10.5 day mouse embryos during a period of organogenesis, but strictly downregulated in 12.5 day embryos [141]. Additional analysis of tissue and cultured cell lines revealed that LIN28 was predominately expressed in undifferentiated embryonic tissue and stem cells, and absent in differentiated cell and tissue types such as fibroblast cells, hepatic and neural tissue [141]. From these data, Moss and Tang inferred that LIN28 was important during early mammalian embryo development and stem cell regulation, and that expression decreased with differentiation. Their conclusion was supported by a transcriptome analysis of human ES cells conducted by Richards et al. [143] who found that *LIN28* was differentially upregulated in human ES cells and strongly downregulated upon differentiation, suggesting *LIN28* was a regulator of pluripotency and could be used as an ES cell marker gene. However, the precise role for LIN28 during mammalian embryonic development has yet to be fully elucidated. Recent experiments by Vogt et al. (2012) to investigate the temporal and functional role of LIN28 suggest that LIN28 is

important during preimplantation mammalian embryo development [144]. Vogt and colleagues suggested that LIN28 may function to regulate the maturation of nucleolar precursor bodies into mature nucleoli, a transition important for the activation of the embryonic transcriptome and the up-regulation of ribosomal subunit production, protein synthesis and cell cycle regulatory mechanisms in early-stage embryos [144]. Vogt et al. observed that LIN28 localized at the periphery of the nucleolar precursor bodies beginning in late 2-cell mouse embryos and concentrating through the 8-cell embryos. As the mouse embryos progressed to blastocysts, LIN28 was concentrated to mature nucleoli in both TE and ICM cells. In contrast, z-stack analysis of 11-cell non-human marmoset blastocysts, showed LIN28 localized to the nucleoli only in the outer blastomeres (precursor cells to what will become the trophectoderm). These data suggest that the temporal patterns of LIN28 expression are different among species, and that LIN28 may have distinct roles for embryonic versus trophectoderm differentiation and development [144].

Transgenic *Lin28* mice created by Zhu et al. [145] demonstrated that aberrant Lin28 expression resulted in altered growth and reproductive phenotypes; global overexpression of *Lin28* resulted in accelerated post-weaning growth trajectories and delayed pubertal onset, whereas *Lin28* knockout pups had lower birth weights and died shortly after parturition [145]. Zhu et al. implied that observations made using the *Lin28* transgenic mice, in conjunction with a meta-analysis of a genome-wide study of human

height conducted by Lettre et al. [146], could be predictive of the importance of LIN28 for regulating human height and pubertal onset.

The potency of *LIN28* as a regulator of pluripotency was demonstrated in experiments by Yu et al. [147], who found that *LIN28* in conjunction with transcription factors *SOX2*, *OCT4* and *NANOG* was sufficient to induce human somatic cells to retrodifferentiate into induced pluripotent stem cells (iPSC). LIN28 has also been implicated as a marker for oncogenic transformation and poor prognostic outcome [148-151]. Aberrant reactivation of LIN28 has been suggested to trigger oncogenic transformation by blocking *lethal-7* (*let-7)* miRNA-mediated inhibition of critical oncogenes such as v-myc myelocytomatosis viral oncogene homolog (avian) (MYC), v-K-ras2 Kirsten rat sarcoma viral oncogene homolog (KRAS) and high mobility group AT-hook 2 (HMGA2) [152, 153], and/or through increased LIN28-meditated translation of oncogenic gene transcripts such as human epidermal growth factor receptor 2 (ERBB2) [154, 155].

Additionally, the *LIN28* mRNA is characterized by an exceptionally long and highly conserved 2.7 kb 3'-UTR that contains many putative miRNA binding sites [141]. Ultimately, the structure of LIN28 connotes the capacity to posttranscriptionally regulate mRNA and miRNA, as well as to be regulated by miRNA, in a double negative feedback fashion.

LIN28 IN MAMMALS

While there is only one *Lin28* gene in nematodes, two *LIN28* homologs have been identified in mammals: *LIN28A* and *LIN28B* [156]. In the human, *LIN28A* and *LIN28B* genes are transcribed from different chromosomes (chromosomes 1 and 6, respectively), resulting in 4014 bp and 5517 nt mRNA sequences. Despite dissimilarities between the gene transcripts, they retain a high degree of structural and functional homology at the protein level [156]. Both genes encode for two RNA-binding domains, a cold-shock domain (CSD), and a zinc-knuckle domain consisting of two cys-cys-his-cys (CCHC) zinc-fingers [141] (Figure 5).

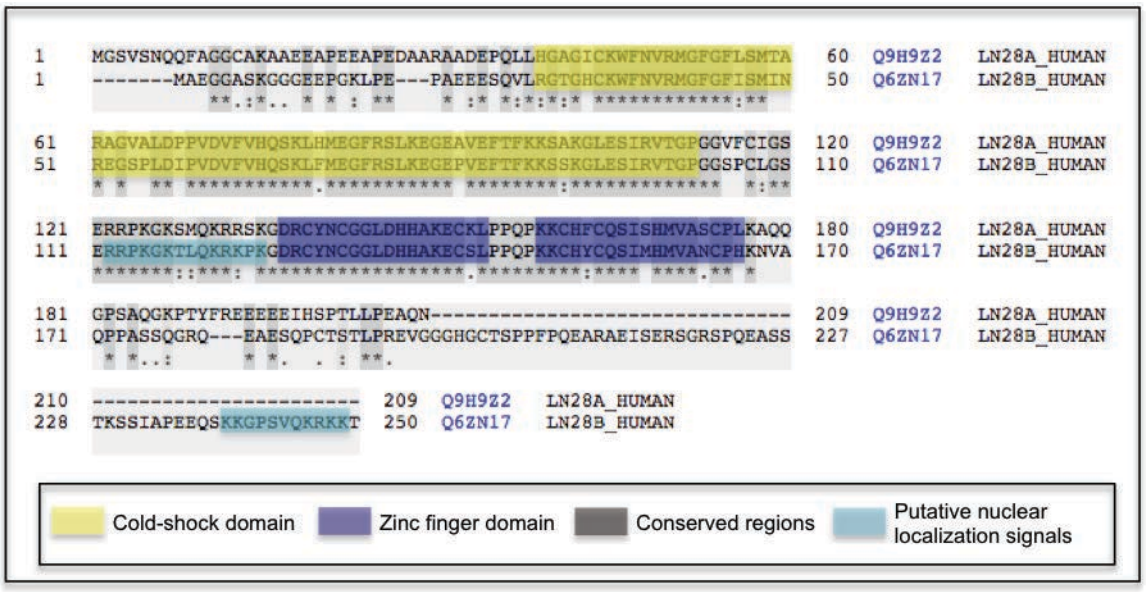

Figure 5. Human LIN28A and LIN28B amino acid alignment.

Alignment demonstrates similarity of the two proteins. The yellow and blue boxes delineate the RNA-binding regions, with yellow indicting the cold-shock domain and the blue indicating the two zinc-finger domains. The gray regions accented with an asterisk indicate regions conserved between the species. The green boxes are putative nuclear localization signals described by Piskounova et al. [157]. Image generated using UNIPROTKB at UniProt.org.

LIN28A mRNA translates into a 209 aa protein which is highly conserved across species (Figure 6).

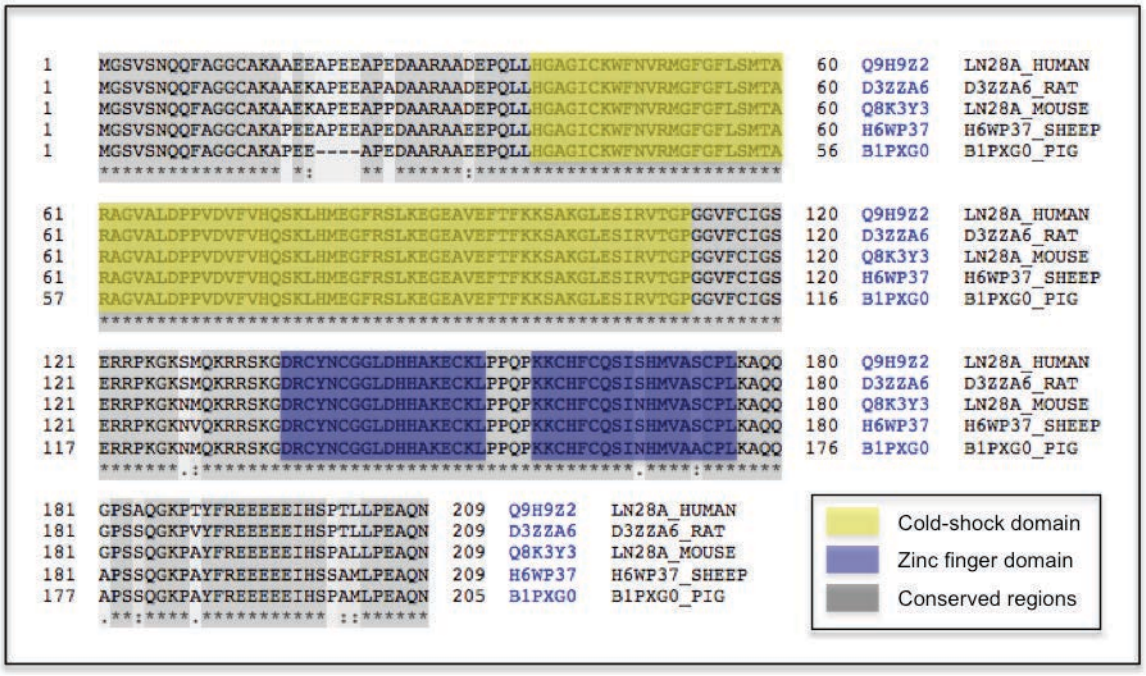

Figure 6. LIN28A protein alignment across species.

Alignment demonstrates a high degree of conservation. The yellow and blue boxes delineate the RNA-binding regions, with yellow indicting the cold-shock domain and the blue indicating the two zinc-finger domains. The gray regions accented with an asterisk indicate regions conserved between the species. Image generated using UNIPROTKB at UniProt.org.

The human *LIN28B* mRNA translates into a 250 aa protein, and in contrast to LIN28A protein, varies in size across species; the mouse *Lin28b* mRNA translates into a 253 aa protein, and the sheep *Lin28b* mRNA translates into a 271 aa protein (Figure 7).

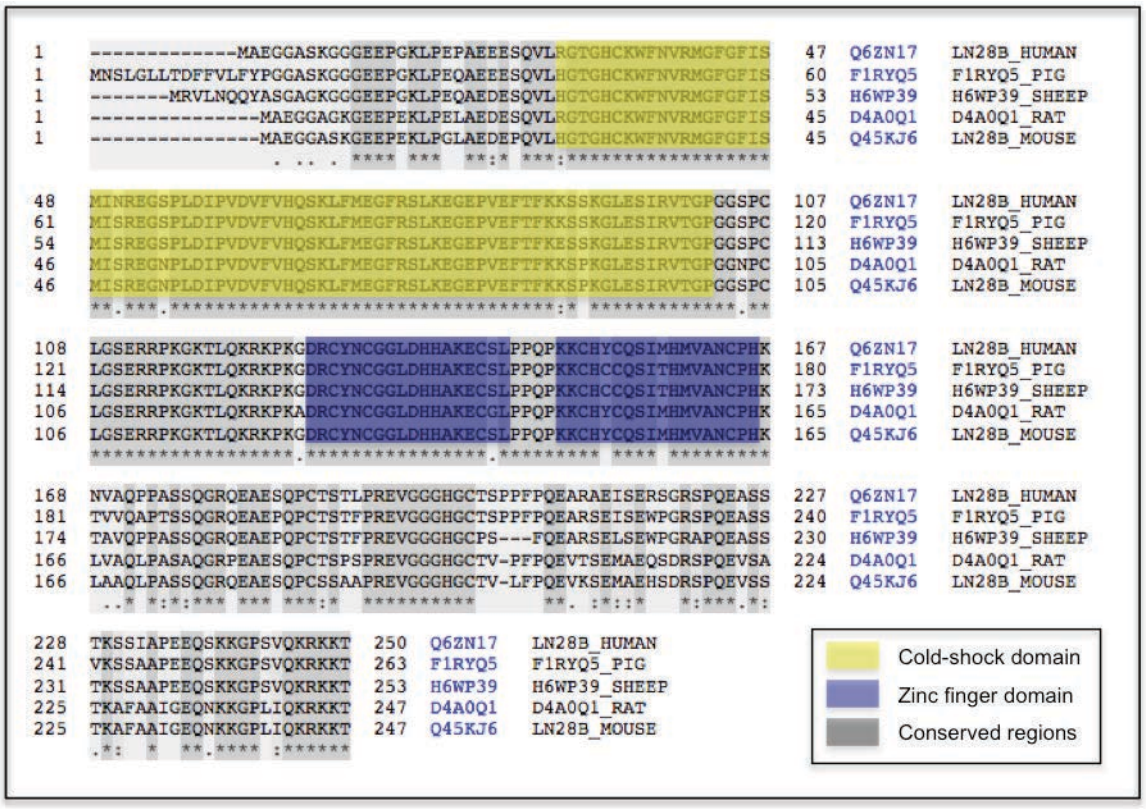

Figure 7. LIN28B protein alignment across species.

The yellow and blue boxes delineate the RNA-binding regions, with yellow indicting the cold-shock domain and the blue indicating the two zinc-finger domains. The gray regions accented with an asterisk indicate regions conserved between the species. Image generated using UNIPROTKB at UniProt.org.

Additionally, some variants for *LIN28B* have been described: three *Lin28b* variants have been described for mouse (Isoform CRA_a, Isoform CRA_b, and Isoform CRA_c, 233, 281 and 96 aa, respectively), and one variant each for human and sheep, 227 aa, 267 aa, respectively (Figure 8). Variant LIN28B proteins in mouse and human are characterized by the addition of amino acids at the N-terminus of the protein sequence. In contrast, the sheep LIN28B variant has additional amino acids inserted at the beginning of the first zinc-finger domain. Theoretically, the location of the sheep variant could affect functionality by extending the linker region between the cold-shock domain and the zinc-knuckle domain affecting RNA binding specificity and/or affinity.

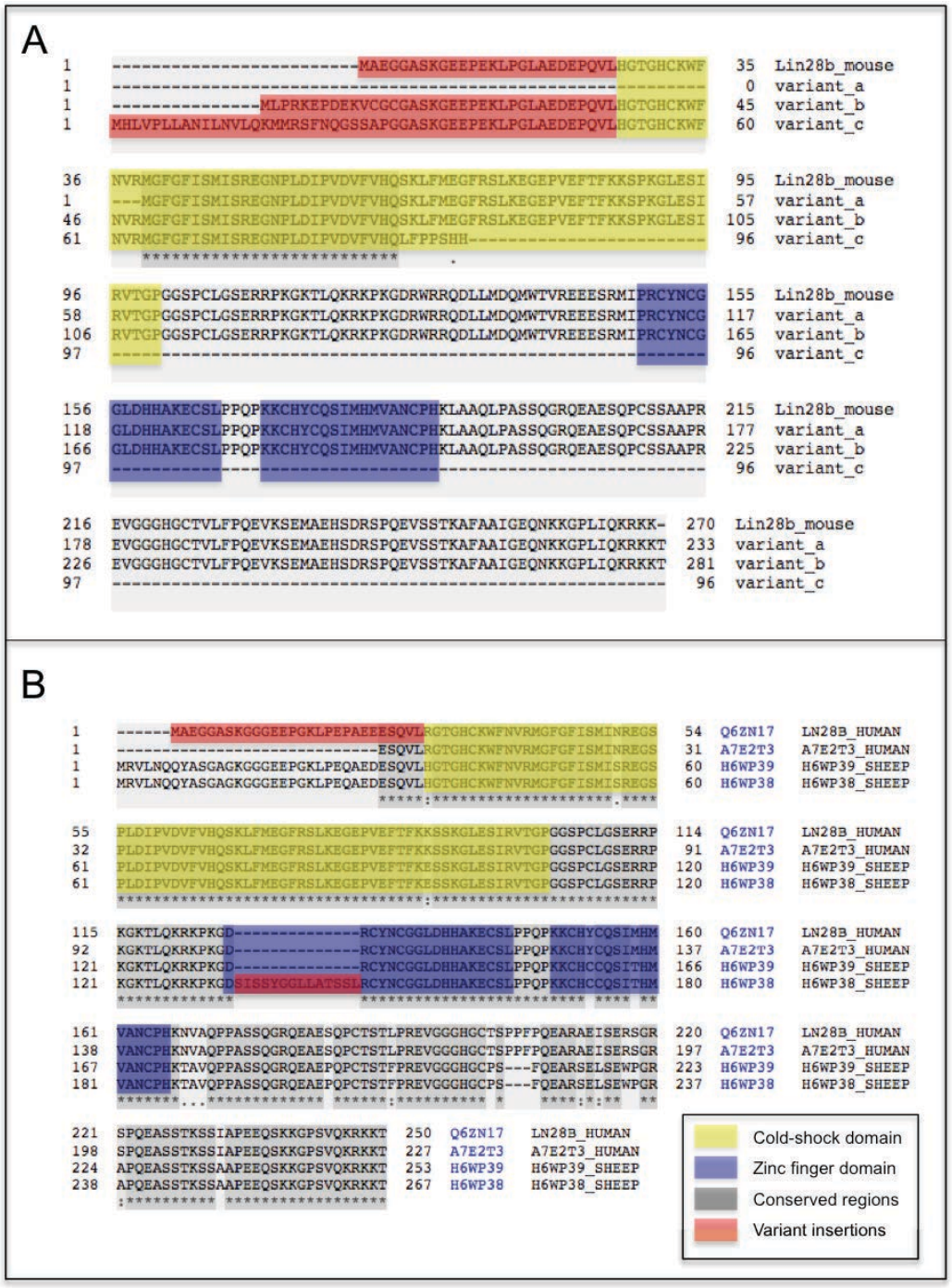

Figure 8. LIN28B protein variants.

The yellow and blue boxes delineate the RNA-binding regions, with yellow indicting the cold-shock domain, blue indicating the two zinc-finger domains, and pink indicating area of variance. The gray regions accented with an asterisk indicate regions conserved between the species. Image generated using UNIPROTKB at UniProt.org.

While LIN28A and LIN28B have a high degree of homology, LIN28B contains two nuclear localization signals, one in an extended C-terminus (KKGPSVQKRKKK) and another in the linker region between the two RNA binding domains (RRPKGKTLQKRKPK), which result in differential localization and ultimately distinct functional mechanisms (discussed below) [157]. To date, LIN28 has been described to have two distinct regulatory roles: the regulation of *let-7* miRNA maturation, and the post-transcriptional regulation of target mRNA.

REGULATION OF MIRNA

MicroRNAs (miRNA) are highly conserved, small (~22 nt), non-coding RNAs, which act to posttranscriptionally regulate target mRNA by binding complementary miRNA response elements (MRE) in the 3'-UTR. The level of complementarity of the miRNA for the target MRE determines the fate of the target mRNA; complete complementarity results in target mRNA degradation, whereas partial complementarity results in translational inhibition.

The *let-7* miRNAs were first described by Reinhart et al. [158] as heterochronic genes important for regulating the larval-adult stage transition in *c. elegans*. The *let-7* miRNA family is comprised of *let-7* miRNA and three other miRNA: *miR-48*, *miR-84* and *miR-241*. These miRNAs are characterized by the complete conservation of eight nucleotide sequence ($^{5'}$UGAGGUAG--$^{3'}$) at their 5' end [159]. *Let-7* miRNAs are transcribed by RNA polymerase II (Pol II) as ~80 nt primary stem-loop *pri-let-7* miRNA structures. Nuclear processing by the RNase III Drosha Microprocessor complex cleaves the

terminal 3’ and 5’ ends, resulting in a ~60 nt hairpin *pre-let-7* miRNA. The *pre-let-7* miRNA is then transported into the cytoplasm by Exportin 5 where RNase III enzyme Dicer cleaves the hairpin resulting in a ~22 nt double-stranded RNA segment, one strand constituting the mature *let-7* miRNA. An RNA helicase unwinds the double-stranded RNA segment, and Dicer facilitates the incorporation of a single strand of the mature *let-7* miRNA into the RNA-induced silencing complex (RISC) [160]. The RISC complex then binds mRNA that contain complementary miRNA response elements (MRE) in their 3’-UTR, represses translation and/or promotes degradation of the target mRNA. Estimates using *in silico* databases identify over five thousand putative mRNA targets, suggesting *let-7* miRNA mediated regulation is extensive.

LIN28 contributes to the maintenance of pluripotency by binding and selectively inhibiting the maturation of *let-7* miRNA by blocking Drosha- and Dicer-mediated processing of *pre-let-7* miRNA. Studies utilizing crystallography, NMR spectroscopy, and binding assays have revealed the mechanisms by which LIN28 binds *pri-* and *pre-let-7* miRNA [161-163]. LIN28 binds to the pre-element (preE), a region in the miRNA hairpin loop, which contains conserved preE stem, preE bulge and preE loop structural elements [161, 164].

The LIN28 CSD binds to a single-stranded region in preE loop. CSD binding causes a section at the 3’ end of the preE bulge, adjacent to the Dicer cleavage site, to melt revealing a conserved GGAG motif [161].

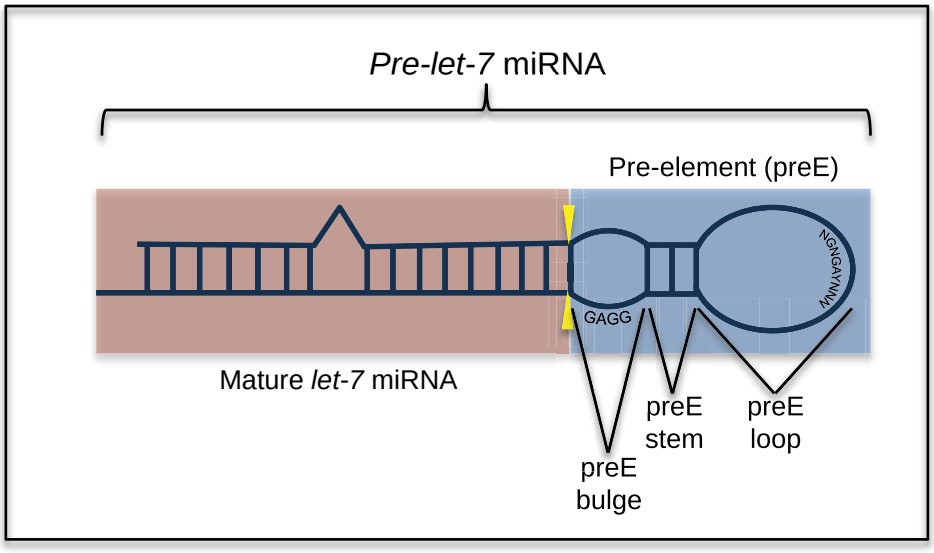

Figure 9. *pre-let-7* miRNA structural elements.

The LIN28 zinc-knuckle domain then binds to the single-stranded GGAG motif and blocks Dicer binding [161-164]. Binding of LIN28 also recruits terminal uridylyl transferase 4 (TUT4), which adds uridine to the 3' end of the bound miRNA signaling for degradation [165] (Figure 10). Using structural and biochemical analyses, Nam et al. [161] identified the amino acid sequence within the *let-7* miRNA preE loop preferentially bound by LIN28 CSD: NGNGAYNN (where Y = pyrimidine, and N = any base). Nam et al. [161] suggested that this flexibility in LIN28 CSD binding specificity could accommodate the variation between individual *let-7* miRNA preE loop sequences.

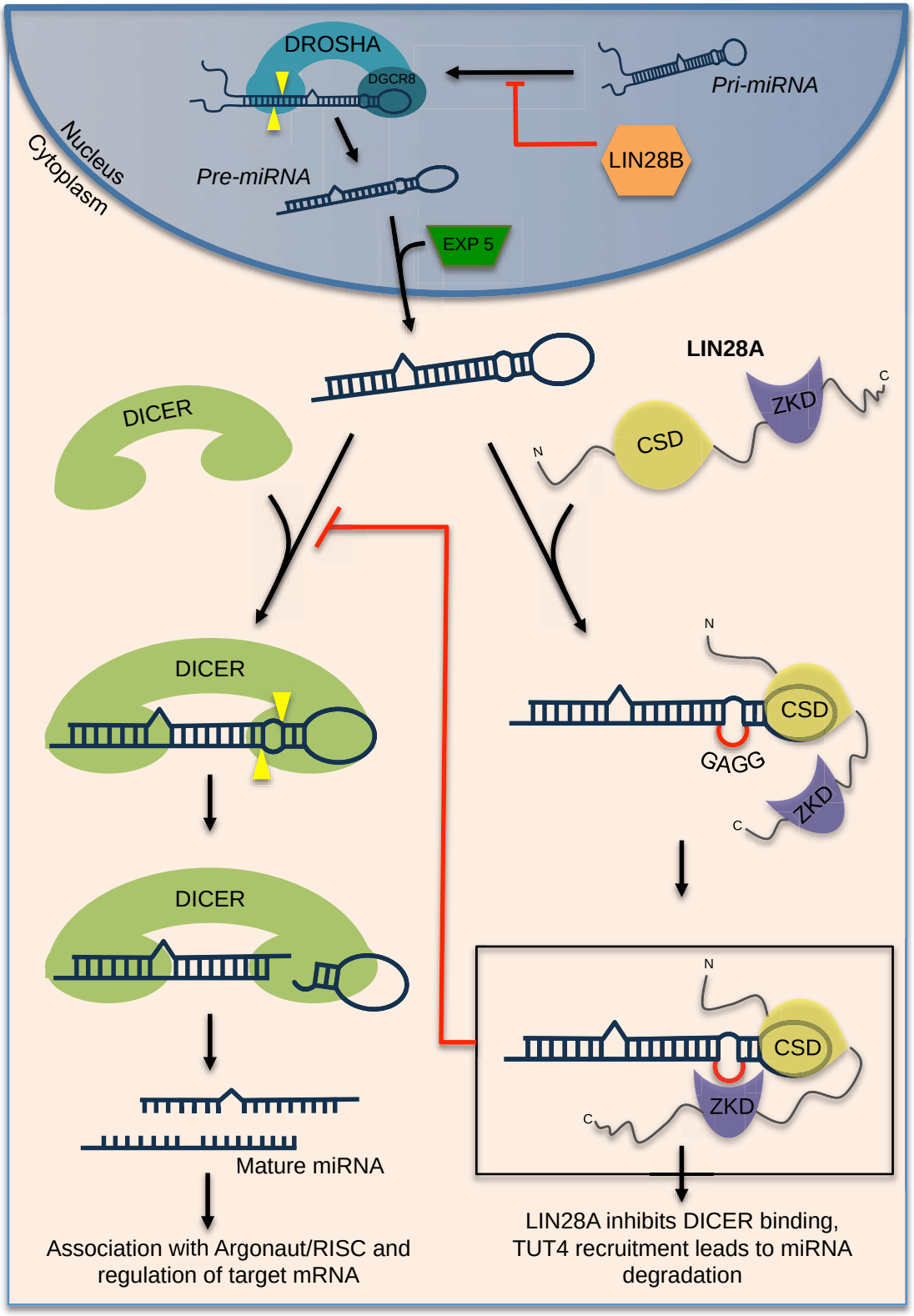

Figure 10. LIN28A mechanism of regulation.

LIN28A binds pre-miRNA and blocks the DICER microprocessor and facilitates miRNA degradation.

LIN28B REGULATION OF MIRNA

In contrast to LIN28A, LIN28B is localized to the nuclear compartment where it sequesters *pri- and pre-let-7* miRNA to the nucleoli (Figure 11) thereby preventing Drosha RNA Microprocessor processing [157]. Whether LIN28A and LIN28B have compensatory or overlapping function, or whether homolog dominance is cell type or developmentally determined, have yet to be fully elucidated.

Ultimately, when LIN28 levels are high, miRNA targets are bound and degraded allowing downstream target mRNA to be translated. When LIN28 levels decrease, mature *let-7* miRNA accumulate, their target mRNAs are repressed and differentiation proceeds. While LIN28A and LIN28B both bind *pre-let-7* miRNA via the conserved CSD and zinc-knuckle RNA-binding domains, differential localization results in two distinct mechanisms of *let-7* miRNA inhibition [157].

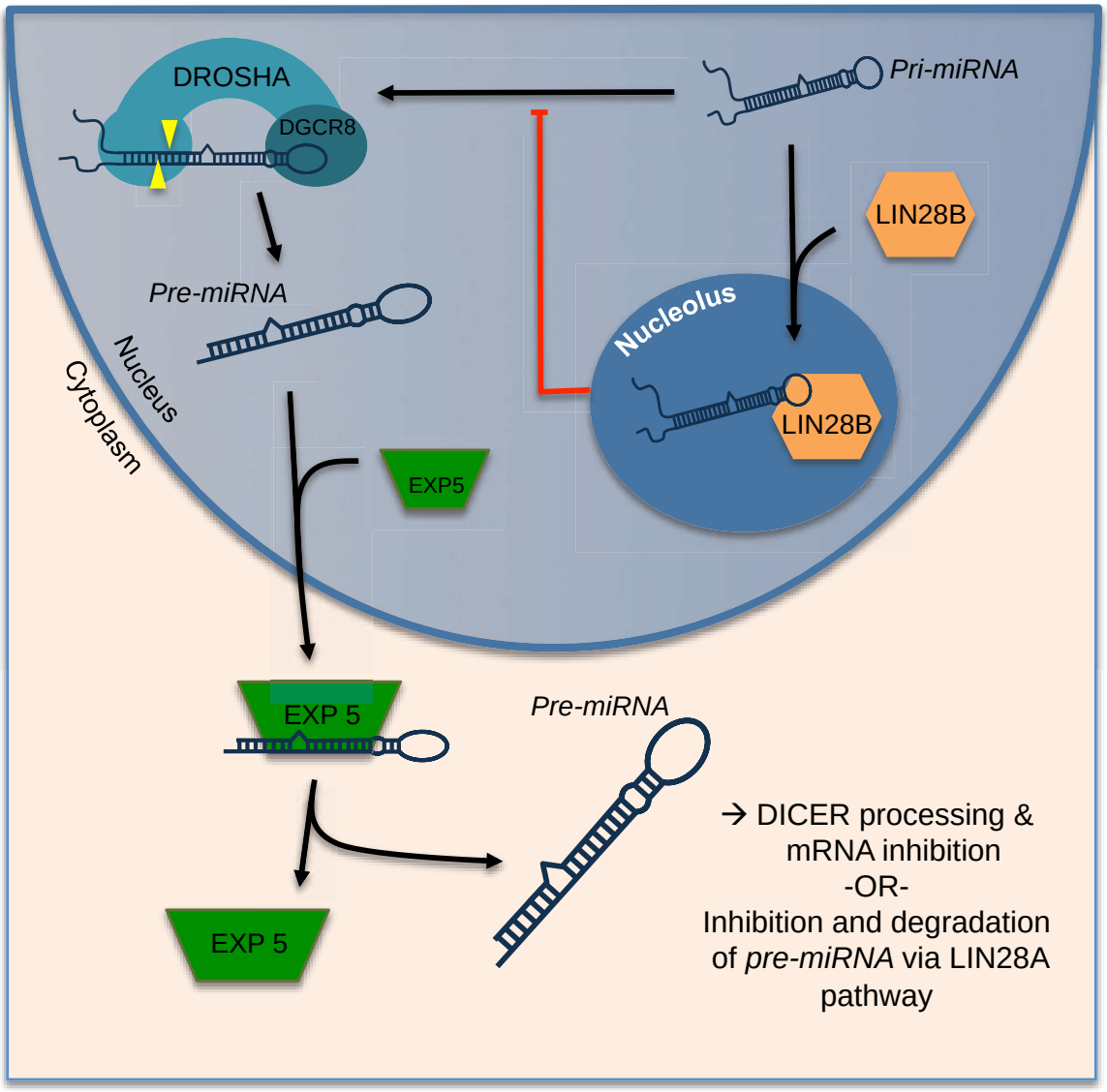

Figure 11. LIN28B mechanism of action.

LIN28B binds *pri-miRNA* and sequesters it to the nucleolar compartment preventing interaction with the DROSHA microprocessor.

REGULATION OF MRNA

In addition to *let-7* miRNA-mediated regulatory pathways, LIN28 has been shown to directly regulate mRNA translation efficiency [166-170]. Balzer and Moss (2007) reported an association between LIN28 and polysomes and actively translating mRNA, the first data to suggest a miRNA-independent regulatory role for LIN28 [168]. A series of experiments has confirmed that LIN28 positively stimulates the translation of the growth factor, IGF2 [171], pluripotency factor OCT4 [170], and a number of genes important for cell-cycle regulation including histone H2a, cdk4 and cyclins A and B [166, 167]. Using immunoprecipitation and deep sequencing, Peng et al. [169] reported that LIN28 selectively bound 4.8% of cellular mRNA, preferentially binding a subset of transcripts for genes important for cell growth and survival. Gene attributes overrepresented in the LIN28 fraction included transcripts for ribosomal proteins and metabolism proteins important for protein biosynthesis, glucose and carbohydrate metabolism, and cholesterol biosynthesis [169]. Peng et al. suggested that this preferential translational stimulation of genes important for growth and metabolism, could be the underlying mechanisms driving the accelerated growth, increased glucose metabolism and insulin sensitivity observed in LIN28-inducible transgenic mice created by Zhu et al. [145]. Notably, in contrast to the findings of Peng et al., Cho et al. [172] recently reported that LIN28 may act as a suppressor of endoplasmic reticulum associated translation of mRNAs in the secretory pathway.

Several studies have suggested that mechanism through which LIN28 promotes translation is through the recruitment of RNA helicase A (RHA) [169, 170, 173], a protein important for facilitating transcription, RNA editing, splicing, nuclear export, and translation [174]. RHA is thought to remodel RNA-RNA and RNA-protein interactions to increase RNA association with ribonucleoprotein (RNP) complexes [174]. Jin et al. (2011) reported that LIN28-interacting domains in the C- and N-termini of RHA bound regions in the C-terminus of LIN28 (interestingly, the LIN28 C-terminal domain is specific for mRNA regulation and is not necessary for *let-7* miRNA regulation [175]); the resulting mRNA-LIN28-RHA complex would act synergistically to remove translational inhibition and improve mRNA translation efficiency [173]. Studies by Lei et al. (2011) identified and characterized the LIN28-response element (LRE), the specific mRNA structural motif required for LIN28 recognition and binding [175]. According to Lei et al., the LRE consists of a secondary structure consisting of three stem-loops, with one stem-loop containing an unmatched, bulging adenine residue (referred to as an A-bulge) flanked by two G:C nucleotide pairs [175]. To date, this LRE motif has been reported in the coding region, as well as in the 5'- and 3'-UTRs of confirmed LIN28-target genes [166, 167, 170, 175]. In addition to being bound by LIN28, Qiao et al. (2012) demonstrated that the LRE motif was bound by the RNAse II Drosha, and that Drosha binding resulted in mRNA destabilization and ultimately decreased translation [176]. Qiao et al. suggested that this Drosha-dependent destabilization of mRNA might serve to counterbalance LIN28-mediated stimulation of mRNA.

LIN28 IN THE PLACENTA

Despite the growing base of research on LIN28, little is known about its role in placenta establishment, differentiation and function. While there has been extensive research into the role of LIN28 in developmental timing and embryonic stem cell (ESC) differentiation, there is little data on whether LIN28 regulates the trophoblast stem cell differentiation important for the establishment and function of trophoblast sub-lineages critical for placenta health. Yang and Moss (2003) observed LIN28 in embryonic day 7.5 mouse trophoblast [177], and Vogt et al. (2012) reported a role for LIN28 at the 2-cell stage in the mouse, implying that LIN28 regulates the maturation of nucleoli required for the transition between maternal and embryonic genome control. Additionally, Vogt et al. reported finding LIN28 isolated to the outer blastomeres in marmoset blastocysts, suggesting a role for LIN28 in early primate trophectoderm development [144].

CHAPTER III: REGULATORY ROLE OF LIN28A IN MOUSE AND HUMAN TROPHOBLAST CELL DIFFERENTIATION[1]

SYNOPSIS

Proper regulation of trophoblast proliferation, differentiation and function are critical for placenta development and function. The RNA-binding protein, LIN28, has been well characterized as a potent regulator of differentiation in embryonic stem cells, however little is known about the function of LIN28 in the placenta. We assessed LIN28 *in vitro* using mouse trophoblast stem cells (mTS) and human trophoblast cells (ACH-3P). We observed that LIN28A decreased and *let-7* miRNA increased when mTS were induced to differentiate into mTGCs upon the removal of FGF4, heparin and conditioned medium. Similarly, we observed that LIN28A decreased in ACH-3P cells induced to

[1] This chapter has been written and formatted with the intention of submitting to the journal, *Biology of Reproduction*, in spring of 2013. Authors and Affiliations: Jill L. Seabrook[#], Jeremy D. Cantlon[#], Austin J. Cooney[^], Erin McWhorter[#], Brittany Fromme[#], Gerrit J. Bouma[#], Russell V. Anthony[#], Quinton A. Winger[#]. [#]Department of Biomedical Sciences, College of Veterinary Medicine and Biomedical Sciences, Colorado State University, Fort Collins, Colorado, USA; [^]Department of Molecular and Cellular Biology, Baylor College of Medicine, Houston, Texas, USA.

syncytialize with forskolin treatment. To assess LIN28 *in vivo* we examined embryonic day 11.5 mouse placenta and observed abundant LIN28A in the chorioallantoic interface and labyrinth layer, with little LIN28A staining in spongiotrophoblast or differentiated trophoblast giant cells (mTGC). Additionally, shRNA-mediated *LIN28A* knockdown in ACH-3P cells resulted in increased spontaneous syncytialization, and increased levels of syncytiotrophoblast markers: hCG, *LGALS13* and *ERVW-1* mRNA. Additionally, targeted degradation of *LIN28A* mRNA increased responsiveness to forskolin-induced differentiation. In contrast, targeted degradation of *Lin28a* mRNA in mTS cells did not alter cell phenotype when maintained under proliferative culture conditions. Together these data establish that LIN28A has a functional role in regulating trophoblast proliferation, differentiation and function. These data also suggest that loss of LIN28A in human trophoblast is sufficient to induce differentiation, but that in the mouse, LIN28A acts in concert with other factors to inhibit trophoblast differentiation.

INTRODUCTION

The initial differentiation event during embryo development is the segregation of pluripotent cells into either trophoblast or inner cell mass cell lineages. Placenta establishment and development originates and depends upon trophoblast stem cell differentiation into specialized trophoblast sub-types. Disruption of temporal or molecular programs regulating the differentiation of trophoblast stem cells can result in insufficient sub-lineage trophoblast populations, and ultimately in compromised invasion or utero-placental vascular remodeling, poor metabolic exchange and/or abnormal

endocrine function. In the human, trophoblast dysfunction is thought to be an underlying cause to the development of increased intervillous blood pressure, perfusion velocity and the development of global hypertension and inflammation associated with placental diseases such as preeclampsia (PE) and intrauterine growth restriction (IUGR) [21, 178-181]. Assessments of placental tissue taken from PE and IUGR pregnancies are associated with lower cytotrophoblast (CT) fusion indices, a higher rate of syncytial apoptosis, and insufficient extravillous trophoblast (EVT) invasion and villus development [182-184]. Immediate implications of placenta dysfunction include fetal growth restriction, fetal distress, preterm delivery and in acute cases, death. However, research also indicates placenta dysfunction contributes to long-term physiological programing of the offspring, manifesting in increased risk of hypertension, cardiac disease, diabetes and obesity [1, 185-187]. Therefore understanding the mechanisms regulating trophoblast differentiation is key to developing means for efficient diagnoses and treatment placenta dysfunction.

LIN28, an RNA binding protein, has been well characterized as a potent post-transcriptional regulator of differentiation in embryonic stem cells with the ability to enhance retrodifferentiation of somatic cells into induced pluripotent stem cells (iPSC) [147, 165, 188, 189]. Additionally, reactivation of LIN28 in terminally differentiated tissue has been implicated in oncogenic transformation and poor prognostic outcome [148-151]. To date, LIN28 has been described to have two distinct regulatory mechanisms for maintaining pluripotency: inhibition of *let-7* miRNA maturation [149], and direct post-

transcriptional regulation of target mRNA [169]. LIN28 blocks *let-7* miRNA maturation in undifferentiated cells by recruiting terminal uridylyl transferase (TUTase) [165, 190, 191]. While there has been extensive research into the role of LIN28 in stem cell (ESC) differentiation [147, 169, 192, 193], there is little data on whether LIN28 regulates the trophoblast stem cell differentiation important for the establishment and function of trophoblast sub-lineages critical for placenta health. Yang and Moss [177] observed LIN28 in embryonic day 7.5 mouse trophoblast, and Vogt et al. [144] reported a role for LIN28 at the 2-cell stage in the mouse, concluding that LIN28 regulates the maturation of nucleoli required for the transition between maternal and embryonic genome control. Additionally, Vogt et al. [144] reported finding LIN28 isolated to the outer blastomeres in marmoset blastocysts, suggesting a role for LIN28 in early primate trophectoderm development.

The aim of this study was to determine whether LIN28 is important for modulating trophoblast differentiation, and ultimately to determine whether disruption of LIN28 would impact trophoblast differentiation and/or function.

MATERIALS AND METHODS

All animal experiments were performed in accordance with protocols approved by the Colorado State University Institutional Animal Care and Use Committee.

CELL LINES.

Mouse trophoblast cells (mTS) were derived from blastocyst-stage embryos at 3.5 days postcoitum (dpc) from naturally bred Black Swiss female mice, using techniques previously described [27, 194]. Briefly, mouse blastocysts were collected and cultured on a feeder layer of mitomycin-C treated mouse embryonic fibroblasts. Trophoblast stem cell colonies were isolated from blastocyst outgrowths and separated from feeder fibroblasts through serial passage. Isolated mTS cells were maintained in 70% mouse embryonic fibroblast conditioned medium and 30% TS medium (RPMI 1640, 2 mM L-glutamine, 30% FBS, 1mM sodium pyruvate, 100uM β-mercaptoethanol, antibiotic-antimycotic solution containing 10,000 IU/mL penicillin, 10,000 ug/mL streptomycin, 25 ug/mL amphotericin) supplemented with 25 ng/mL FGF4 and 1 ug/mL heparin. mTS cell differentiation into mouse trophoblast giant cells (mTGC) was induced by removal of conditioned medium, FGF4 and heparin for six days.

ACH-3P cells (a generous gift from Ursula Hiden, Medical University of Graz, Austria), a cell line derived from the fusion of AC1-1 cells with primary first trimester human trophoblast cells [29], were grown in F-12 Medium (10% FBS, 2 mM L-glutamine, antibiotic-antimycotic solution containing 10,000 IU/mL penicillin, 10,000 ug/mL streptomycin, 25 ug/mL amphotericin). ACH-3P cells were induced to differentiate into syncytiotrophoblast by treatment with 40 uM forskolin for 48 hours; forskolin is known to induce morphological fusion of cultured trophoblast cells, which closely resembles morphology of natural syncytiotrophoblast [195].

REAL-TIME RT-PCR.

Total RNA was extracted from cells using miRNA Mini Kit (Qiagen, Valencia, CA) according to manufacturer's directions. For mRNA analysis, cDNA was generated from 1 ug of total cellular RNA using qScript cDNA Supermix (product no. 95048; Quanta Biosciences, Gaithersburg, MD) and quantitative real-time RT-PCR (qPCR) of mRNA was performed as described previously [194]. Briefly, each 1X 20 uL qPCR reaction consisted of 10 uL LightCycler 480 Probes Master mix (product no. 04707494001; Roche, Mannheim, Germany), 1 uL of 150 nM TaqMan Gene Expression Assay (Applied Biosystems, Carlsbad, CA) and 9 uL of cDNA template diluted to 90 uL. qPCR was performed using the Light Cycler 480 thermal cycler (Roche) with the following parameters: 10 minute pre-incubation at 95°C, 45 cycles of amplification which included denaturation at 95°C for 10 seconds, annealing at 60°C for 30 seconds and extension at 72°C for 1 second, followed by a final cooling cycle at 40°C for 5 min. Normalization of mRNA levels in mTS cells was calculated using levels of glyceraldehyde-3-phosphate dehydrogenase (*Gapdh)*. Normalization of mRNA in human cells was using the geometric mean of TATA box biding protein mRNA (*TBP)* and mitochondrial ribosomal protein S15 mRNA (*MRPS15)*.

For miRNA analysis, cDNA was generated from 500 ng of total cellular RNA using miScript II RT Kit (product no. 218161; Qiagen). The 1X 10 uL miRNA qPCR reaction consisted of 5 uL LightCycler 480 SYBR Green I Master mix (product no. 04707516001; Roche) 1 uL of forward primer, 1 uL universal reverse primer (SBI System Biosciences,

Mountain View, CA for mouse *let-7* miRNA primers, Qiagen miScript for human *let-7* miRNA primers), and 8 uL of cDNA template. miRNA qPCR was performed using the Light Cycler 480 thermal cycler (Roche) with the following cycling parameters: 15 minute enzyme activation step at 95°C, followed by 45 cycles of amplification which included denaturation at 94°C for 15 seconds, annealing at 55°C for 30 seconds and extension at 70°C for 30 seconds, followed by a melting curve analysis to confirm amplification quality and specificity. Normalization of *let-7* miRNA levels in mTS cells was calculated using the geometric mean of ncRNA (*U6)* snRNA and small nucleolar RNA, C/D box 43 (*RNU43)* snoRNA. Normalization of *let-7* miRNA levels in human cells was calculated using the geometric mean of small nucleolar RNA, C/D box 41 *(SNORD41)* and small nucleolar RNA, C/D box 44 (*SNORD44)* miRNAs.

Relative expression was determined for all qPCR data using the comparative Ct method [196]. Statistics: We used Student's t-test to compare relative expression of genes in wild-type trophoblast, non-target controls, *LIN28A* KD and forskolin treated cells from each of the experimental models. We used the Newman-Keul's Multiple-Comparison Test with an alpha value of 0.05 to compare *let-7* miRNA levels between mTS *Lin28a* KD and non-target control (Figure 3B).

WESTERN BLOT.

Cellular protein was assessed by western blot analysis, similarly to procedures described previously [194, 197, 198]. Briefly, cells were lysed in RIPA buffer (20 mM Tris, 137 mM NaCl, 10% glycerol, 1% Nonidet P-40, 3.5 mM SDS, 1.2 mM sodium

deoxycholate, 1.6 mM EDTA, pH 8) supplemented with 10% protease/phosphatase inhibitor cocktail (product no. P8340; Sigma-Aldrich, St. Louis, MO), and 1 mM phenylmethanesulfonyl fluoride (PMSF). Protein concentration was determined using the Bradford assay method [199]; absorbance was measured at λ 595 nm using the Biotek Synergy 2 Microplate Reader (Biotek, Winooski, VT). Protein was electrophoresed through 4-12% Bis-Tris gels, then transferred to 0.45 um pore nitrocellulose membrane at a constant 100 V on ice for one hour. Membranes were blocked in 10% milk-TBST (50 mM Tris, 150 mM NaCl, 0.05% Tween 20, pH 7.6) overnight at 4°C to reduce non-specific binding, then incubated with primary antibody at ambient temperature for two hours. Membranes were washed in TBST, and then incubated with a horseradish peroxidase-conjugated secondary antibody for one hour at ambient temperature. For assessment of LIN28A protein in human and mouse whole cell lysate, a polyclonal antibody to LIN28A (1:1000 dilution; product no. ab63740; Abcam, Inc., Cambridge, MA) was used in conjunction with a horseradish peroxidase-conjugated secondary (1:2000 dilution; product no. sc-2004; Santa Cruz Biotechnology, Inc., Dallas, TX). An antibody to beta-actin (1:2000 dilution; product no. sc-47778; Santa Cruz Biotechnology, Inc.), or an antibody to GAPDH (1:2000 dilution; product no. ab37168; Abcam, Inc.), was used in conjunction with horseradish peroxidase-conjugated secondary as loading control and to normalize LIN28A protein in cell lysates (1:2000 dilution; product no. 1858413; Pierce, Rockford, IL; or 1:2000 dilution; product no. sc-2004; Santa Cruz Biotechnology). Membranes were developed using ECL Western Blotting Detection Reagent chemiluminescent kit (product no. RPN2132;

Amersham, Pittsburgh, PA), and membranes were imaged using the ChemiDoc XRS+ chemiluminescence system (BioRad, Hercules, CA). Densitometry calculations were performed using the Image Lab Software (BioRad). Fold change was calculated as a percent of non-target control protein after normalization.

IMMUNOHISTOCHEMISTRY.

Mouse placentas were collected on embryonic day 11.5 from naturally bred Black Swiss female mice. Placenta tissue was fixed in 4% paraformaldehyde and paraffin embedded. Immunohistochemistry was performed as previously described [197]. Briefly: 6 micrometer sections were cut, sections were dewaxed in xylene and rehydrated through serial ethanol dilutions, then treated with 3% H_2O_2 to reduce endogenous peroxidase activity. Sections were blocked in SuperBlock Blocking Buffer (product no. 37580; ThermoScientific, Waltham, MA) overnight at 4°C to reduce non-specific binding. Cells were incubated with an antibody to LIN28A overnight at 4°C (1:200 dilution; product no. ab63740; Abcam, Inc.). For negative controls, primary antibody was preabsorbed with antibody-specific synthetic antigen (2:1 ratio; product no. ab64578; Abcam, Inc.). The VectaStain Elite ABC Kit (Rabbit IgG) biotinylated anti-rabbit secondary antibody was used according to manufacturer's directions, and positive immunostaining was visualized using the avidin-biotin complex (ABC) system (product no. PK-6101; Vector Laboratories, Burlingame, CA). Diaminobenzedine (DAB) was used as the final chromogen (product no. SK-4100; Vector Laboratories) and Harris modified hematoxylin was used to counterstain.

LIN28A KNOCKDOWN.

Stably transduced *Lin28a* mRNA knockdown (KD) and non-target control cell lines were created using commercially available MISSON shRNA Lentiviral Transduction Particles, lentiviral based pLKO.1-puro vectors (Sigma-Aldrich). The pLKO.1-puro vectors used contained an shRNA sequence cassette downstream of a modified U6 shRNA promoter and a puromycin resistance gene for selection downstream of a human phosphoglycerate kinase (hPGK) eukaryotic promoter. The lentiviral based pLKO.1-puro vector used to knockdown *Lin28a* in mTS cells contains an shRNA sequence designed to target mouse *Lin28a* mRNA for degradation (clone no. TRCN0000102578; Sigma-Aldrich) (see Table 1).

The lentiviral based pLKO.1-puro vector used to knockdown *LIN28A* in ACH-3P cells contains a shRNA sequence designed to target human *LIN28A* mRNA for degradation (clone no. TRCN0000021802; Sigma-Aldrich) (see Table 1). Both ACH-3P and mTS non-target control cell lines were created using a pLKO.1-puro vector with an shRNA sequence designed to target no known mammalian genes (product no. SHC002V; Sigma-Aldrich) (see Table 1). mTS cells were infected in three replicate experiments with either *Lin28a* mRNA targeted particles or non-target particles at a multiplicity of infection (MOI) of 100 viral particles per cell. Infected mTS cells were selected by treatment with 2 ug/mL puromycin for 14 d or until all untreated control cells were dead. ACH-3P cells were infected in three replicate experiments with either the *LIN28A* mRNA targeted particles or the non-target control particles at a MOI of 500 viral particles per

cell. Infected ACH-3P cells were selected by treatment with 8 ug/mL puromycin for 14 days or until all untreated control cells were dead. The degree of LIN28 mRNA and protein knockdown was determined by qPCR and western blot, as described previously.

Table 1. shRNA clone sequences

mLin28a	CCGGCAAAGGAGACAGGTGCTACAACTCGAGTTGTAGCACCTGTCTCCTTTGTTTTTG
hLIN28A	CCGGACCTACTTTCGAGAGGAAGAACTCGAGTTCTTCCTCTCGAAAGTAGGTTTTTT
Non-target	CCGGGCGCGATAGCGCTAATAATTTCTCGAGAAATTATTAGCGCTATCGCGCTTTT

ELISA.

ACH-3P non-target and LIN28A KD cells were plated in 6-well culture dishes with 25,000 cells per well and six replicates per treatment. Cell culture medium (1.5 mL/replicate) was collected after 48 hours, and cells were collected and counted. Concentrations of hCG were quantified using an hCG ELISA kit utilizing a mouse monoclonal anti-hCG (specific to beta-hCG) conjugated to horseradish peroxidase according to manufacturer's instructions (product no. 25-HCGHU-E01; ALPCO Diagnostics, Salem NH).

Experimental replicates were assayed in triplicate, and absorbance was measured at λ 450 nm. Soluble hCG concentrations (mIU/mL) were calculated by plotting sample mean absorbance values against the mean values calculated from duplicate standard curve values. The standard curve consisted of 0, 5, 20, 50, 150 and 300 mIU/mL hCG

standards. Soluble hCG concentrations were then normalized to the number of cells at the time of collection. We used the Student's t-test to compare hCG concentrations between non-target controls and *LIN28A* KD ACH-3P cell medium. P-values of less than 0.05 were considered to be statistically significant.

IMMUNOFLUORESCENCE.

ACH-3P non-target and LIN28A KD cells were plated on 18 mm glass coverslips in 6-well culture dishes with 10,000 cells per well and six replicates per treatment. To determine ACH-3P cells positive for hCG, immunofluorescence was performed similarly as previously described [200]. Briefly, cells were grown for 48 hours, medium was aspirated, cells were rinsed with PBS (137 mM NaCl, 2.7 mM KCl, 10 mM Na_2HPO_4, 1.8 mM KH_2PO_4, pH 7.4) and then fixed in 100% ice-cold acetone for 10 minutes at -20 °C. Cells were rinsed with PBS and then blocked in 10% goat serum in PBS-0.1% Tween for 20 minutes at ambient temperature. Cells were incubated with anti-beta-hCG primary antibody (1:50 dilution; product no. RB-059-A; ThermoScientific) overnight at 4°C with gentle agitation. Cells were rinsed with PBS-0.1% Tween and incubated for one hour at ambient temperature with AlexFluor 488-conjugated secondary antibody (1:1000 dilution; product no. A11008; Invitrogen, Carlsbad, CA). Cells were incubated with a plasma membrane stain (CellMask Orange, Invitrogen) according to manufacturer's directions, rinsed and then incubated with 5 ug/mL Hoechst 33342 for 10 minutes at ambient temperature to visualize cell nuclei.

To assess ACH-3P cell fusion, ACH-3P cells were plated on 18 mm glass coverslips in 6-well culture dishes with 10,000 cells per well and six replicates per treatment. Cells were rinsed with PBS and then incubated with the plasma membrane stain, Concanavalin A, AlexaFluor 488 conjugate for 10 minutes at ambient temperature (1:1000 dilution; product no. C11252; Invitrogen). Cells were fixed in 100% ice-cold acetone for 10 minutes at -20 °C, rinsed in PBS and then treated with 500 nM propidium iodide for 10 minutes at ambient temperature.

RESULTS

LEVELS OF LIN28 AND LET-7 MIRNA IN MOUSE TROPHOBLAST CELLS.

Mouse trophoblast stem cells (mTS) were used to determine if levels of LIN28 changed with differentiation into trophoblast giant cells (mTGC). mTS cells grown for six days in the absence of FGF4, heparin and fibroblast conditioned medium differentiated from proliferative mTS into mTGCs. mTS cell differentiation was characterized by typical morphological transformation from compact proliferative mTS cells into expanded endoreduplicating mTGCs (Figure 12 A-B). Day six mTGCs had a 13-fold decrease in *Lin28a* mRNA ($P < 0.01$) compared to mTS maintained in proliferative culture conditions (Figure 12 C). The decreases observed in *Lin28a* mRNA data were corroborated by decreases in LIN28A protein, as determined by western blot of whole cell lysate and immunohistochemistry (Figure 12 D-F). The decreased levels of LIN28 mRNA and protein in mTGCs was accompanied by significantly increased levels of *let-7* miRNA:

19-fold increased levels of *let-7a* miRNA ($P < 0.01$), 24-fold increased levels of *let-7c* miRNA ($P < 0.01$), 29-fold increased levels of *let-7d* miRNA ($P < 0.01$), 22-fold increased levels of *let-7e* miRNA ($P < 0.01$), 34-fold increased levels of *let-7f* miRNA ($P < 0.01$), 31-fold increased levels of *let-7g* miRNA ($P < 0.01$), and 26-fold increased levels of *let-7i* miRNA ($P < 0.05$) (Figure 12 G). These data suggest that mTS cell differentiation may be a LIN28-mediated event, and that LIN28 acts to inhibit *let-7* miRNA maturation in proliferative mTS cells.

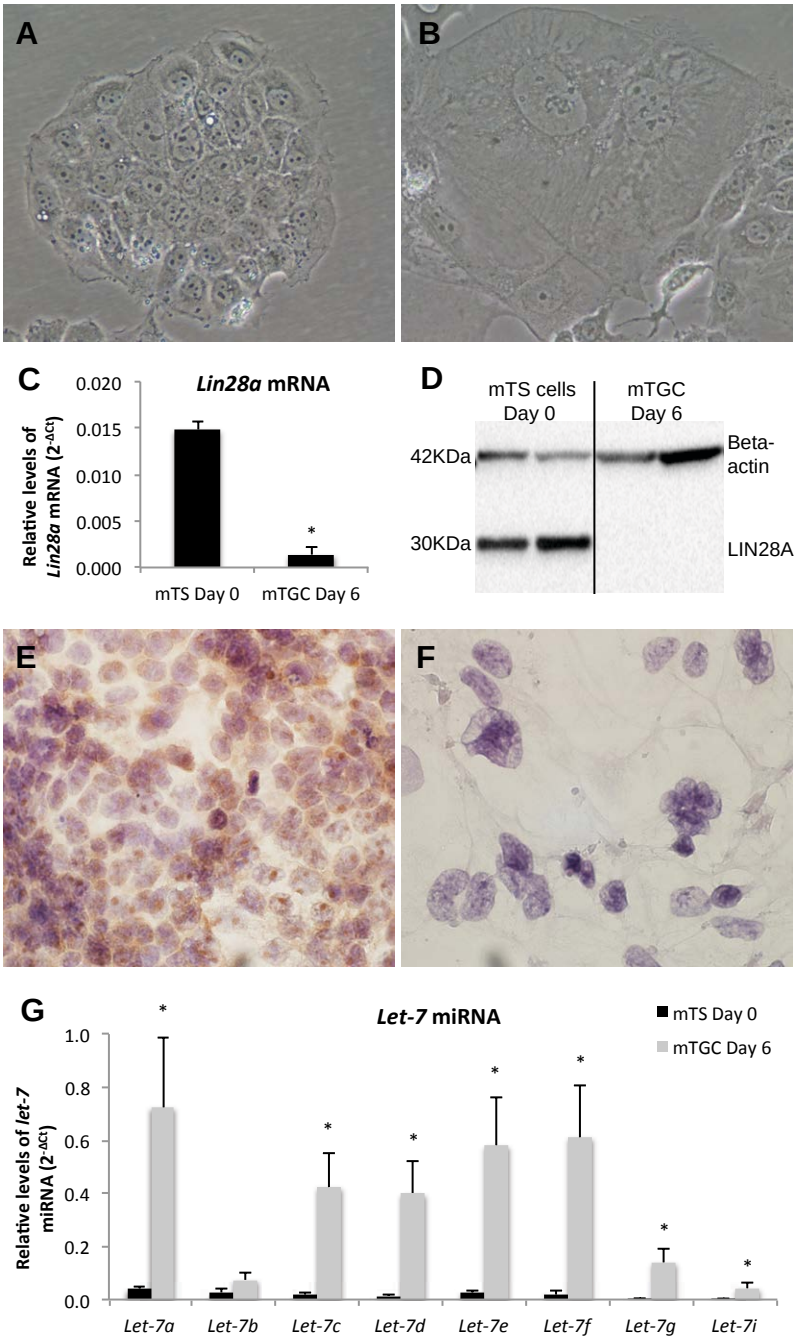

Figure 12.LIN28A and *let-7* miRNA levels in proliferative mTS cells and differentiated mTGCs.

A-B) Brightfield microscopy (20X) depicts mTS cell morphology under proliferative and differentiation conditions. C-D) LIN28A mRNA and protein levels are decreased in differentiated mTGCs compared to proliferative mTS. E-F) Immunohistochemistry demonstrates LIN28A in proliferating mTS is decreased when cells differentiate into mTGCs after 6 days without FGF4, heparin or conditioned medium. G) Levels of *let-7* miRNA were increased in mTGCs grown under differentiating conditions for 6 days.

IN VIVO LOCALIZATION OF LIN28A IN EMBRYONIC DAY 11.5 MOUSE PLACENTA.

Immunohistochemistry, using serial sections of embryonic day 11.5 (E 11.5) mouse placenta, was used to determine *in vivo* LIN28A protein localization during mid-gestation. Distinct areas along the chorioallantoic interface, as well as the extraembryonic membranes stained positive for LIN28A (Figure 13 A1 & B1). The trophoblast cells of the labyrinth layer had strong, diffuse LIN28A staining throughout (Figure 13 A2 & B2). Allantois, spongiotrophoblast, and mTGCs in the junctional zone had little or no LIN28A reactivity (Figure 13 A3 & B3). Maternal decidua also had little to no LIN28 staining. These data demonstrate that LIN28A protein is present in mid-gestational mouse placenta, and may have a role in the regulation of trophoblast differentiation and/or function.

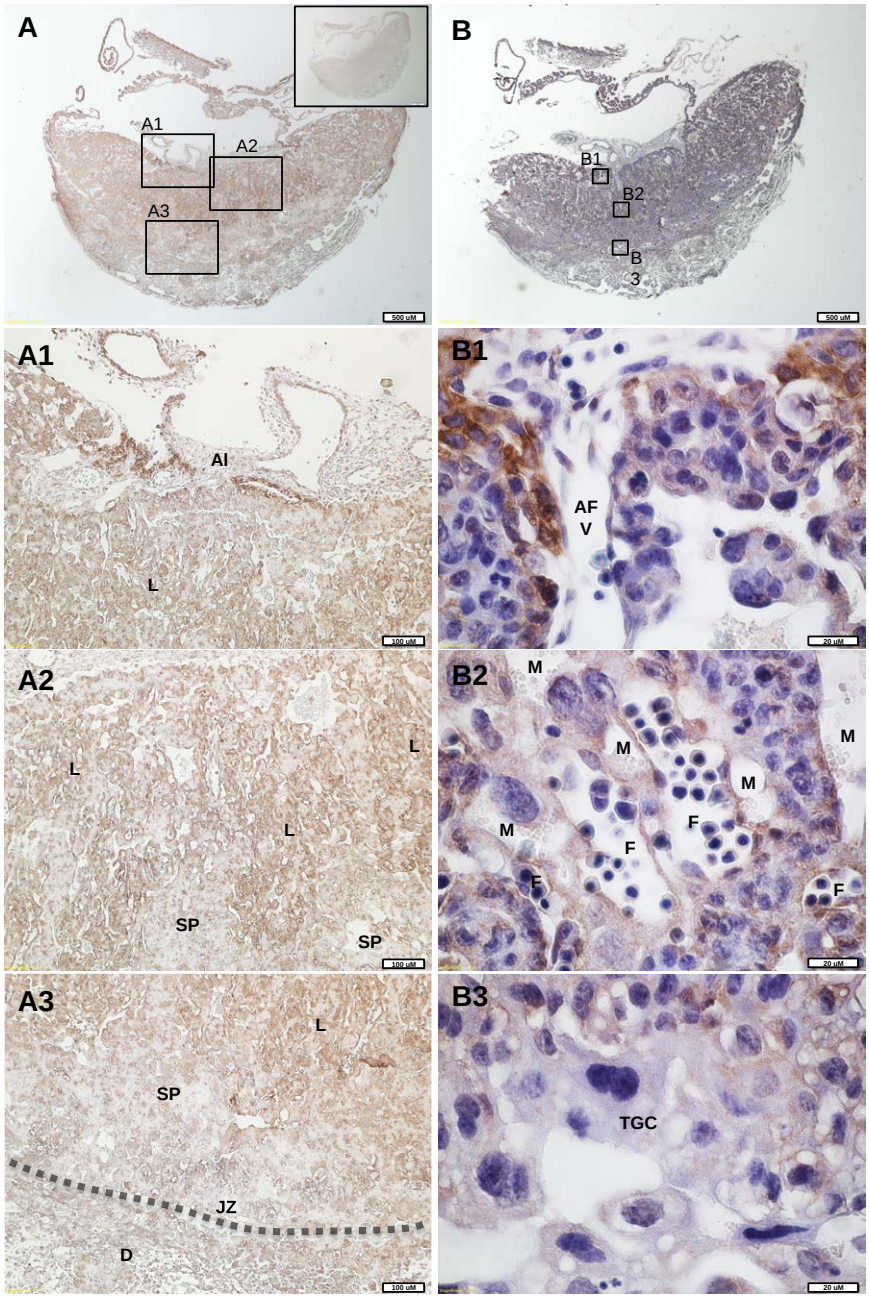

Figure 13. LIN28A in E11.5 mouse placenta.

A) E11.5 mouse placenta stained for LIN28A (2X). Boxed areas represent areas of (10X) magnification depicted in figures A1-A3. Inset shows preabsorbed control. B) E11.5 mouse placenta stained for LIN28A and counterstained with hematoxylin (2X). Boxed areas represent areas of (60X) magnification depicted in figures B1-B3. Allantois (Al), labyrinth layer (L), spongiotrophoblast (SP), junctional zone (JZ and dashed line), decidua (D), allantoic-derived fetal vessel (AFV), maternal vessel (M), fetal vessel (F), trophoblast giant cell (TGC).

LOSS OF LIN28A MRNA IN MOUSE TROPHOBLAST CELLS.

To determine the role of LIN28 in mouse trophoblast stem cell differentiation and function, a *Lin28a* mRNA knockdown (KD) mTS cell line was created. Decreased levels of LIN28A protein was confirmed in *Lin28a* KD mTS cells via western blot (Figure 14 A). Densitometry analysis of the western blot data demonstrated a 86% reduction of LIN28A in *Lin28a* KD mTS cells, compared to a 95% reduction of LIN28A observed in mTGC after six days without FGF4, heparin and conditioned medium. *Lin28a* KD mTS cells resulted in increased levels of *let-7* miRNA similar to mTGC differentiated for six days without FGF4, heparin or conditioned medium (Figure 14 B). These miRNA data suggest that 86% loss of LIN28A is sufficient to induce a comparable increase in the levels of *let-7* miRNA as is achieved by removal of FGF4, heparin and fibroblast-conditioned medium. Notably, when *Lin28a KD* mTS cells were induced to differentiate by the removal of FGF4, heparin and conditioned medium, *let-7a, let-7d and let-7g* miRNA levels exceeded the levels observed in non-target control cells (Figure 14 C). Despite losses of LIN28A mRNA and protein, increases in *let-7* miRNA, and an apparent increased capacity for *let-7* miRNA responsiveness, *Lin28a* KD mTS cells did not demonstrate increased levels of spontaneous differentiation, or loss of proliferative capacity over 15 passages in proliferative culture conditions (Figure 15).

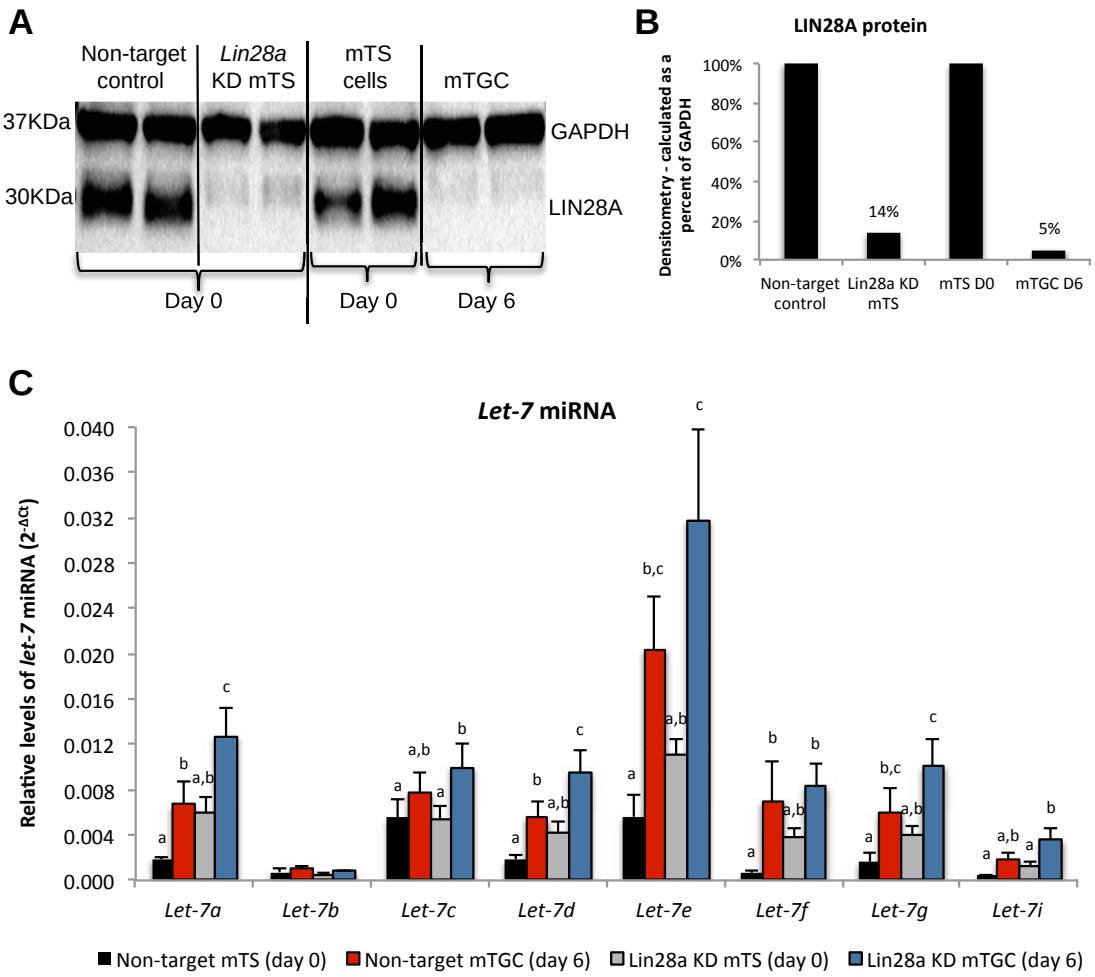

Figure 14.shRNA-mediated *Lin28a* knockdown in mTS cells results in increased levels of *let-7* miRNA.

A) LIN28A protein levels in *Lin28a* KD and non-target control mTS cells (columns 1-4) in relation to mTS cells at day 0 and after six days in differentiation medium (columns 5-8). Densitometry analysis of LIN28A protein bands: calculations made as a percent of GAPDH protein. B) Densitometry analysis of western blot. C) Levels of *let-7* miRNA in *Lin28a* KD and non-target control mTS cells, and mTS cells collected at day 0 and after six days in differentiation medium.

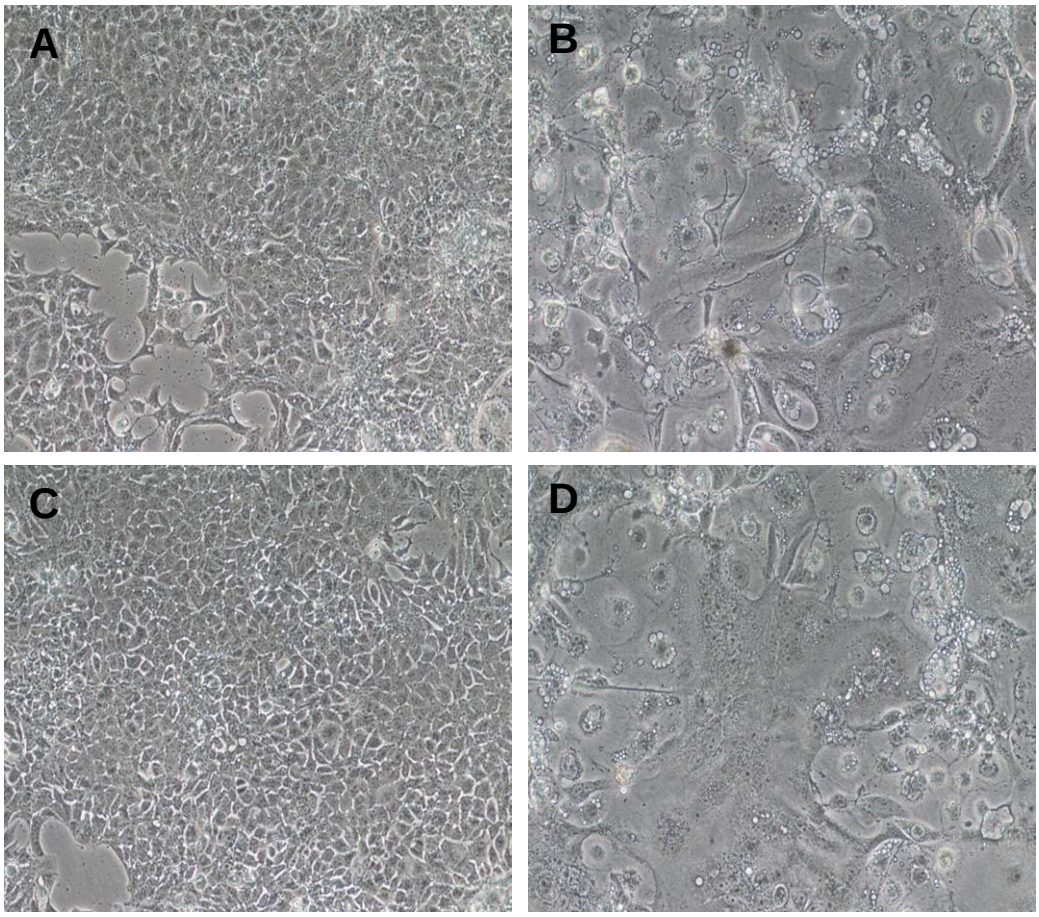

Figure 15.mTS cell morphology.

Brightfield microscopy (20X). A) Proliferative mTS morphology of non-target control mTS cells at day 0, and (B) the expected mTGC morphology after six days in differentiation medium. C) *Lin28a* KD mTS cells had a proliferative morphology at day 0 and (D) mTGC morphology after six days in differentiation medium.

LIN28A mRNA AND PROTEIN IN CULTURED HUMAN TROPHOBLAST CELLS.

The immortalized first-trimester human trophoblast cell line, ACH-3P, was used to determine if LIN28 had a role in regulating human trophoblast differentiation and function. ACH-3P cells were treated with 40 uM forskolin to induce differentiation, and responded with a 6-fold increase in soluble hCG-beta in culture medium compared to

DMSO controls, demonstrating that forskolin treatment was effective at inducing differentiation of ACH-3P (Figure 16 A). Forskolin-induced differentiated cells had decreased LIN28A mRNA and protein (24%, 62%, respectively, $P < 0.05$) compared to DMSO treated controls (Figure 16 B-D).

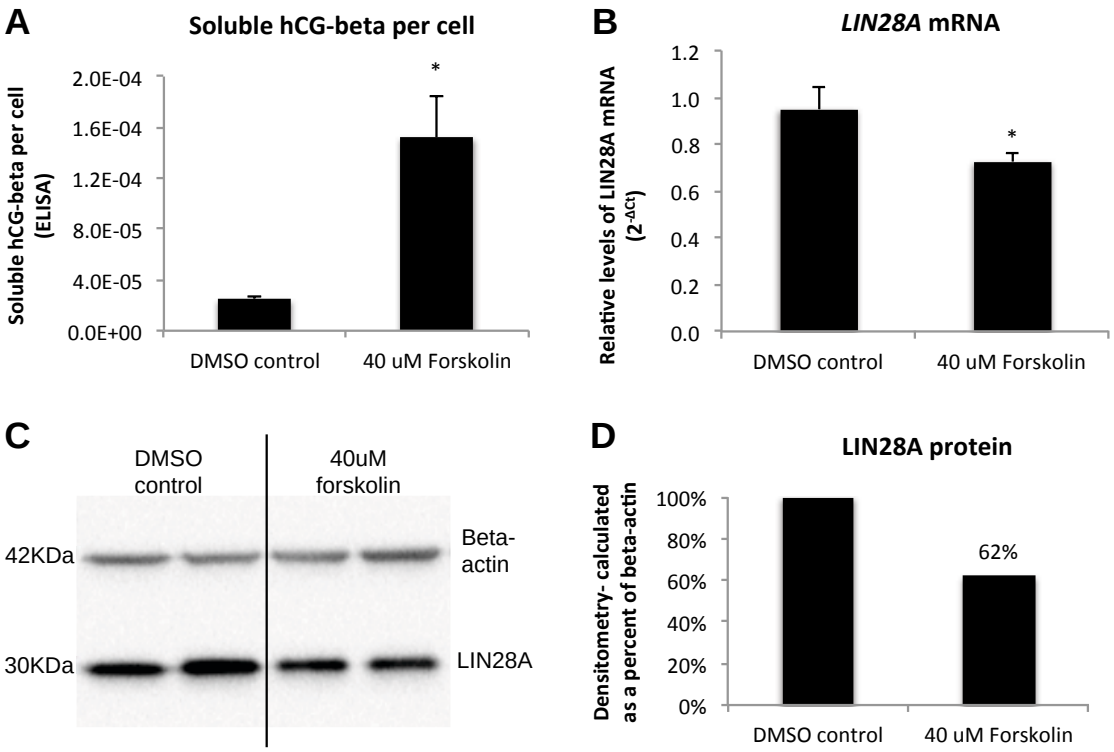

Figure 16.LIN28A response to forskolin-induced differentiation.

A) ELISA analysis of LIN28A in cell culture medium. B) *LIN28A* mRNA (qPCR). C-D) LIN28A protein and densitometry analysis.

To determine if loss of *LIN28A* was sufficient to induce differentiation in human trophoblast, a *LIN28A* KD ACH-3P cell line was established. *LIN28A* mRNA KD resulted in a 96% reduction of *LIN28A* mRNA ($P < 0.01$) and 95% reduction in protein (densitometry not shown) compared to non-target control ACH-3P cells (Figure 17 A-B).

The resulting *LIN28A* KD ACH-3P cells had increased levels of miRNAs *let-7c, let-7d* and *let-7e* ($P < 0.05$) (Figure 17 C).

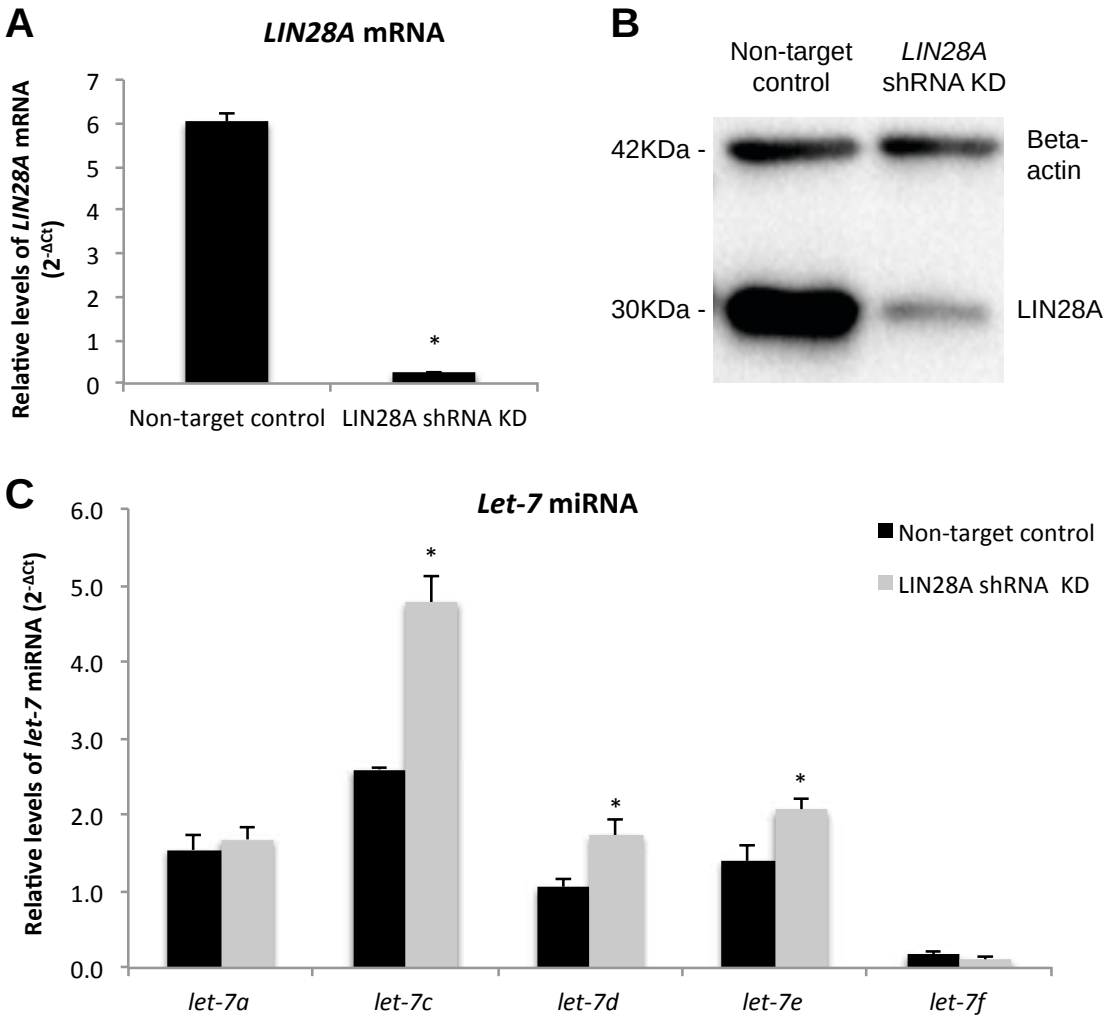

Figure 17.LIN28A and *let-7* miRNA in *LIN28A* KD ACH-3P cells.

A-B) LIN28A mRNA (qPCR) and protein. C) *let-7* miRNA in *LIN28A* KD ACH-3P cells.

ELISA analysis of culture medium collected from *LIN28A* KD ACH-3P cells had 13-fold ($P < 0.01$) increased per-cell concentrations of soluble hCG-beta (Figure 18 A), as well

as an increased hCG-beta immunostaining (Figure 18 C-D) compared to non-target control cells. The increased level of hCG protein was accompanied by elevated levels of mRNA for both the alpha (*CGA*) and beta (*CGB*) polypeptide subunits (1.8-, 3.5-fold, respectively, $P < 0.01$) compared to non-target control cells (Figure 18 B).

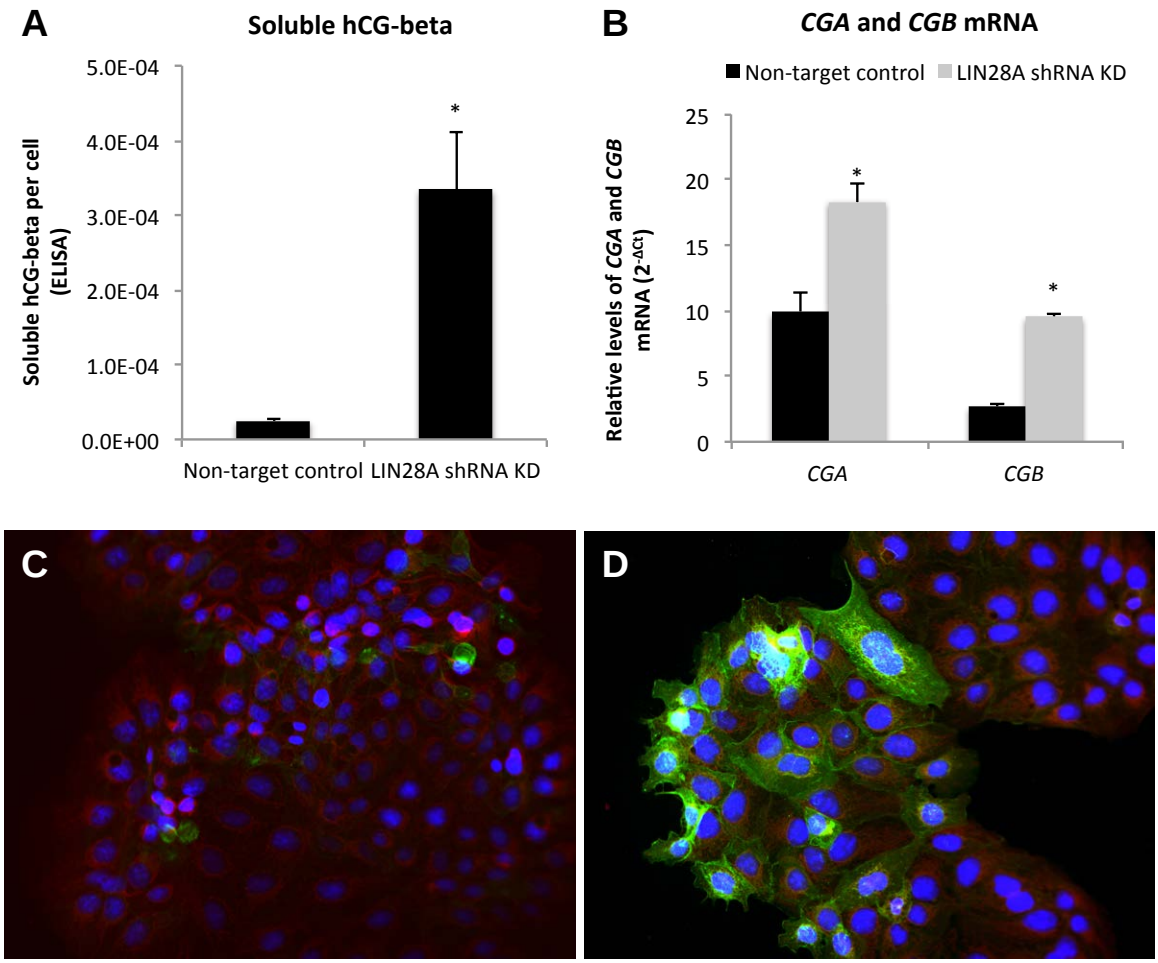

Figure 18.hCG in *LIN28A* KD ACH-3P cells.

A) ELISA analysis of LIN28A in culture medium from *LIN28A* KD ACH-3P cells. B) Levels of *CGA* and *CGB* mRNA (qPCR) compared to non-target control ACH-3P cells. C-D) Immunofluorescence (20X); red, plasma membrane; blue, nuclei; green, hCG-beta.

In addition to increased hCG production, *LIN28A* KD ACH-3P cells had 6-fold higher levels of *LGALS13* mRNA ($P < 0.01$), a syncytiotrophoblast-specific marker (Figure 19 A), 3.5-fold increased levels of *ERVW-1* mRNA, which encodes for the fusion protein syncytin-1 ($P < 0.01$) (Figure 19 B), as well as increased morphological differentiation characterized by an increased spontaneous formation of large multinucleated syncytial plaques (Figure 19 C-D). These data suggest that LIN28 may contribute to the regulation of human trophoblast differentiation into the syncytiotrophoblast sub-lineage.

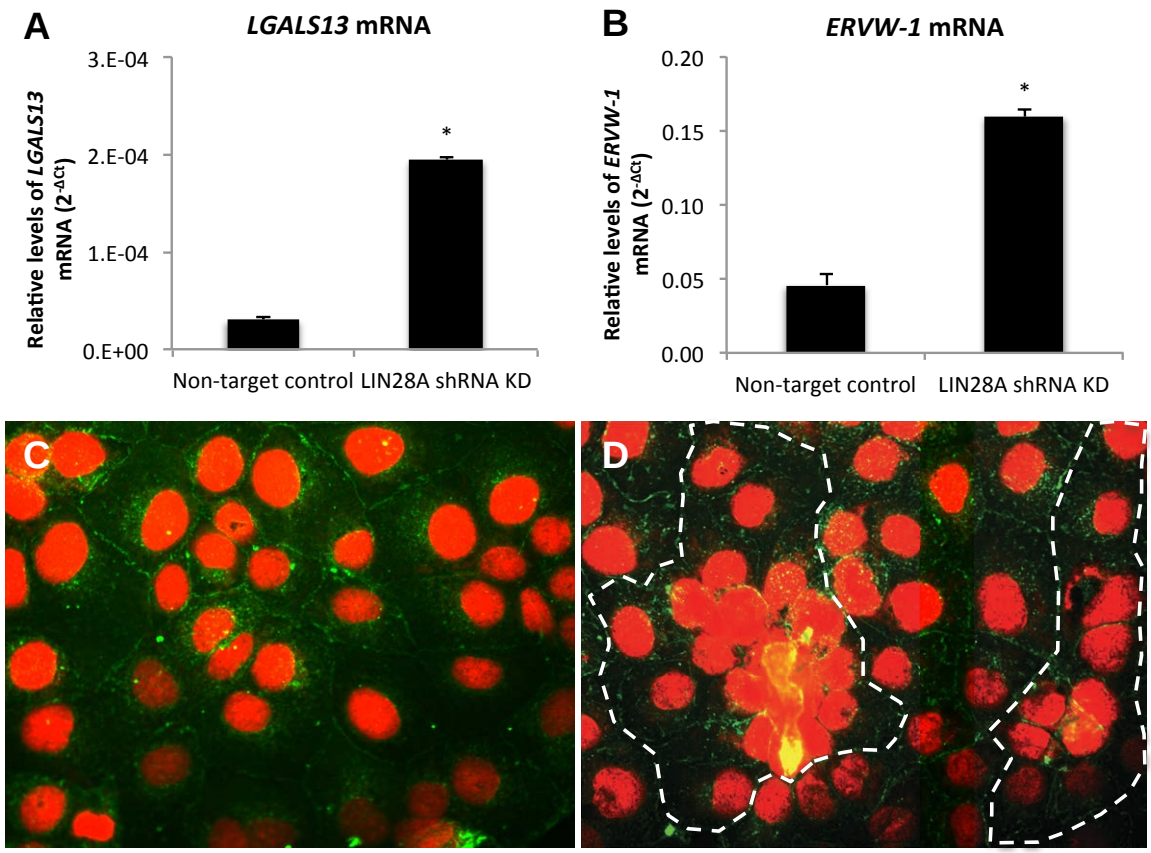

Figure 19.Spontaneous syncytialization in *LIN28A* knockdown in ACH3P cells.

A-B) *LGALS13* and *ERVW-1* mRNA (qPCR) in *LIN28A* KD ACH-3P cells. C-D) Immunofluorescence; red, nuclei; green, plasma membrane; dashed line signifies boundary of multinucleated cell plaque.

Finally, *LIN28A* KD ACH-3P cells treated with 40 uM forskolin had additional losses of *LIN28A* mRNA ($P < 0.01$) (Figure 20 A). While levels of *ERVW-1* mRNA did not increase in *LIN28A* KD ACH-3P cells treated with 40 uM forskolin (Figure 20 B), levels of *LGALS13* mRNA increased an additional 15-fold ($P < 0.01$) (Figure 20 C), and soluble hCG in the culture medium rose an additional 7-fold ($P < 0.01$) over DMSO controls (Figure 20 D). These data suggest that, like *Lin28a* KD mTS cells, *LIN28A* KD ACH-3P cells have an increased potential for differentiation.

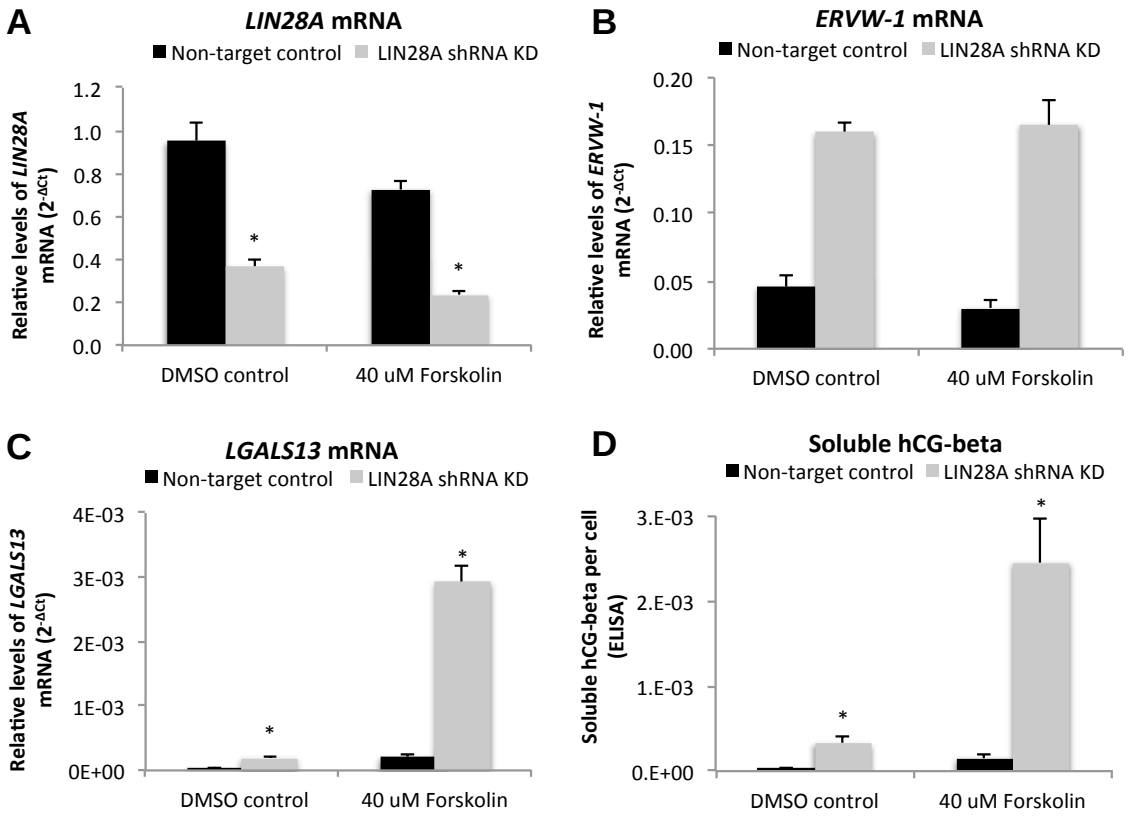

Figure 20.Differentiation markers in *LIN28A* KD ACH-3P cells treated with forskolin.

A-C) *LIN28A, ERVW-1* and *LGALS13* mRNA (qPCR) in *LIN28A* KD ACH-3P treated with 40 uM forskolin. ELISA analysis of hCG-beta in cell culture medium of *LIN28A* KD ACH-3P cells treated with forskolin.

DISCUSSION

Proper regulation of trophoblast proliferation, differentiation and function are the fundamental mechanisms supporting proper placenta development and function. However, ethical dictates limit the extent to which human pregnancy is studied, so surrogate models are often necessary to understand trophoblast function. Human embryonic stem cells (hESC) are one such model, and have been used to understand the molecular mechanisms regulating the initial differentiation of trophectoderm and subsequent differentiation events resulting in trophoblast cell lineages [201-203]. To

date, LIN28 has been demonstrated to be a potent regulator of pluripotency in hESC, regulating the initiation of differentiation down embryonic cell lineages [147, 149, 165, 188]. Conservation of LIN28 expression and function in trophoblast stem progenitors demonstrates there is a fundamental role for LIN28 in the regulation of trophoblast pluripotency and differentiation, and ultimately in placenta development.

Our data demonstrate that LIN28 is present in mouse placenta tissue, as well as mouse and human trophoblast cells, suggesting that in addition to being a potent regulator of pluripotency in hESC, there may be a conserved functional role for LIN28 in trophoblast differentiation. Our qPCR data found *Lin28a* mRNA to be significantly decreased, and *let-7* miRNA to be significantly increased in mouse trophoblast giant cells (mTGC) compared to proliferative trophoblast stem cells (mTS). Western blot assessment of LIN28A in cultured mTS cells confirmed qPCR data, suggesting that trophoblast differentiation was a LIN28-regulated event, and that it was possibly acting through *let-7* miRNA mediated pathways similar to those observed in ES cells [147, 192, 193].

Using immunohistochemistry assessment of serial sections of mid-gestational mouse placenta we found distinct LIN28A immunostaining in the fetal membranes, along the chorioallantoic interface, and throughout the labyrinth layer, suggesting these areas may maintain progenitor cell populations. Our data is consistent with observations made by Yang and Moss (2003), who noted that early gestational mouse trophoblast and yolk epithelium were positive for LIN28 [177]. In the mouse, labyrinthine differentiation

begins at embryonic day 8.5 when the chorionic and allantoic layers come together to form a trilaminar structure composed of mononuclear trophoblast giant cells in direct contact with maternal blood, overlaying two layers of multinucleated syncytiotrophoblast layers [204, 205]. Co-culture of trophoblast cells with allantois has demonstrated a direct effect on trophoblast morphological differentiation [205], suggesting these tissues have a direct role in regulating trophoblast differentiation and function. Our observation that LIN28A is present along the chorioallantoic interface and throughout the labyrinth layer suggest that continued expression of pluripotency factors such as LIN28 may be necessary for continued trophoblast differentiation and remodeling through mid-gestation. Additionally, the mid-gestation chorio-allantoic interface has been reported to be the site of hematopoietic progenitor stem cells [206, 207], suggesting that pluripotency factors such as LIN28 may be functioning to maintain stem cell progenitor niches in these tissues. Decreased levels of LIN28A immunostaining in the spongiotrophoblast, and the mTGC along the junctional zone suggest that, by mid-gestation, these cells have undergone terminal differentiation [208].

Our *Lin28a* KD mTS cell line demonstrates that LIN28A inhibits *let-7* miRNA in trophoblast cells, as demonstrated in human ES cells [209]. However, despite significant decreases in *Lin28a* mRNA and concomitant increases in *let-7* miRNA, mTS cell proliferation or differentiation was not affected. This suggests that while decreased levels of LIN28A and increased levels of *let-7* miRNA may be necessary for differentiation to proceed, it is not sufficient to induce differentiation in mTS. It is

important to note that FGF4, heparin and embryonic fibroblast-derived growth factors present in the proliferative culture medium are potent regulators of the cell cycle, and may act to prevent mTGC differentiation, and their presence in the mTS culture medium may ultimately override any effects resulting from the loss of *Lin28a*.

While *Lin28a* KD mTS cells did not exhibit a phenotypic change, when we applied the same strategy for *LIN28A* mRNA KD in the ACH-3P cells, increased levels of *let-7* miRNA were accompanied by increased levels of spontaneous biochemical and morphological differentiation. Differentiation was characterized by increased levels of human chorionic gonadotropin (hCG), syncytiotrophoblast-specific *LGALS13* mRNA, and *ERVW-1* mRNA (the transcript encoding for the fusion protein, syncytin-1), and the spontaneous formation of large multinucleated cell plaques. These data suggested that *LIN28A* KD was inducing ACH-3P cells to differentiate toward the syncytiotrophoblast trophoblast sub-lineage.

Despite the increased levels of spontaneous syncytialization, the *LIN28A* KD ACH-3P cells continued to passage, suggesting that loss of *LIN28A* and increased levels of *let-7* miRNA, were not sufficient to completely suppress proliferation. However, when *LIN28A* KD ACH-3P cells were treated with forskolin, LIN28A levels decreased further and syncytiotrophoblast markers, hCG, and *LGALS13* mRNA increased substantially beyond the levels observed in forskolin-treated non-target controls. This increased differentiation potential in the *LIN28A* KD ACH-3P cells was similar to what we observed

in the *Lin28a* KD mTS cells, suggesting that LIN28A was acting to inhibit trophoblast differentiation, rather than directly initiate differentiation. These data are consistent with data presented by Yu et al. (2007), which demonstrated that overexpression of *Lin28* alone was not sufficient for initiating retrodifferentiation into iPSC or for maintaining resulting colonies, but improved the frequency of iPSC reprogramming events [147].

It is important to note that LIN28 has been shown to directly regulate mRNA translation efficiency, stimulating the translation of the growth factor IGF2, pluripotency factor OCT4, and a number of genes important for cell-cycle regulation including histone H2a, cdk4 and cyclins A and B [166-171]. This would suggest that LIN28A likely has regulatory roles independent of *let-7* miRNA-mediated pathways, and may act in concert with a number of factors to regulate trophoblast differentiation. Such *let-7* miRNA-independent regulatory pathways may explain the differences in effects observed between human and mouse trophoblast cell lines.

Our data demonstrate that LIN28A is present in the mouse placenta and may have a conserved functional role in the regulation of human and mouse trophoblast differentiation into the sub-lineages vital for proper placenta development. We conclude from these data that LIN28A likely acts in concert with a number of factors to regulate the progression of trophoblast differentiation through *let-7* miRNA dependent and independent pathways, and that loss of *LIN28* results in an increased potential for trophoblast differentiation to proceed, rather than actively initiating differentiation (Figure

21). While this study provides evidence for LIN28's role in the regulation of trophoblast differentiation, additional experiments are needed to determine the mechanisms of LIN28 regulation of trophoblast, and how LIN28 contributes to placenta development and health.

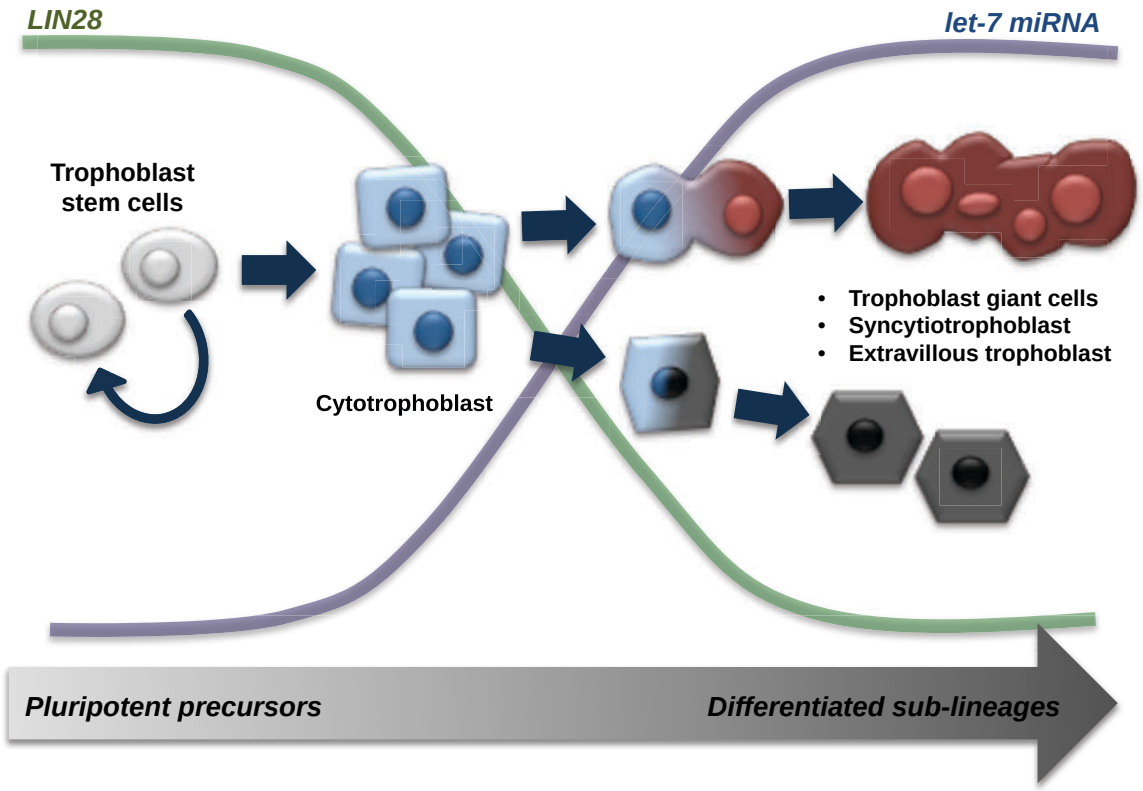

Figure 21.Proposed mechanism for LIN28 regulation of trophoblast cell differentiation.

LIN28 functions to maintain pluripotency in proliferative trophoblast progenitors, suppressing *let-7* miRNA inhibition of mRNA and supporting translational activation of downstream targets. As LIN28 decreases with differentiation, *let-7* miRNA are allowed to mature suppressing downstream mRNA targets. Additionally, translational activation directly mediated by LIN28 binding target mRNA is lost. Consequently, inhibition to differentiation is removed, and cells progressively differentiate into trophoblast sub-lineages.

CHAPTER IV: LIN28A AND LIN28B IN TROPHOBLAST CELLS AND PLACENTA TISSUE

INTRODUCTION

In the human, *LIN28A* and *LIN28B* genes are transcribed from different chromosomes (chromosomes 1 and 6, respectively), resulting in 4014 bp and 5517 nt mRNA sequences. Despite dissimilarities between the gene transcripts, they retain a high degree of structural and functional homology at the protein level [156]. Both genes encode for two RNA-binding domains, a cold-shock domain (CSD), and a zinc-knuckle domain consisting of two cys-cys-his-cys (CCHC) zinc-fingers [141]. While LIN28A and LIN28B have a high degree of homology, there are some distinct differences. LIN28B contains two nuclear localization signals, one in an extended C-terminus (KKGPSVQKRKKK) and another in the linker region between the two RNA binding domains (RRPKGKTLQKRKPK), which may result in differential localization and ultimately distinct functional mechanisms [157]. Additionally, LIN28B has a greater degree of variability across species, translating into a 250 aa protein, a 253 aa protein, or a 271 aa protein, in the human, mouse and sheep, respectively. Additionally, three LIN28B variants have been described for mouse (Isoform CRA_a, Isoform CRA_b, and Isoform CRA_c, 233, 281 and 96 aa, respectively), and one variant each for human and sheep, 227 aa, 267 aa, respectively. Variant LIN28B proteins in mouse and human are characterized by the addition of amino acids at the N-terminus of the protein sequence. In contrast, the sheep LIN28B variant has additional amino acids inserted at the

beginning of the first zinc-finger domain. Ultimately, these variations could affect localization and function, suggesting LIN28B may have different regulatory functions across species. To date, LIN28 has been described to have two distinct regulatory roles: the regulation of *let-7* miRNA maturation, and the post-transcriptional regulation of target mRNA.

The impetus for looking at LIN28A in the placenta arose from a microarray comparing proliferating mouse trophoblast (mTS) cells to differentiated mouse trophoblast giant cells (mTGC). During the transition from proliferative mTS to mTGC, *Lin28a* was significantly downregulated, whereas *Lin28b* was not only much less abundant, but levels of *Lin28b* did not change due to the differentiation to mTGC. Consequently, our initial focus, and the data we collected for Chapter III, was on LIN28A. However, while *Lin28b* levels were low in mTS, and did not seem to have a regulatory role in mTS cell differentiation, we found that LIN28B levels in the human trophoblast cells lines were significantly higher than LIN28A. These data suggested that LIN28B may have a functional role in the regulation of human trophoblast differentiation distinct from the regulation observed in mTS cell differentiation. Therefore, we wanted to determine the relationship between LIN28A and LIN28B, and determine any functional species differences important for the regulation of trophoblast proliferation and differentiation.

Additionally, through collaboration with Dr. Russ Anthony, we obtained access to *ex vivo* first trimester placenta tissue, term placenta tissue and IUGR term placenta tissue. This

provided us the opportunity to assess LIN28A and LIN28B in primary human placenta tissue, both under normal and pathologic physiologic states.

MATERIALS AND METHODS

All animal experiments were performed in accordance with protocols approved by the Colorado State University Institutional Animal Care and Use Committee.

CELL LINES.

The following human trophoblast cell lines were grown in F-12 Medium (10% FBS, 2 mM L-glutamine, antibiotic-antimycotic solution containing 10,000 IU/mL penicillin, 10,000 ug/mL streptomycin, 25 ug/mL amphotericin): ACH-3P (a generous gift from Ursula Hiden, Medical University of Graz, Austria) [29], HTR-8/SVneo [30], BeWo [28] and Swan 71 (a generous gift from Gil Mor, Yale University School of Medicine, New Haven, CT) [34]. Cells were induced to differentiate into syncytiotrophoblast by treatment with 40 uM forskolin for 48 hours; forskolin is known to induce morphological fusion of cultured trophoblast cells, which closely resembles morphology of natural syncytiotrophoblast [195]. Cells were induced to invade by plating on Matrigel Basement Membrane Matrix diluted with serum-free culture medium (6 mg/mL) (product no. 354234; BD Biosciences, Bedford, MA) for a period of 48 hours.

Mouse trophoblast cells (mTS) were derived from blastocyst-stage embryos at 3.5 days postcoitum (dpc) from naturally bred Black Swiss female mice, using techniques previously described [27, 194]. Briefly, mouse blastocysts were collected and cultured

on a feeder layer of mitomycin-C treated mouse embryonic fibroblasts. Trophoblast stem cell colonies were isolated from blastocyst outgrowths and separated from feeder fibroblasts through serial passage. Isolated mTS cells were maintained in 70% mouse embryonic fibroblast conditioned medium and 30% TS medium (RPMI 1640, 2 mM L-glutamine, 30% FBS, 1mM sodium pyruvate, 100uM β-mercaptoethanol, antibiotic-antimycotic solution containing 10,000 IU/mL penicillin, 10,000 ug/mL streptomycin, 25 ug/mL amphotericin) supplemented with 25 ng/mL FGF4 and 1 ug/mL heparin. mTS cell differentiation into mouse trophoblast giant cells (mTGC) was induced by removal of conditioned medium, FGF4 and heparin for six days.

REAL-TIME RT-PCR.

Total RNA was extracted from cells using miRNA Mini Kit (Qiagen, Valencia, CA) according to manufacturer's directions. For mRNA analysis, cDNA was generated from 1 ug of total cellular RNA using qScript cDNA Supermix (product no. 95048; Quanta Biosciences, Gaithersburg, MD) and quantitative real-time RT-PCR (qPCR) of mRNA was performed as described previously [194]. Briefly, each 1X 20 uL qPCR reaction consisted of 10 uL LightCycler 480 Probes Master mix (product no. 04707494001; Roche, Mannheim, Germany), 1 uL of 150 nM TaqMan Gene Expression Assay (Applied Biosystems, Carlsbad, CA) and 9 uL of cDNA template diluted to 90 uL. qPCR was performed using the Light Cycler 480 thermal cycler (Roche) with the following parameters: 10 minute pre-incubation at 95 °C, 45 cycles of amplification which included denaturation at 95°C for 10 seconds, annealing at 60°C for 30 seconds and extension at 72°C for 1 second, followed by a final cooling cycle at 40°C for 5 min. Normalization of

mRNA was using the geometric mean of TATA box biding protein mRNA (*TBP)* and mitochondrial ribosomal protein S15 mRNA (*MRPS15)*.

Relative expression was determined for all qPCR data using the comparative Ct method [196]. Statistics: We used Student's t-test to compare relative expression of genes between treatments.

WESTERN BLOT.

Cellular protein was assessed by western blot analysis, similarly to procedures described previously [194, 197, 198]. Briefly, cells were lysed in RIPA buffer (20 mM Tris, 137 mM NaCl, 10% glycerol, 1% Nonidet P-40, 3.5 mM SDS, 1.2 mM sodium deoxycholate, 1.6 mM EDTA, pH 8) supplemented with 10% protease/phosphatase inhibitor cocktail (product no. P8340; Sigma-Aldrich, St. Louis, MO), and 1 mM phenylmethanesulfonyl fluoride (PMSF). Protein concentration was determined using the Bradford assay method [199]; absorbance was measured at λ 595 nm using the Biotek Synergy 2 Microplate Reader (Biotek, Winooski, VT). Protein was electrophoresed through 4-12% Bis-Tris gels, then transferred to 0.45 um pore nitrocellulose membrane at a constant 100 V on ice for one hour. Membranes were blocked in 10% milk-TBST (50 mM Tris, 150 mM NaCl, 0.05% Tween 20, pH 7.6) overnight at 4°C to reduce non-specific binding, then incubated with primary antibody at ambient temperature for two hours. Membranes were washed in TBST, and then incubated with a horseradish peroxidase-conjugated secondary antibody for one hour at ambient temperature. For assessment of LIN28 protein, a polyclonal antibody to LIN28A

(1:1000 dilution; product no. ab63740; Abcam, Inc., Cambridge, MA), and a polyclonal antibody to LIN28B (1:1000 dilution; product no. A303-589A; Bethyl Laboratories, Inc., Montgomery, TX) were used in conjunction with horseradish peroxidase-conjugated secondary antibodies (1:2000 dilution; product no. sc-2004; Santa Cruz Biotechnology, Inc., Dallas, TX). An antibody to beta-actin (1:2000 dilution; product no. sc-47778; Santa Cruz Biotechnology, Inc.), or an antibody to GAPDH (1:2000 dilution; product no. ab37168; Abcam, Inc.), was used in conjunction with horseradish peroxidase-conjugated secondary as loading control and to normalize LIN28 protein in cell lysates (1:2000 dilution; product no. 1858413; Pierce, Rockford, IL; or 1:2000 dilution; product no. sc-2004; Santa Cruz Biotechnology). Membranes were developed using ECL Western Blotting Detection Reagent chemiluminescent kit (product no. RPN2132; Amersham, Pittsburgh, PA), and membranes were imaged using the ChemiDoc XRS+ chemiluminescence system (BioRad, Hercules, CA). Densitometry calculations were performed using the Image Lab Software (BioRad). Fold change was calculated as a percent of non-target control protein after normalization.

LIN28 KNOCKDOWN.

Stably transduced *LIN28A and LIN28B* mRNA knockdown (KD) and non-target control cell lines were created using commercially available MISSON shRNA Lentiviral Transduction Particles, lentiviral based pLKO.1-puro vectors (Sigma-Aldrich). The pLKO.1-puro vectors used contained an shRNA sequence cassette downstream of a modified U6 shRNA promoter and a puromycin resistance gene for selection downstream of a human phosphoglycerate kinase (hPGK) eukaryotic promoter. The

lentiviral based pLKO.1-puro vector used to knockdown *LIN28A* in cells contained an shRNA sequence designed to target human *LIN28A mRNA* (clone no. TRCN0000021802; Sigma-Aldrich), or *LIN28B* mRNA (clone no. TRCN0000122599; Sigma-Aldrich) for degradation (see Table 2). Non-target control cell lines were created using a pLKO.1-puro vector with an shRNA sequence designed to target no known mammalian genes (product no. SHC002V; Sigma-Aldrich) (see Table 2). Cells were infected in three replicate experiments with either the *LIN28* mRNA targeted particles or the non-target control particles at a MOI of 500 viral particles per cell. Infected cells were selected by treatment with 8 ug/mL puromycin for 14 days or until all untreated control cells were dead. The degree of LIN28 mRNA and protein knockdown was determined by qPCR and western blot, as described previously.

Table 2. shRNA clone sequences

hLIN28A	CCGGACCTACTTTCGAGAGGAAGAACTCGAGTTCTTCCTCTCGAAAGTAGGTTTTTT
hLIN28B	CCGGGCCTTGAGTCAATACGGGTAACTCGAGTTACCCGTATTGACTCAAGGCTTTTTTG
Non-target	CCGGGCGCGATAGCGCTAATAATTTCTCGAGAAATTATTAGCGCTATCGCGCTTTT

LIN28 OVEREXPRESSION.

A stably transduced *LIN28A* overexpressing ACH-3P cell line was created using commercially available Lentiviral Transduction Particles, designed to natively express the full human *LIN28A* coding sequence under a suCMV promoter, and a blasticidin resistance gene and red fluorescent protein (RFP) selection marker downstream of a RSV promoter (product no. SC-022; BioPioneer Inc., San Diego, CA). A control ACH-3P

cell line was created using the RFP control lentivial particles expressing codon optimized RFP under suCMV promoter, and a blasticidin gene under PGK promoter (product no. SC-030; BioPioneer).

ELISA.

Non-target and LIN28 KD cells were plated in 6-well culture dishes with 25,000 cells per well and six replicates per treatment. Cell culture medium (1.5 mL/replicate) was collected after 48 hours, and cells were collected and counted. Concentrations of hCG were quantified using an hCG ELISA kit utilizing a mouse monoclonal anti-hCG (specific to beta-hCG) conjugated to horseradish peroxidase according to manufacturer's instructions (product no. 25-HCGHU-E01; ALPCO Diagnostics, Salem NH).

Experimental replicates were assayed in triplicate, and absorbance was measured at λ 450 nm. Soluble hCG concentrations (mIU/mL) were calculated by plotting sample mean absorbance values against the mean values calculated from duplicate standard curve values. The standard curve consisted of 0, 5, 20, 50, 150 and 300 mIU/mL hCG standards. We used the Student's t-test to compare hCG concentrations between non-target controls and *LIN28* KD cell medium. P-values of less than 0.05 were considered to be statistically significant.

IMMUNOHISTOCHEMISTRY.

Term human placentas were collected as described previously, and in accordance with the Committee of Ethics, Medical University of Bialystok, Bialystok, Poland [210]. Immunohistochemistry was performed as previously described [197]. Briefly: 6 micrometer sections were cut, sections were dewaxed in xylene and rehydrated through serial ethanol dilutions, then treated with 3% H_2O_2 to reduce endogenous peroxidase activity. Sections were blocked in SuperBlock Blocking Buffer (product no. 37580; ThermoScientific, Waltham, MA) overnight at 4°C to reduce non-specific binding. Sections were incubated with an antibody to LIN28A (dilution 1:1000; product no. ab63740; Abcam), or LIN28B (dilution 1:1000; product no. A303-589A; Bethyl Laboratories, Inc.) overnight at 4°C (1:200 dilution; product no. ab63740; Abcam, Inc.). For negative controls, primary antibody was either withheld and/or preabsorbed with antibody-specific synthetic antigen (LIN28A: 2:1 ratio; product no. ab64578; Abcam, Inc.; LIN28B: 5:1 ratio; product no. A303-589BP; Bethyl Laboratories, Inc.). The VectaStain Elite ABC Kit (Rabbit IgG) biotinylated anti-rabbit secondary antibody was used according to manufacturer's directions, and positive immunostaining was visualized using the avidin-biotin complex (ABC) system (product no. PK-6101; Vector Laboratories, Burlingame, CA). Diaminobenzedine (DAB) was used as the final chromogen (product no. SK-4100; Vector Laboratories) and propidium iodide (60 ug/mL) was used to counterstain.

miRNA mimic.

Cells were treated with the following miScript miRNA mimics in conjunction with HiPerFect transfection reagent according to manufacturer's directions (Qiagen) (see Table 3).

Table 3. miRNA mimic sequences

hsa-miR-9	UCUUUGGUUAUCUAGCUGUAUGA
hsa-miR-30b	UGUAAACAUCCUACACUCAGCU
hsa-miR-125a	UCCCUGAGACCCUUUAACCUGUGA
hsa-miR-1	UGGAAUGUAAAGAAGUAUGUAU

Briefly, 15,000 cells were plated to 24-well culture dishes and treated twice, at 24 hour intervals, for a period of 72 hours with a 1X reaction consisting of 100 uL serum-free culture medium, 6 uL HiPerFect transfection reagent, and 1 uL of miRNA mimic (1 nM).

RESULTS

Levels of LIN28A and LIN28B in human trophoblast cell lines

Levels of LIN28A and LIN28B varied between cell lines. HTR-8/SVneo and ACH-3P cell lines had higher levels of *LIN28A* mRNA compared to *LIN28B* mRNA, BeWo cells had higher levels of *LIN28B* mRNA compared to *LIN28A* mRNA, and Swan 71 cells had higher levels of *LIN28A* mRNA, however compared to the other cell lines, Swan 71 cells had low levels of both *LIN28A* and *LIN28B* mRNA (Figure 22 A). LIN28A levels were confirmed by western blot (Figure 22 B).

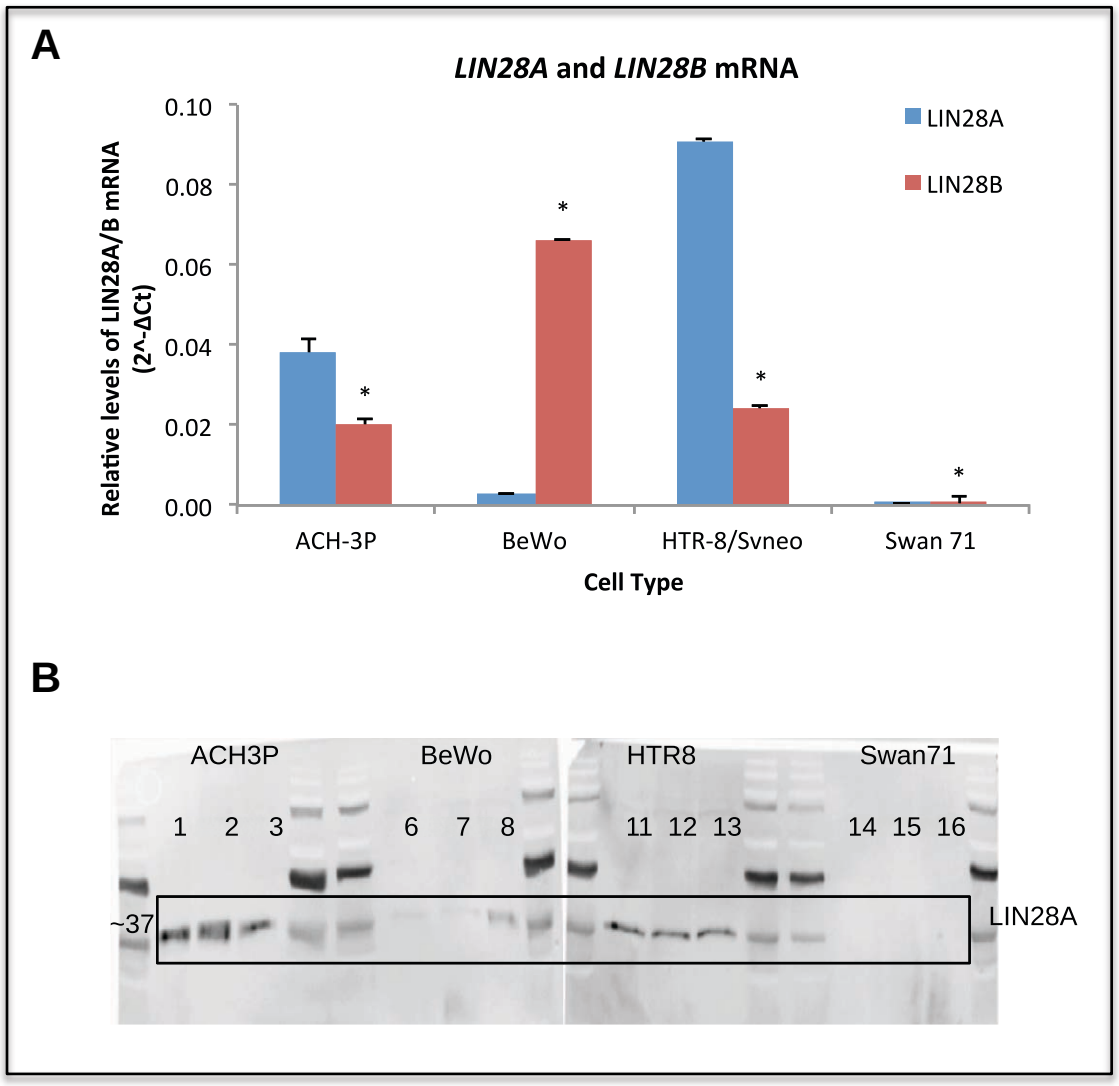

Figure 22. LIN28 in immortalized human trophoblast cell lines.

A) Levels of *LIN28A* and *LIN28B* mRNA in human trophoblast cell lines (qPCR). B) Levels of LIN28A protein in human trophoblast cell lines (western blot).

LIN28A AND *LIN28B* IN PRIMARY HUMAN PLACENTA TISSUE

Levels of LIN28B mRNA and protein were higher than levels of LIN28A in first-trimester human placenta tissue. (Figure 23 A-D). Levels of *LIN28B* mRNA were higher than *LIN28A* mRNA in term placenta tissue (Figure 23 E-F). Additionally, levels of *LIN28A*

and *LIN28B* mRNA were lower in tem placenta tissue from IUGR pregnancies compared to normal controls, suggesting deregulated *LIN28A* and *LIN28B* may have a contributive role in the development of IUGR (Figure 23 E-F). Immunohistochemistry using serial sections of term placenta tissue demonstrated a diffuse presence of LIN28A and LIN28B protein throughout what appears to be mesenchyme in term placenta villi (Figure 24 and Figure 25).

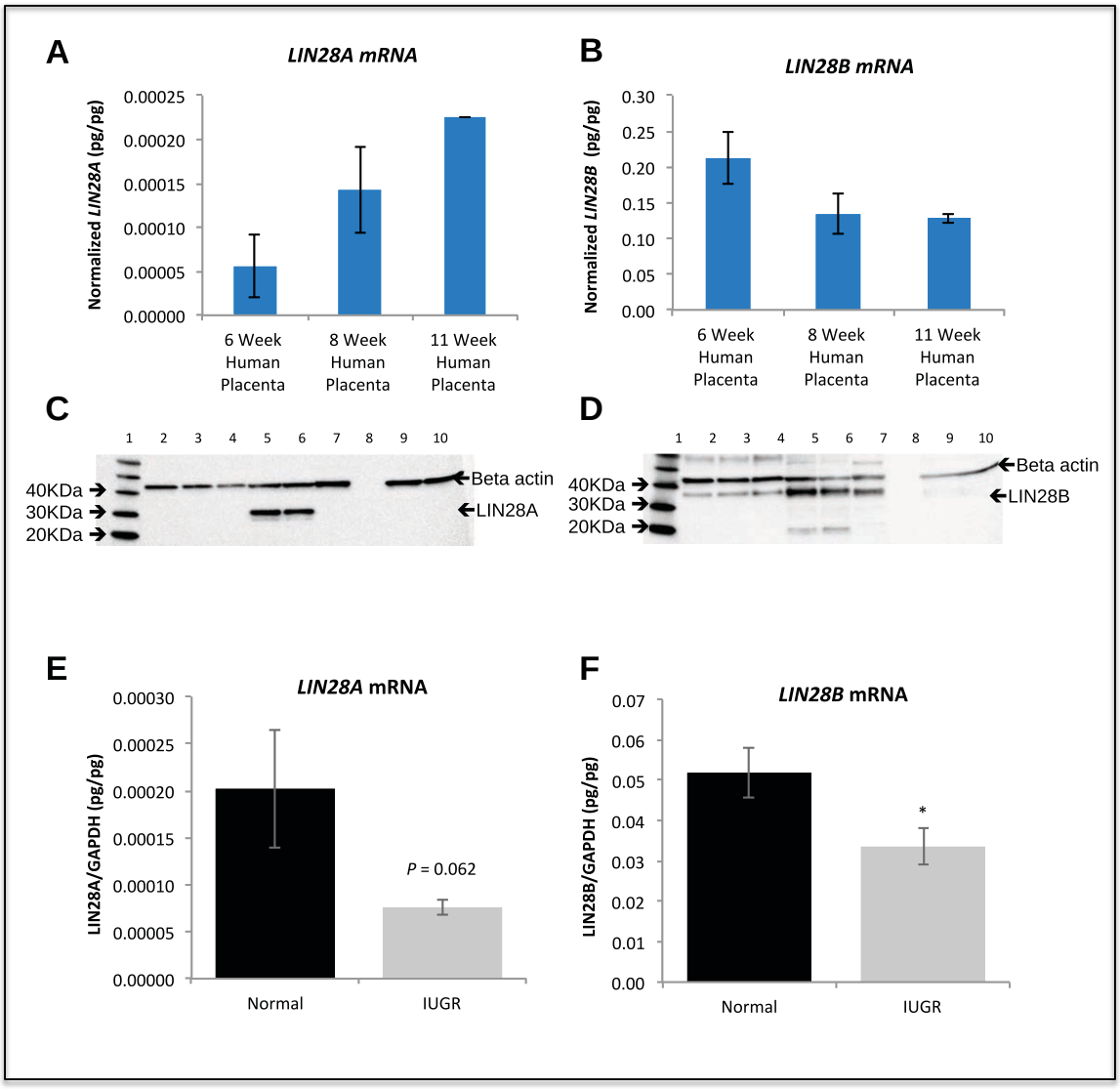

Figure 23. LIN28 in human placenta tissue.

A-B) *LIN28A* and *LIN28B* in first-trimester human placenta tissue. C-D) LIN28A and LIN28B protein in BeWo, ACH-3P cells, and first-trimester and term placenta tissue. Load order: Lane1: Invitrogen MagicMark XP (LC5602) ladder, Lane2-4: Bewo, Lane5-6: ACH3P, Lane7: term placenta #23, Lane8: blank, Lane9: 6.2 wk first trimester, Lane10: 11 week first trimester. E-F) LIN28A and LIN28B mRNA in term and IUGR term placenta tissue. Figures A, B, E and F were produced and analyzed by Dr. Russ Anthony's lab, and reproduced here with his permission. Materials and methods for RT-qPCR performed by Dr. Anthony's lab are as described elsewhere [211].

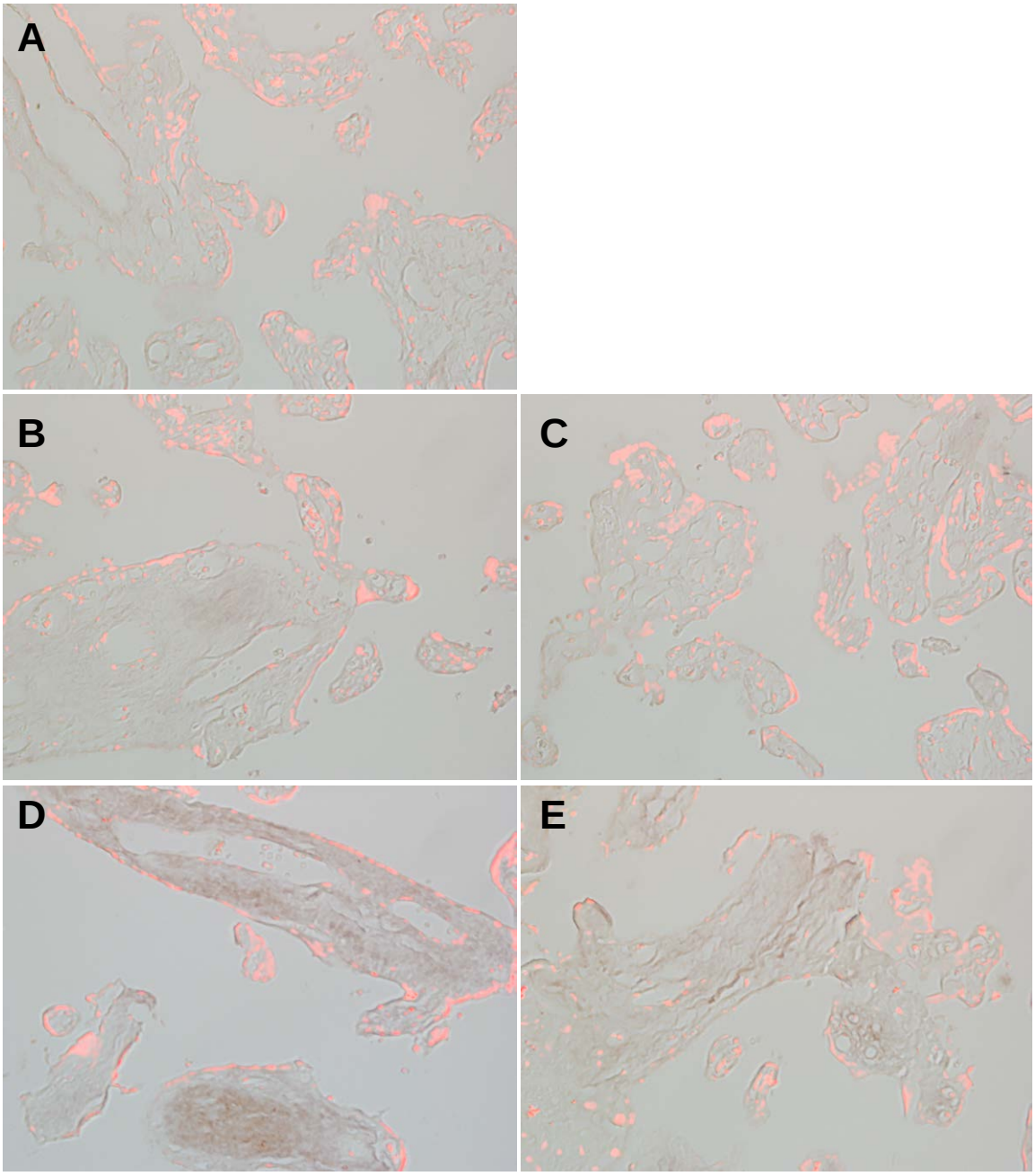

Figure 24. LIN28A protein in term placenta tissue.

20X magnification. A) No primary antibody. B-C) Preabsorbed primary antibody ratio of 1:2. D-E) LIN28A 1:1000 dilution. Counterstained with 60 ug/mL propidium iodide.

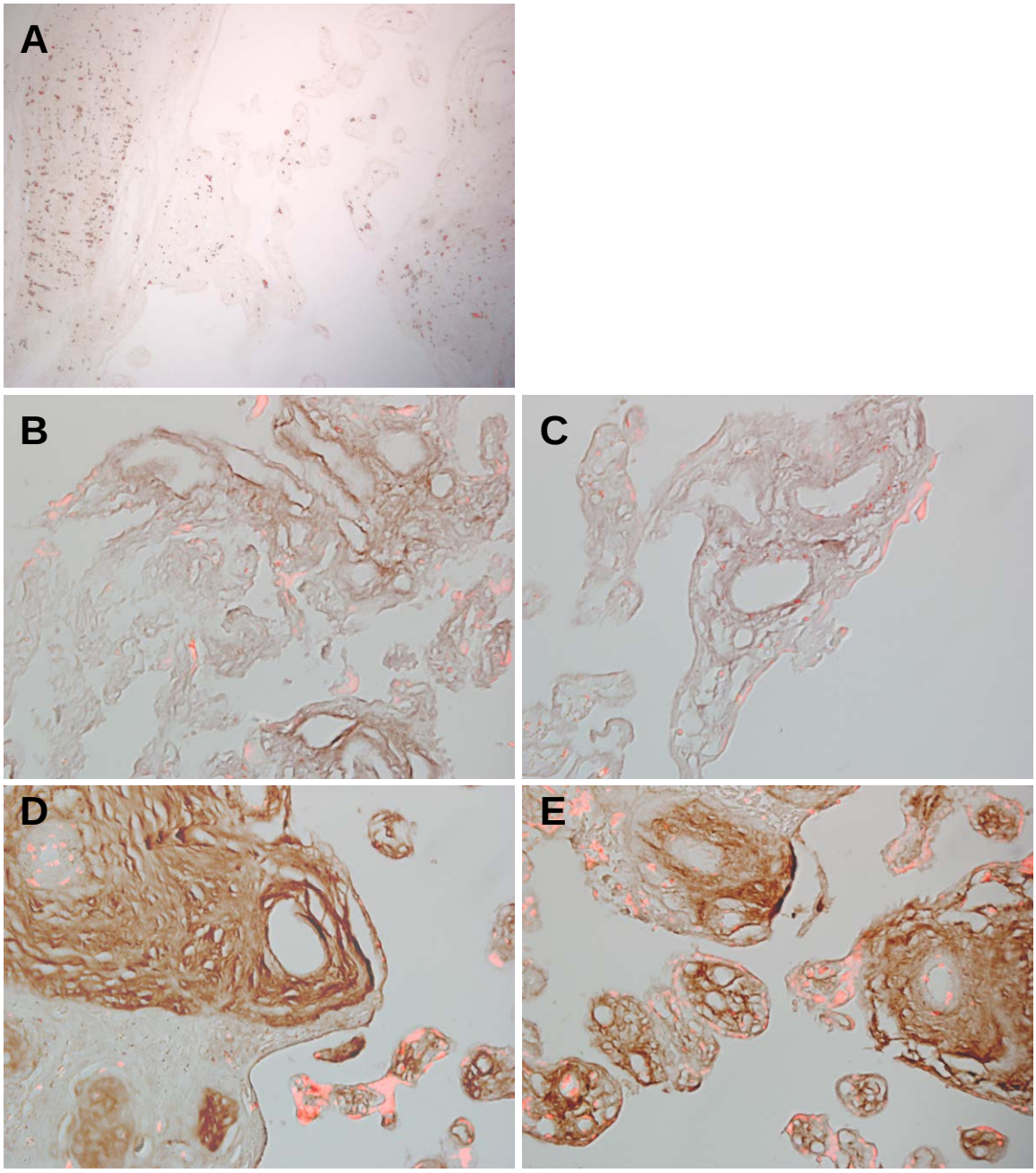

Figure 25. LIN28B protein in term placenta tissue.

20X magnification. A) No primary antibody. B-C) Preabsorbed primary antibody ratio of 1:5. D-E) LIN28B 1:1000 dilution. Counterstained with 60 ug/mL propidium iodide.

LIN28 IN MOUSE AND SHEEP PLACENTA TISSUE

Mouse

As determined in previous experiments (Chapter III), levels of LIN28A are high in day 0 proliferative mouse trophoblast stem cells (mTS), and decreased over six days without FGF4, heparin and conditioned medium as cells differentiated into trophoblast giant cells (mTGC) (LIN28A protein data reproduced here). However mTS cells did not have detectable levels of LIN28B in mTS or mTGC (Figure 26). It should be noted that we have not identified a mouse LIN28B positive control tissue to confirm that this antibody is working for mouse tissue. Although we did not have a positive control for LIN28B, these data confirm our preliminary microarray data, which demonstrated that *Lin28a* was more abundant in proliferative mTS than *Lin28b*, and that only *Lin28a* decreased with differentiation into mTGC.

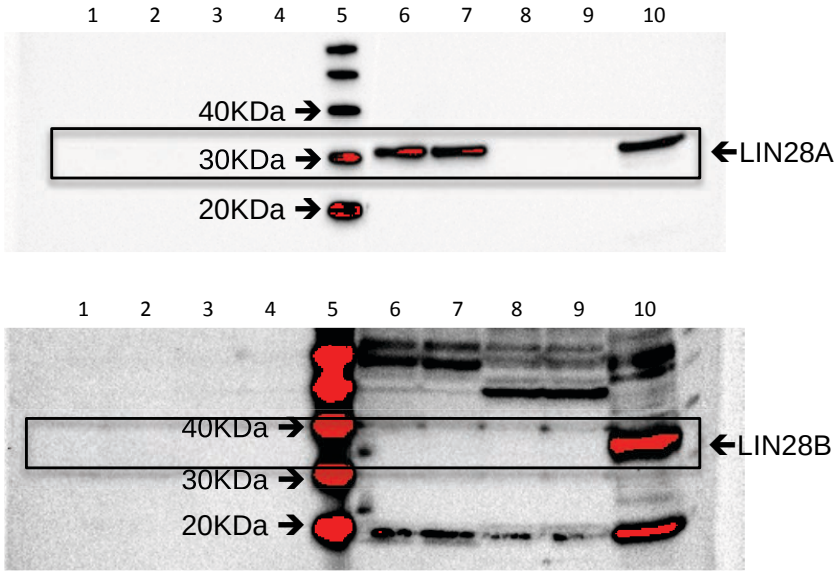

Figure 26. LIN28 protein in mTS cells.

Load order: Lane1: mTS day 0 #1 –PREABSORBED PRIMARY ANTIBODY, Lane2: mTS day 0 #2 –PREABSORBED PRIMARY ANTIBODY, Lane3: mTS day 6 #1 –PREABSORBED PRIMARY ANTIBODY, Lane4: mTS day 6 #2 –PREABSORBED PRIMARY ANTIBODY, Lane5: Invitrogen MagicMark XP (LC5602) ladder, Lane6: mTS day 0 #1, Lane7: mTS day 0 #2, Lane8: mTS day 6 #1, Lane9: mTS day 6 #2, Lane10: ACH3P WT positive control

Sheep

Collaborative projects performed by Dr. Russ Anthony's lab, assessed levels of *Lin28a* and *Lin28b* mRNA levels in sheep conceptuses at embryonic days 13, 15, 16, 17, 21 and 30. Levels of *Lin28b* mRNA were significantly higher than *Lin28a* mRNA at all time points (Figure 27). Levels of *Lin28a* mRNA were highest at embryonic day 13, significantly declined at embryonic day 15 and remained low through embryonic day 30 (Figure 27). *Lin28b* mRNA demonstrated the opposite pattern, with lower expression observed at embryonic days 13 – 17 before increasing significantly at embryonic days 21 and 30 (Figure 27). Together these data suggest that, LIN28B may have a more

significant regulatory role in sheep placenta development than LIN28A, and that the sheep may be a better model than mouse for assessing the role of LIN28 in human placenta.

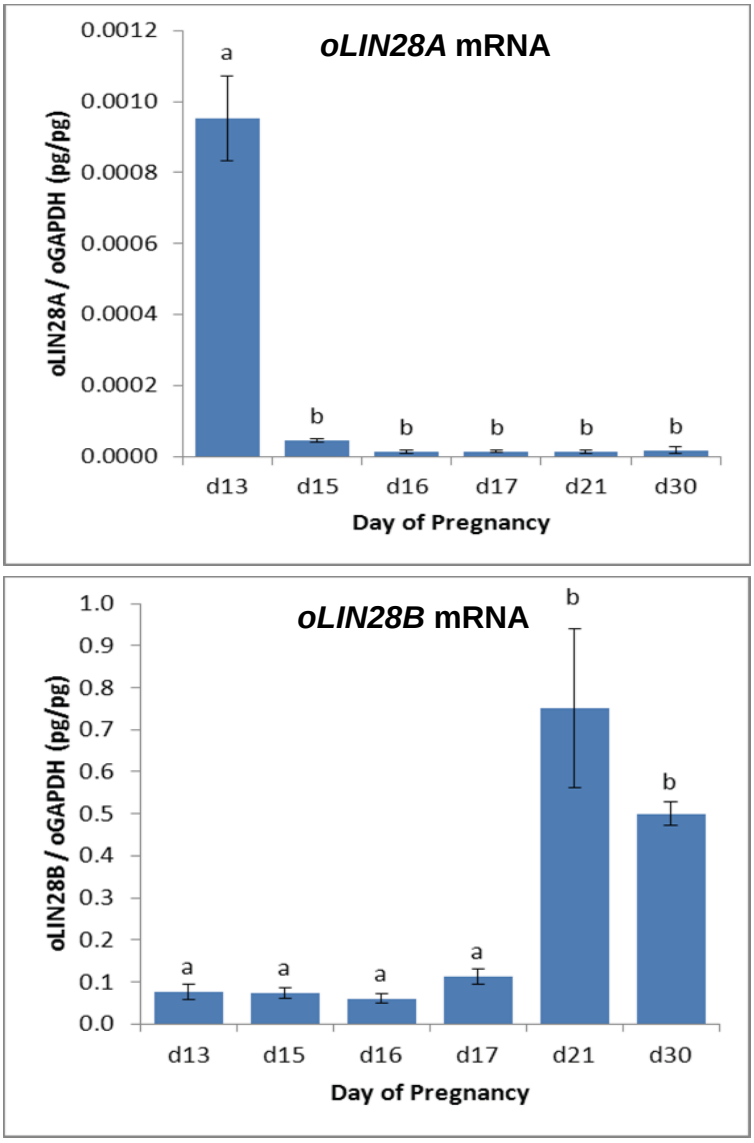

Figure 27. *Lin28* mRNA in sheep placenta.

Data collected and analyzed by Dr. Anthony's lab. Data reproduced here with Dr. Anthony's permission. Materials and methods for RT-qPCR performed by Dr. Anthony's lab are as described elsewhere [211].

LIN28 IN HUMAN AND SHEEP TROPHOBLAST CELLS GROWN ON MATRIGEL

ACH-3P cells grown on Matrigel had distinctly different growth morphology when grown on Matrigel compared to cells grown on plastic (Figure 28).

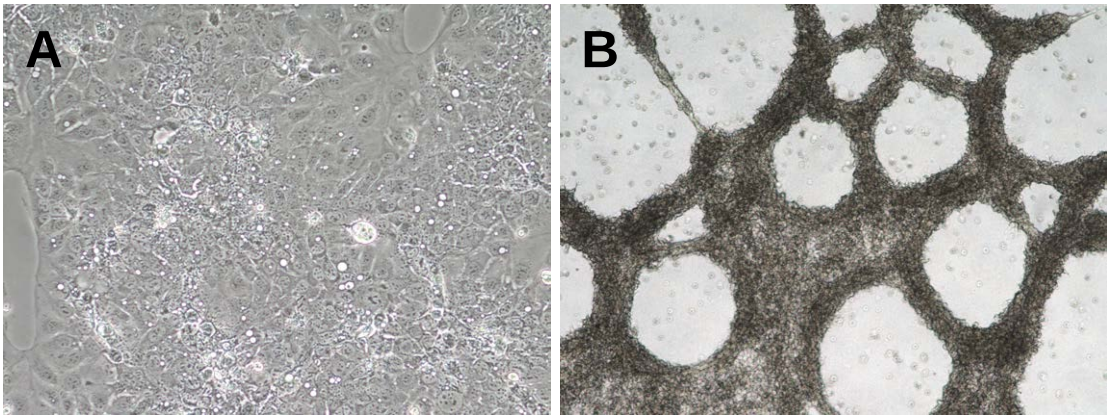

Figure 28. ACH-3P cells on Matrigel.

ACH-3P cells induced to invade when grown on Matrigel extracellular matrix (B) have a very distinct morphology compared to proliferative cells grown on plastic (A).

In ACH-3P cells grown on Matrigel, *LIN28A* mRNA levels increased, whereas *LIN28B* mRNA decreased. These data are in contrast to the decreased levels of LIN28A observed in ACH-3P cells treated with forskolin, suggesting that LIN28A's role in cytotrophoblast to syncytiotrophoblast differentiation may be different than cytotrophoblast to extravillous trophoblast differentiation. These data also suggest that LIN28B may function to regulate the differentiation of cytotrophoblast into the extravillous trophoblast sub-lineages in human trophoblast (Figure 29).

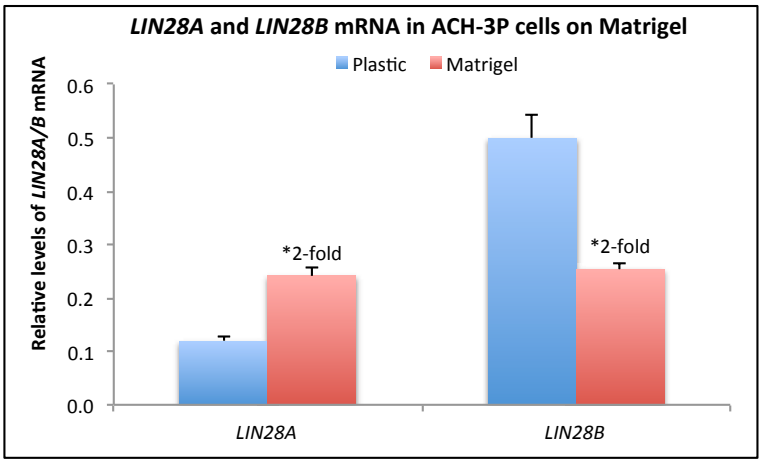

Figure 29. *LIN28* mRNA in ACH-3P human trophoblast cells grown on Matrigel extracellular matrix.

The increased levels of *LIN28A* mRNA we observed in ACH-3P cells grown on Matrigel was confirmed separately by Dr. Russ Anthony's group using primary ovine trophoblast (oTR) cells. However in oTR cells, levels of *LIN28B* mRNA did not change when grown on Matrigel (Figure 30).

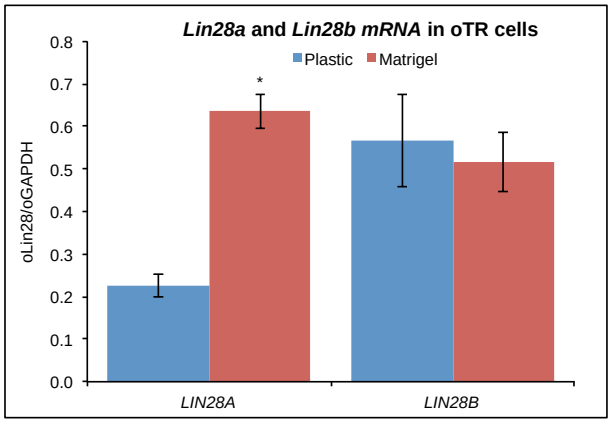

Figure 30. *Lin28* mRNA in primary ovine trophoblast cells (oTR) grown on Matrigel extracellular matrix.

Data collected and analyzed by Dr. Anthony's lab. Data are reproduced with the permission of Dr. Anthony. Materials and methods for RT-qPCR performed by Dr. Anthony's lab are as described elsewhere [211].

LIN28 LEVELS IN HUMAN TROPHOBLAST CELLS TREATED WITH FORSKOLIN

Forskolin-induced differentiation caused decreases in *LIN28A* mRNA in both ACH-3P and BeWo human trophoblast cell lines. However, levels of *LIN28B* mRNA increased in ACH-3P cells treated with forskolin and did not change in BeWo cells treated with forskolin. These data suggest that LIN28A regulation of cytotrophoblast to syncytiotrophoblast differentiation may be the same in both ACH-3P cell lines, however regulatory role for LIN28B may be different.

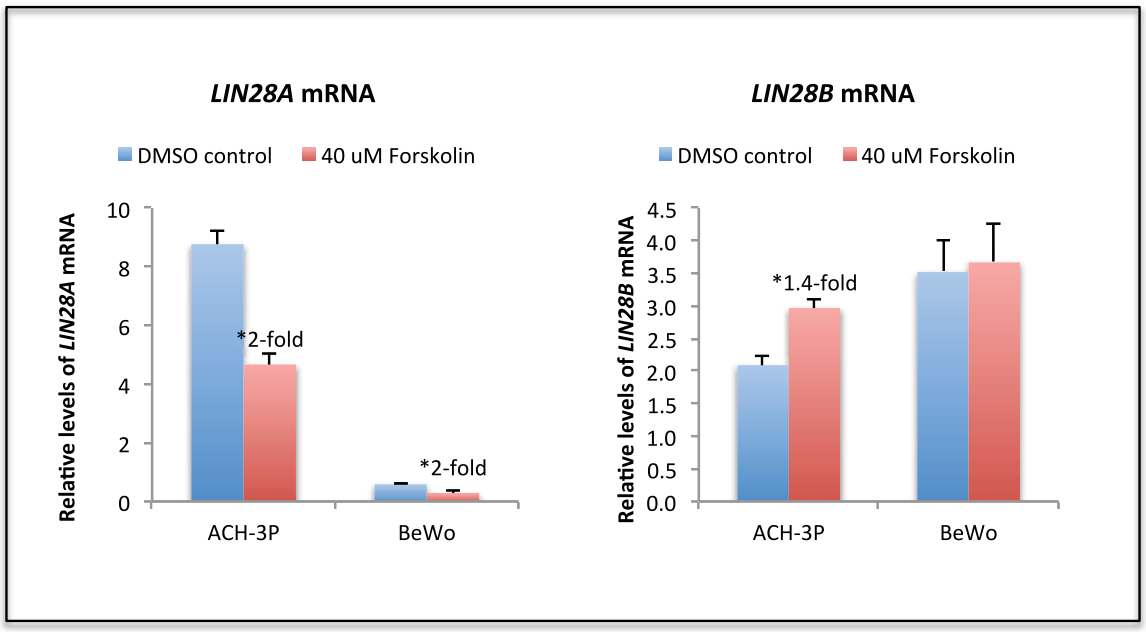

Figure 31. ***LIN28*** **mRNA in forskolin-treated ACH-3P and BeWo cell lines.**

EFFECTS OF LIN28 KNOCKDOWN IN ACH-3P CELLS

Levels of LIN28A and LIN28B were confirmed in *LIN28A* and *LIN28B* shRNA KD ACH-3P cells by qPCR and western blot (Figure 32).

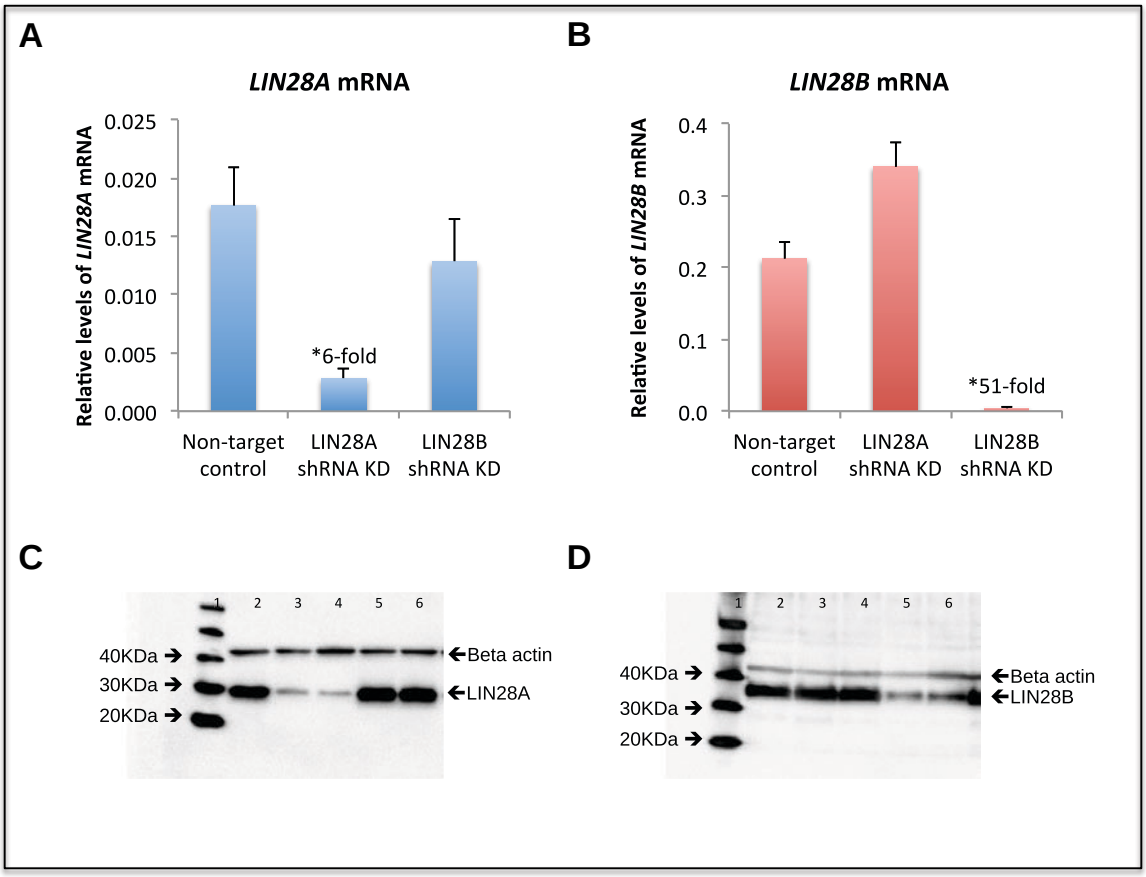

Figure 32. LIN28A and LIN28B in *LIN28A* and *LIN28B* shRNA knockdown ACH-3P cells.

A-B) Levels of LIN28 mRNA in ACH-3P shRNA KD ACH-3P cells (qPCR). C-D) Load order (same for both gels): Lane1: Invitrogen MagicMark XP (LC5602) ladder, Lane2: ACH-3P non-target control, Lane3: ACH3P LIN28A shRNA KD #1, Lane4: ACH3P LIN28A shRNA KD #2, Lane5: ACH3P LIN28B shRNA KD clone2 #1, Lane6: ACH3P LIN28B shRNA KD clone2 #2 (western blot).

LIN28A shRNA KD ACH-3P cells had increased levels of soluble hCG-beta on a per-cell basis, however soluble hCG-beta in cell culture medium from LIN28B shRNA KD ACH-3P cells was not different from non-target control cell medium (Figure 33A). While *ERVW-1* mRNA was not different in *LIN28A* shRNA KD cells, it was decreased in *LIN28B* shRNA KD cells (Figure 33B). *LIN28A* and *LIN28B* shRNA KD had opposite

effects on syncytiotrophoblast marker *LGALS13* mRNA, with loss of *LIN28A* resulting in increased *LGALS13* mRNA and loss of *LIN28B* resulting in decreased *LGALS13* mRNA (Figure 33C). Additionally, extravillous trophoblast specific marker *HLA-G* mRNA was increased in *LIN28A* shRNA KD cells but did not change with loss of *LIN28B* (Figure 33D).

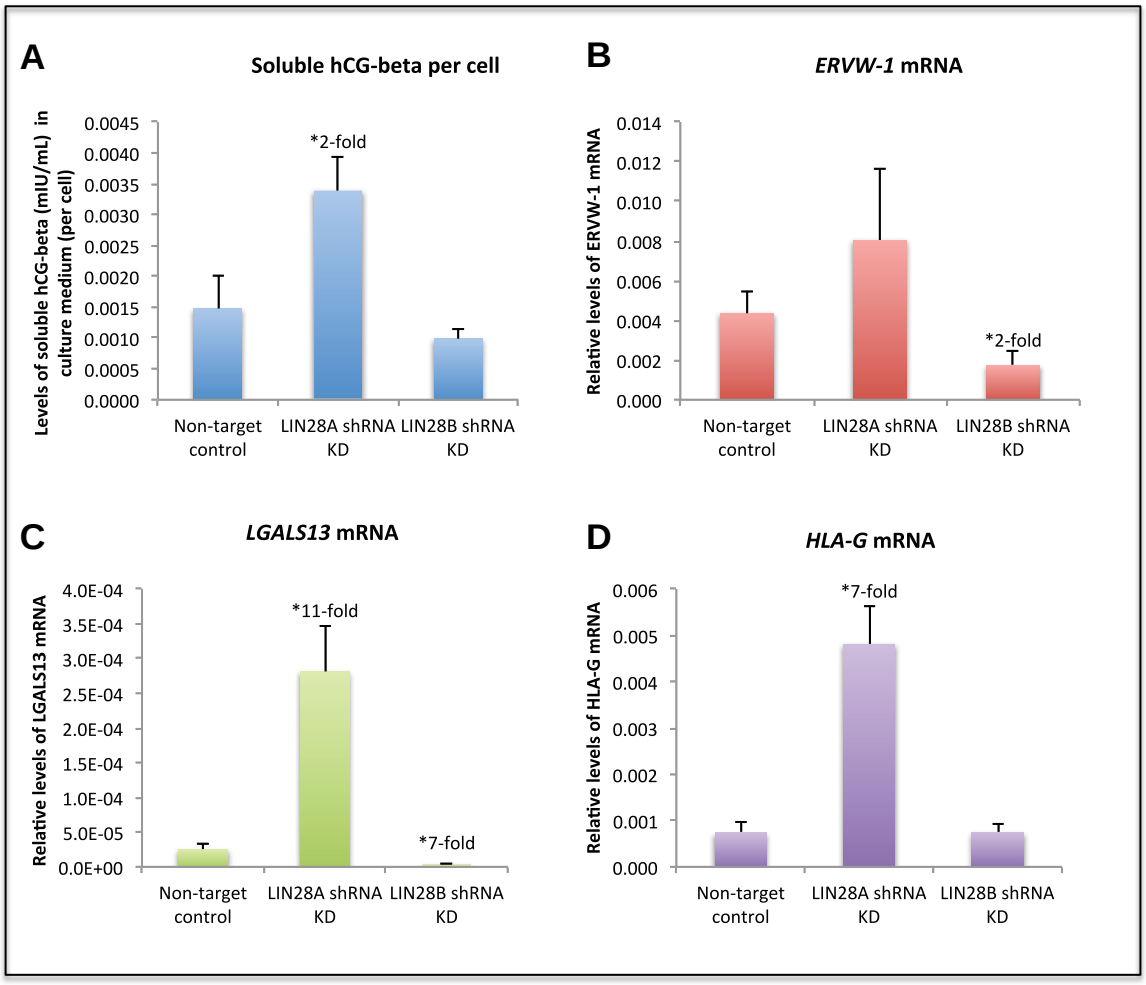

Figure 33. Differentiation markers in *LIN28* shRNA knockdown ACH-3P cells.

EFFECTS OF LIN28A OVEREXPRESSION IN ACH-3P CELLS

Levels of *LIN28A* mRNA were higher in *LIN28A* overexpressing (OE) ACH-3P cells compared to RFP control cells (Figure 34).

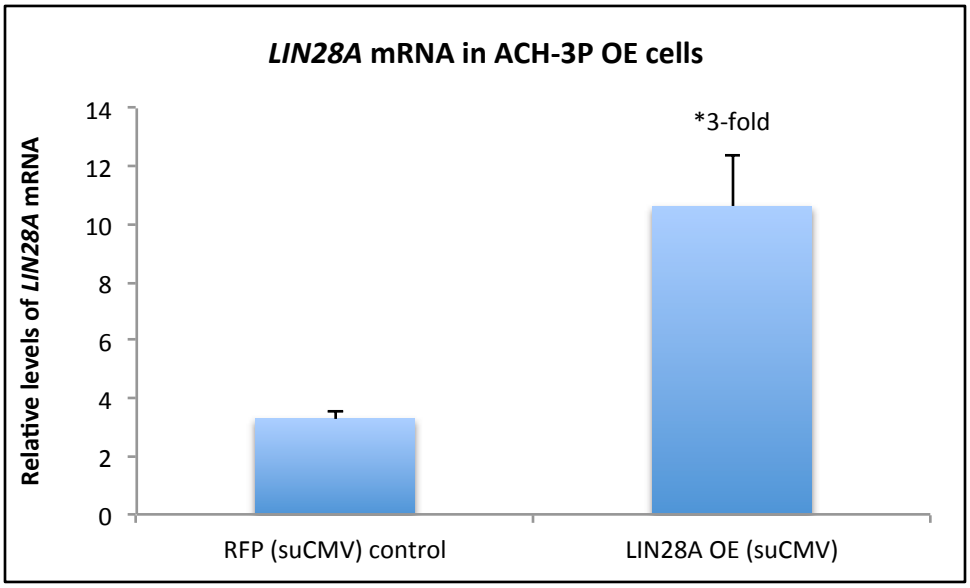

Figure 34. *LIN28A* mRNA in *LIN28A* OE (CMV) ACH-3P cells.

Despite increased *LIN28A* mRNA, *LIN28A* OE cells had increased levels of soluble hCG-beta in cell culture medium compared to RFP control cells. Additionally, forskolin treatment resulted in increased levels of hCG-beta in culture medium despite increased levels of *LIN28A* (Figure 35).

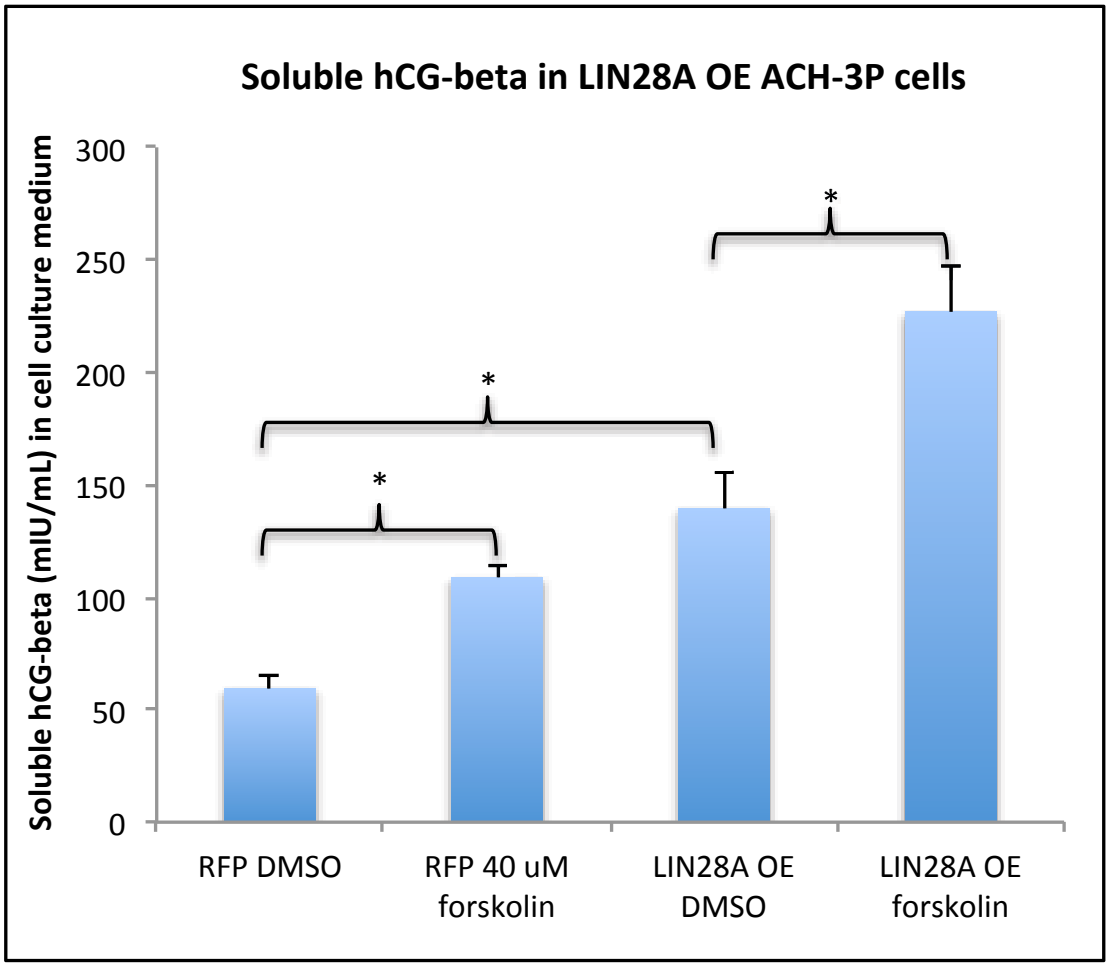

Figure 35. hCG-beta in culture medium from *LIN28A* overexpressing ACH-3P cells treated with DMSO or forskolin.

MICRORNA REGULATION OF LIN28A AND LIN28B

There is some data to suggest that in embryonic stem cells and cancer cells, LIN28 is regulated by miRNAs *miR-9*, *miR-30* and *miR-125* [192]. In order to assess whether this miR-LIN28 regulatory pathway was conserved in trophoblast cells, we treated wild-type ACH-3P cells with miRNA *hsa-miR-9, hsa-miR-30b* and *hsa-miR-125a* mimics and assessed levels of soluble hCG-beta. We found that *miR-9* and *miR-30b* resulted in the most significant decreases in levels of *LIN28A* and *LIN28B* mRNA in ACH-3P cells (Figure 36).

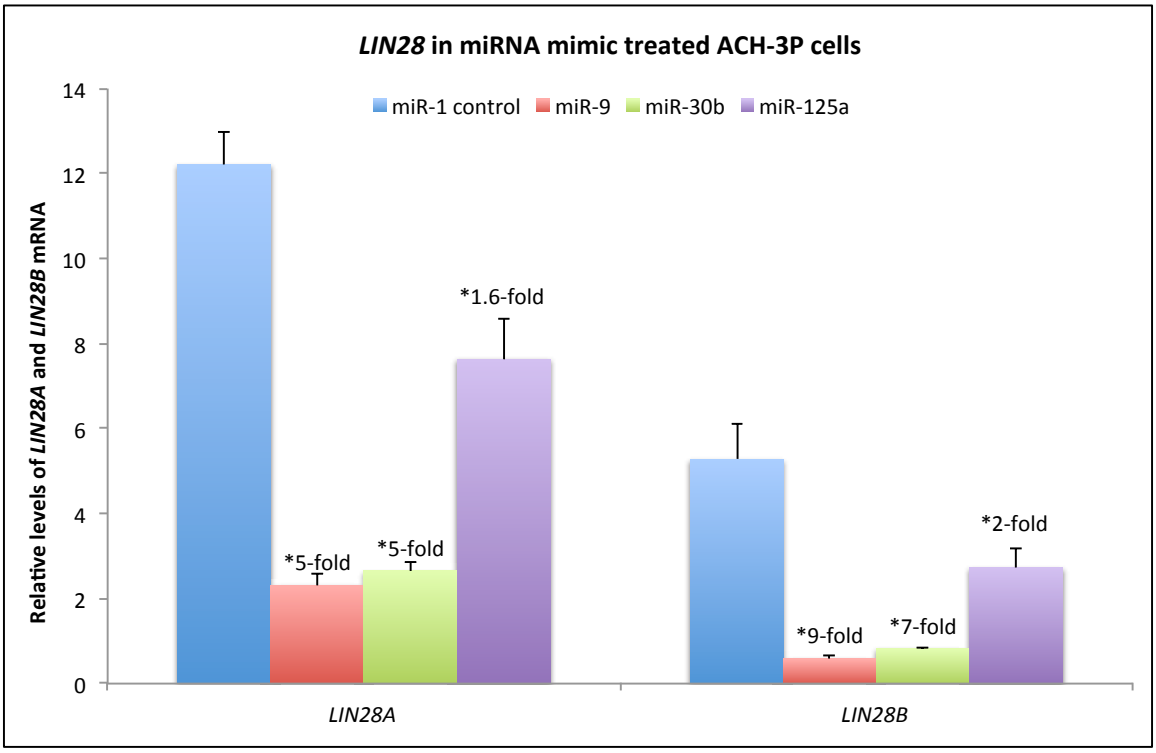

Figure 36. *LIN28* mRNA in ACH-3P cells treated with miRNA mimics.

The effects of miRNA mimics *miR-9*, *miR-30b* and *miR-125a* on *LIN28* mRNA levels.

However, when ACH-3P cells were treated with a combination of *hsa-miR-9* and *hsa-miR-30b*, levels of soluble hCG-beta in the culture medium decreased rather than increased (Figure 37). These data were in contrast to the increased levels of hCG-beta observed in the *LIN28A* shRNA KD ACH-3P cells. These data suggest that *miR-9* and *miR-30b* inhibition of LIN28 have distinctly different regulatory effects compared to shRNA-mediated LIN28A inhibition.

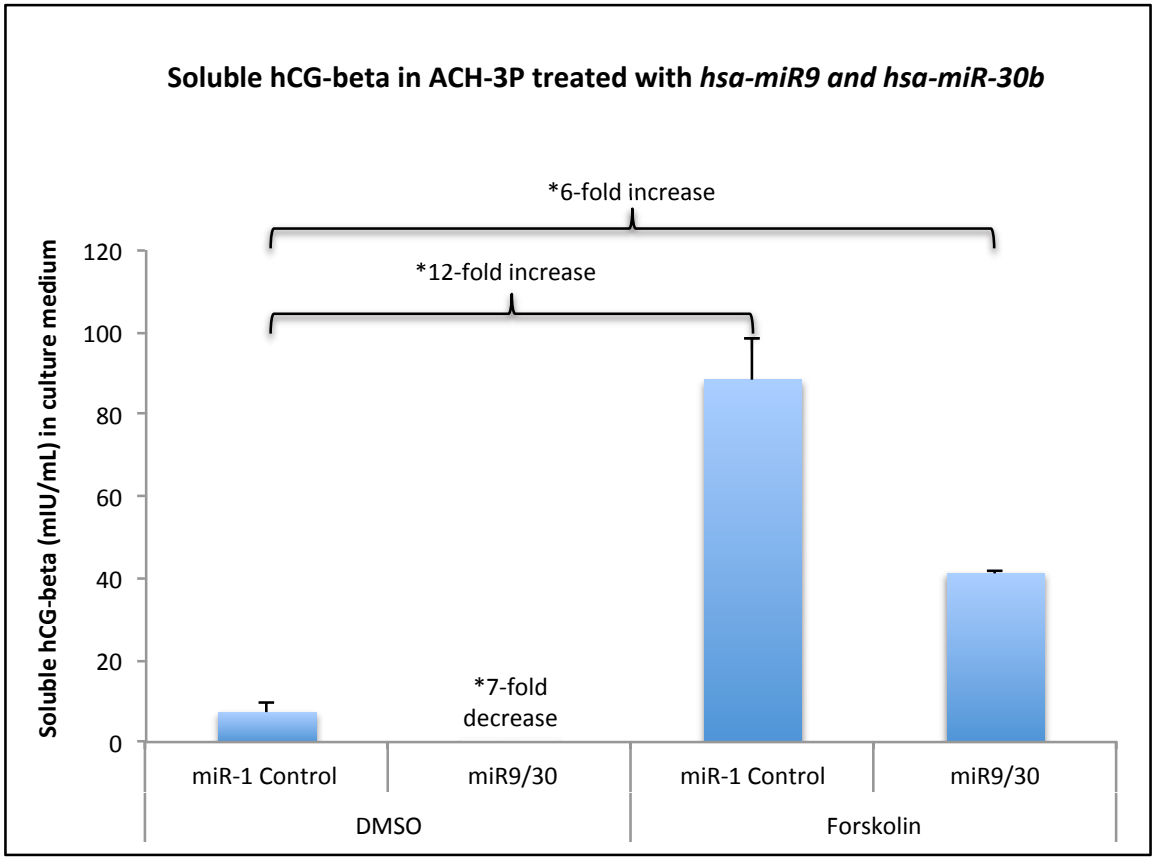

Figure 37. Effects of miRNA mimic treatment on forskolin-induced differentiation.

DISCUSSION

We found that each immortalized human trophoblast cell line had a distinct pattern of LIN28 expression, with ACH-3P and HTR-8/SVneo cells having high levels of both, BeWo cells having high levels of LIN28B and Swan 71 cells having low expression of both LIN28A and LIN28B. Importantly, assessment of *LIN28* in first-trimester and term primary human placenta tissue, found *LIN28B* to be significantly higher than *LIN28A* suggesting LIN28B may have a more significant regulatory role in the human placenta than LIN28A. Interestingly, in sheep there is a significant increase in *LIN28B* mRNA at embryonic day 17 that correlates with a period of development that includes adhesion, attachment and placenta development. These data are in striking contrast to the LIN28 expression patterns observed in primary mouse tissue, where LIN28A levels were higher than LIN28B, and mTS – mTGC differentiation was characterized by significant decreases in LIN28A. Together these data suggest that there may be important differences in LIN28 expression and placenta regulation between species, and may also suggest that in regards to LIN28, the sheep may be a better model for the human, than the mouse.

We found that mediated differentiation using forskolin or Matrigel substrate induced different LIN28 responses *in vitro*. Growth on Matrigel substrate was accompanied by increased levels of *LIN28A* mRNA in ACH-3P and primary oTR cells, whereas *LIN28B* levels decreased in ACH-3P cells and remained unchanged in oTR cells. These data could suggest that the induction of an invasive phenotype is associated with

dedifferentiation, as indicated by increased *LIN28A*, or it could suggest that invasion is a LIN28B-mediated event. Comprehensive comparisons and assessments using these Matrigel data are not recommended as each preliminary experiment was conducted by different labs and analyzed using different techniques. Additionally, markers to assess degree of invasion and cytotrophoblast to extravillous trophoblast (EVT) differentiation (such as MMPs, or HLA-G) were not used. Future controlled experiments are needed to further clarify the role of LIN28 during trophoblast invasion.

Experiments conducted in Chapter III describe the effects of forskolin treatment on *LIN28A* in ACH-3P cells. In Chapter IV, we assessed the effects of forskolin treatment on *LIN28B*, and in BeWo cells. We found that, like in ACH-3P cells, *LIN28A* decreased in BeWo cells treated with forskolin. However, the response of *LIN28B* was variable, with levels of *LIN28B* increasing in ACH-3P cells and unaltered in BeWo cells. Again, conclusions from these preliminary data are purely speculative: BeWo cells, historically, are considered a better model for assessing syncytialization lending credence to the suggestion that cytotrophoblast fusion into syncytiotrophoblast may be a LIN28A regulated event, however, given the low overall levels of LIN28A in primary human placenta tissue, more studies are needed.

The effects of shRNA-mediated *LIN28A* knockdown (KD) in ACH-3P cells are thoroughly described in Chapter III. Here we describe the effects of shRNA-mediated *LIN28B* KD in the ACH-3P cells. There were no differences in soluble hCG-beta or *HLA*-

G mRNA differentiation markers in *LIN28B* KD ACH-3P cells compared to non-target control cells. However, *LIN28B* KD ACH-3P cells had lower levels of *ERVW-1* and *LGALS13* mRNA compared to non-target control cells. These data are contrary to the effects observed with loss of *LIN28A,* where *LIN28A* KD ACH-3P cells had higher levels of all differentiation markers. Experiments using *LIN28A* overexpressing (OE) ACH-3P cells did little to confirm or clarify our findings, with *LIN28A* OE ACH-3P cells having increased levels of hCG-beta compared to RFP controls, and persistence of forskolin responsiveness. The confounding nature of the data may be the result of inherent differences in the cell lines: differences could be due to immortalization through the fusion with choriocarcinoma, due to variation between trophoblast parental lines, due to natural variation in native levels of LIN28A and LIN28B, or due to response predisposition and/or capacity to various stimuli such as forskolin or Matrigel substrate.

Finally, we demonstrated that miRNAs *miR-9*, *miR-30b* and *miR-125a* are associated with the effective inhibition of *LIN28A* and *LIN28B* mRNA in ACH-3P cells, although miRNA-mediated loss of *LIN28* was not associated with increased levels of trophoblast differentiation observed in shRNA-mediated loss of *LIN28A*. Differences may be due to the fact that mimic treatment resulted in the loss of both *LIN28A* and *LIN28B*, rather than the *LIN28A*-specific losses mediated by targeted shRNA. Decreases observed in hCG-beta are unlikely the result of direct miRNA regulation, as the 3'-UTR regions of the hCG subunits (CGA and CGB) are diminutive with few or no relevant miRNA binding sites (Figure 38).

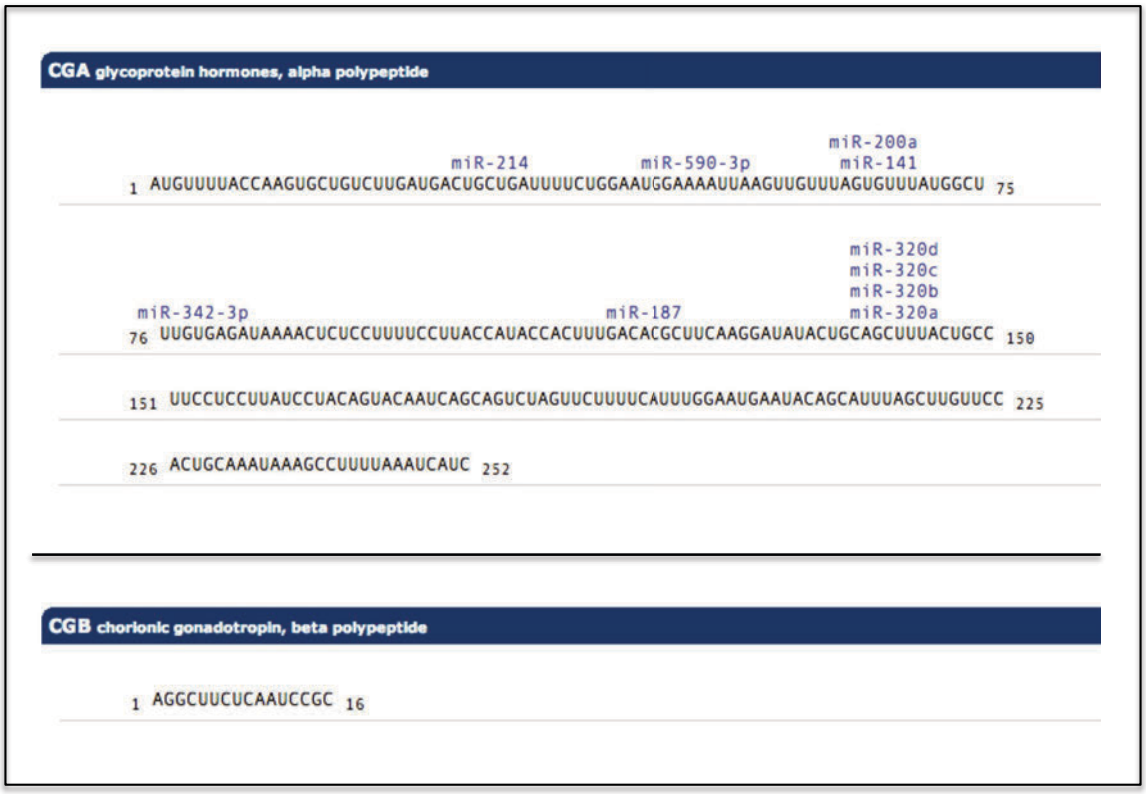

Figure 38.Putative miRNA biding sites in the 3'-UTR of hCG subunits (CGA and CGB).

Figure generated using microRNA.org *in silico* database.

Additionally, each individual miRNA typically has many predicted mRNA targets (*miR-9* and *miR-30b* have an estimated 8,778 and 6,218 mRNA targets, respectively). Therefore, the addition of miRNA mimic likely has expansive regulatory effects.

In conclusion, given the variability between the immortalized cell lines, and the innate complexity of LIN28 regulation, a prudent approach would be to assess LIN28 regulatory patterns in primary isolated human trophoblast cells in order to adequately design experiments utilizing appropriate models.

CHAPTER V: SUMMARY

The overall goal of these studies was to determine the role of LIN28 in the regulation of trophoblast proliferation and/or differentiation important for placenta development and function.

Proper regulation of trophoblast proliferation, differentiation and function are the fundamental mechanisms supporting proper placenta development and function. The initial differentiation event during embryo development is the segregation of pluripotent cells into either trophoblast or inner cell mass cell lineages. Disruption of temporal or molecular programs regulating the differentiation of trophoblast stem cells can result in insufficient sub-lineage trophoblast populations, and ultimately in compromised invasion or utero-placental vascular remodeling, poor metabolic exchange and/or abnormal endocrine function. Beyond being an immediate and exigent pregnancy-related issue, placenta dysfunction contributes significantly to the 500,000 maternal deaths each year, is a contributive factor in preterm delivery, and leads to increased risk for developing long-term health complications for children born from these pregnancies. Understanding the molecular mechanisms regulating trophoblast proliferation, differentiation and function is important for understanding, diagnosing, and ultimately treating placental disease.

LIN28, an RNA binding protein, has been well characterized as a potent post-transcriptional regulator of differentiation in embryonic stem cells with the ability to contribute to the dedifferentiation of somatic cells into induced pluripotent stem cells (iPSC). To date, LIN28 has been described to have two distinct regulatory mechanisms for maintaining pluripotency: inhibition of *let-7* miRNA maturation and direct post-transcriptional regulation of target mRNA. While there has been extensive research into the role of LIN28 in stem cell (ESC) differentiation, there is little data on whether LIN28 regulates the trophoblast stem cell differentiation important for the establishment and function of trophoblast sub-lineages critical for placenta health.

Experiments described in Chapter III demonstrate that LIN28A is present in the mouse placenta and may have a conserved functional role in the regulation of human and mouse trophoblast differentiation into the sub-lineages vital for proper placenta development. We conclude from these data that LIN28A likely acts in concert with a number of factors to regulate the progression of trophoblast differentiation through *let-7* miRNA dependent and independent pathways, and that loss of *LIN28* results in an increased potential for trophoblast differentiation to proceed, rather than actively initiating differentiation.

Experiments in Chapter IV suggest that levels of LIN28A, and levels of its homolog LIN28B, demonstrate species-specific expression patterns, and that the LIN28 homologs may have distinct regulatory roles in the modulation of trophoblast

proliferation and differentiation unique to each species (see Figure 39). Additionally, currently available *in vitro* cell lines show considerable variation in the levels of LIN28A and LIN28B, so careful consideration should be made when extrapolating *in vitro* data as a meaningful representation of *in vivo* reality.

While together these experiments demonstrate that LIN28 is present in placenta tissue, with a regulatory role in trophoblast differentiation that is likely important for proper placenta development and function, further studies are needed to determine species-specific variation.

Ultimately, progress in our understanding of the molecular mechanisms regulating trophoblast proliferation and differentiation will contribute to our understanding of placenta development and disease, which will not only contribute to an improvement in pregnancy outcome, but also will contribute to improving the long-term health of individuals from pregnancies complicated by placental disease.

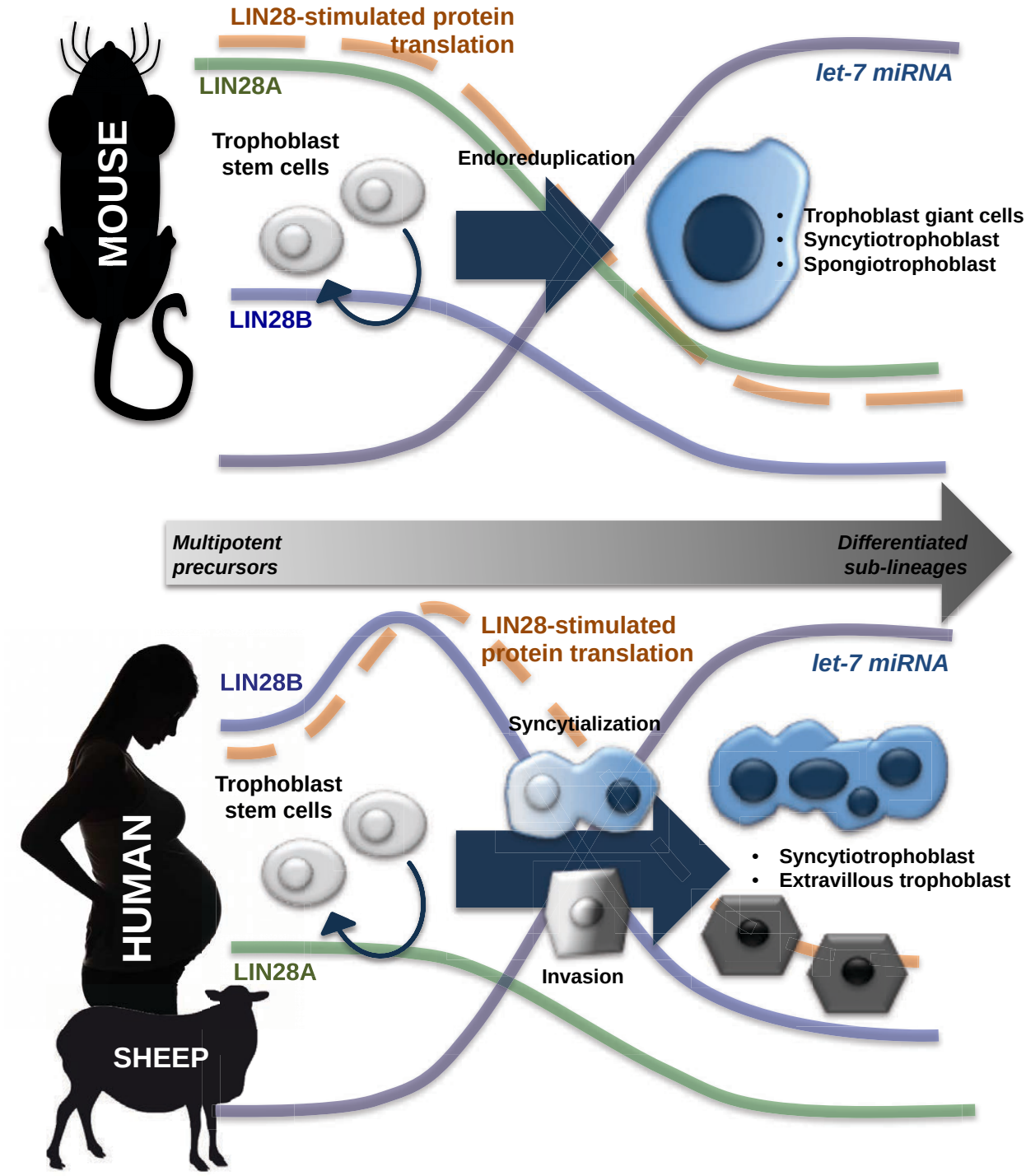

Figure 39.Proposed mechanism of LIN28 regulation of trophoblast differentiation in mouse, human and sheep.

REFERENCES

1. Bellamy L, Casas J-P, Hingorani AD, Williams DJ. Pre-eclampsia and risk of cardiovascular disease and cancer in later life: systematic review and meta-analysis. BMJ 2007; 335:974.

2. Saura B, Capestro M, Bova H. CONTINUITY OF BODIES: THE INFANT'S PLACENTA AND THE ISLAND'S NAVEL IN EASTERN POLYNESIA. The Journal of the Polynesian Society 2002; 111:127-145.

3. Birdsong WM. The placenta and cultural values. Western journal of medicine 1998; 168:190.

4. Helsel DG, Mochel M. Afterbirths in the Afterlife: Cultural Meaning of Placental Disposal in a Hmong American Community. Journal of Transcultural Nursing 2002; 13:282-286.

5. Aston WG. Nihongi: Chronicles of Japan from the Earliest of Times to AD 697. Tuttle Publishing; 2005.

6. Cadkin AV, Ginsberg NA, Pergament E, Verlinski Y. Chorionic villi sampling: a new technique for detection of genetic abnormalities in the first trimester. Radiology 1984; 151:159-162.

7. Gottesfeld K, Thompson H, Holmes J, Taylor E. Ultrasonic Placentography-A New Method for Placental Localization. Obstetrical & Gynecological Survey 1967; 22:250-252.

8. Benirschke K. Pathology of the human placenta. Berlin ;: Springer; 2012.

9. Nicholl C. Leonardo da Vinci flights of the mind. New York, N.Y., U.S.A.: Viking Penguin; 2004.

10. Kemp M. Leonardo. Oxford ;: Oxford University Press; 2011.

11. Comparative reproductive biology. Ames, Iowa: Blackwell Pub; 2007.

12. Wooding FB. The role of the binucleate cell in ruminant placental structure. Journal of reproduction and fertility. Supplement 1982; 31:31-39.

13. Martin R. Evolution of Placentation in Primates: Implications of Mammalian Phylogeny. Evolutionary Biology 2008; 35:125-145.

14. Pardi G, Marconi AM, Cetin I. Placental-fetal Interrelationship in IUGR Fetuses: A Review. Placenta 2002; 23, Supplement A:S136-S141.

15. Adamson SL, Lu Y, Whiteley KJ, Holmyard D, Hemberger M, Pfarrer C, Cross JC. Interactions between Trophoblast Cells and the Maternal and Fetal Circulation in the Mouse Placenta. Developmental Biology 2002; 250:358-373.

16. Carter AM. Animal Models of Human Placentation: A Review. Placenta 2007; 28, Supplement:S41-S47.

17. Malassine A, Frendo JL, Evain-Brion D. A comparison of placental development and endocrine functions between the human and mouse model. Human Reproduction Update 2003; 9:531-539.

18. Dreyfus M, Becmeur Fo, Schwaab C, Baldauf J-J, Philippe L, Ritter J. The pregnant ewe: an animal model for fetoscopic surgery. European Journal of Obstetrics & Gynecology and Reproductive Biology 1997; 71:91-94.

19. Morrison JL. Sheep models of intrauterine growth restriction: fetal adaptations and consequences. Clinical and Experimental Pharmacology and Physiology 2008; 35:730-743.

20. Anthony R, Scheaffer A, Wright C, Regnault T, Campbell B, Webb R, Dobson H, Doberska C. Ruminant models of prenatal growth restriction. In: Reproduction in domestic ruminants V. Proceedings of the Sixth International Symposium on Reproduction in Domestic Ruminants held in Crieff, Scotland, UK, August 2002.: Society for Reproduction and Fertility; 2003: 183-194.

21. Regnault TRH, Galan HL, Parker TA, Anthony RV. Placental Development in Normal and Compromised Pregnancies: A Review. Placenta 2002; 23, Supplement A:S119-S129.

22. Enders A, Blankenship T. Modification of endometrial arteries during invasion by cytotrophoblast cells in the pregnant macaque. Cells Tissues Organs 1997; 159:169-193.

23. Ramsey EM, Harris JW. Comparison of uteroplacental vasculature and circulation in the rhesus monkey and man. Carnegie Institution of Washington; 1966.

24. Enders A. Transition from lacunar to villous stage of implantation in the macaque, including establishment of the trophoblastic shell. Cells Tissues Organs 1995; 152:151-169.

25. Palmer AE, London WT, Sly DL, Rice JM. Spontaneous preeclamptic toxemia of pregnancy in the patas monkey (Erythrocebus patas). Laboratory animal science 1979; 29:102-106.

26. Schramm R, Bavister B. A macaque model for studying mechanisms controlling oocyte development and maturation in human and non-human primates. Human Reproduction 1999; 14:2544-2555.

27. Tanaka S, Kunath T, Hadjantonakis A-K, Nagy A, Rossant J. Promotion of Trophoblast Stem Cell Proliferation by FGF4. Science 1998; 282:2072-2075.

28. Pattillo RA, Gey GO. The Establishment of a Cell Line of Human Hormone-synthesizing Trophoblastic Cells in Vitro. Cancer Research 1968; 28:1231-1236.

29. Hiden U, Wadsack C, Prutsch N, Gauster M, Weiss U, Frank H-G, Schmitz U, Fast-Hirsch C, Hengstschlager M, Potgens A, Ruben A, Knofler M, et al. The first trimester human trophoblast cell line ACH-3P: A novel tool to study autocrine/paracrine regulatory loops of human trophoblast subpopulations - TNF-alpha stimulates MMP15 expression. BMC Developmental Biology 2007; 7:137.

30. Graham C, Hawley T, Hawley R, MacDougall J, Kerbel R, Khoo N, Lala P. Establishment and characterization of first trimester human trophoblast cells with extended lifespan. Exp Cell Res 1993; 206:204 - 211.

31. Khoo NKS, Bechberger JF, Shepherd T, Bond SL, McCrae KR, Hamilton GS, Lala PK. SV40 Tag transformation of the normal invasive trophoblast results in a premalignant phenotype. I. Mechanisms responsible for hyperinvasivess and resistance to anti-invasive action of TGFβ. International Journal of Cancer 1998; 77:429-439.

32. Morales-Prieto DM, Chaiwangyen W, Ospina-Prieto S, Schneider U, Herrmann J, Gruhn B, Markert UR. MicroRNA expression profiles of trophoblastic cells. Placenta 2012; 33:725-734.

33. Noguer-Dance M, Abu-Amero S, Al-Khtib M, Lefevre A, Coullin P, Moore GE, Cavaille J. The primate-specific microRNA gene cluster (C19MC) is imprinted in the placenta. Human Molecular Genetics 2010; 19:3566-3582.

34. Straszewski-Chavez SL, Abrahams VM, Alvero AB, Aldo PB, Ma Y, Guller S, Romero R, Mor G. The Isolation and Characterization of a Novel Telomerase Immortalized First Trimester Trophoblast Cell Line, Swan 71. Placenta 2009; 30:939-948.

35. Kliman HJ. Uteroplacental Blood Flow: The Story of Decidualization, Menstruation, and Trophoblast Invasion. The American Journal of Pathology 2000; 157:1759-1768.

36. Kaufmann P, Black S, Huppertz B. Endovascular trophoblast invasion: implications for the pathogenesis of intrauterine growth retardation and preeclampsia. Biol Reprod 2003; 69:1 - 7.

37. Pijnenborg R, Vercruysse L, Brosens I. Deep placentation. Best Practice & Research Clinical Obstetrics & Gynaecology 2011; 25:273-285.

38. Thornburg KL, Jacobson S-L, Giraud GD, Morton MJ. Hemodynamic changes in pregnancy. Seminars in Perinatology 2000; 24:11-14.

39. Kim JJ, Jaffe RC, Fazleabas AT. Blastocyst invasion and the stromal response in primates. Human Reproduction 1999; 14:45-55.

40. Lockwood CJ, Krikun G, Hausknecht V, Wang EY, Schatz F. Decidual Cell Regulation of Hemostasis during Implantation and Menstruation. Annals of the New York Academy of Sciences 1997; 828:188-193.

41. Gellersen B, Brosens J. Cyclic AMP and progesterone receptor cross-talk in human endometrium: a decidualizing affair. Journal of Endocrinology 2003; 178:357-372.

42. Iwahashi M, Muragaki Y, Ooshima A, Yamoto M, Nakano R. Alterations in distribution and composition of the extracellular matrix during decidualization of the human endometrium. Journal of Reproduction and Fertility 1996; 108:147-155.

43. Gellersen B, Reimann K, Samalecos A, Aupers S, Bamberger A-M. Invasiveness of human endometrial stromal cells is promoted by decidualization and by trophoblast-derived signals. Human Reproduction 2010; 25:862-873.

44. Jones RL, Salamonsen LA, Findlay JK. Activin A Promotes Human Endometrial Stromal Cell Decidualization in Vitro. Journal of Clinical Endocrinology & Metabolism 2002; 87:4001-4004.

45. Oreshkova T, Dimitrov R, Mourdjeva M. A Cross-Talk of Decidual Stromal Cells, Trophoblast, and Immune Cells: A Prerequisite for the Success of Pregnancy. American Journal of Reproductive Immunology 2012; 68:366-373.

46. Lala PK, Chatterjee-Hasrouni S, Kearns M, Montgomery B, Colavincenzo V. Immunobiology of the Feto-Maternal Interface. Immunological Reviews 1983; 75:87-116.

47. Cross JC, Werb Z, Fisher SJ. Implantation and the Placenta: Key Pieces of the Development Puzzle. Science 1994; 266:1508-1518.

48. Rossant J, McMahon A. "Cre"-ating mouse mutants-a meeting review on conditional mouse genetics. Genes Dev 1999; 13:142 - 145.

49. Rossant J, Tam PPL. Blastocyst lineage formation, early embryonic asymmetries and axis patterning in the mouse. Development 2009; 136:701-713.

50. Rinkenberger JL, Cross JC, Werb Z. Molecular genetics of implantation in the mouse. Developmental Genetics 1997; 21:6-20.

51. Mouse development patterning, morphogenesis, and organogenesis. San Diego, Calif.: Academic; 2002.

52. Gasperowicz M, Natale DRC. Establishing Three Blastocyst Lineages: Then What? Biology of Reproduction 2011; 84:621-630.

53. Johnson MH. From Mouse Egg to Mouse Embryo: Polarities, Axes, and Tissues. Annual Review of Cell and Developmental Biology 2009; 25:483-512.

54. Gardner RL. Origin and differentiation of extraembryonic tissues in the mouse. International review of experimental pathology 1983; 24:63-133.

55. Werling U, Schorle H. Transcription Factor Gene AP-2 Gamma Essential for Early Murine Development. Molecular and Cellular Biology 2002; 22:3149-3156.

56. Cross JC, Baczyk D, Dobric N, Hemberger M, Hughes M, Simmons DG, Yamamoto H, Kingdom JCP. Genes, Development and Evolution of the Placenta. Placenta 2003; 24:123-130.

57. Guzman-Ayala M, Ben-Haim N, Beck Sv, Constam DB. Nodal protein processing and fibroblast growth factor 4 synergize to maintain a trophoblast stem cell microenvironment. Proceedings of the National Academy of Sciences of the United States of America 2004; 101:15656-15660.

58. Nishioka N, Inoue K-i, Adachi K, Kiyonari H, Ota M, Ralston A, Yabuta N, Hirahara S, Stephenson RO, Ogonuki N, Makita R, Kurihara H, et al. The Hippo Signaling Pathway Components Lats and Yap Pattern Tead4 Activity to Distinguish Mouse Trophectoderm from Inner Cell Mass. Developmental Cell 2009; 16:398-410.

59. Kidder BL, Palmer S. Examination of transcriptional networks reveals an important role for TCFAP2C, SMARCA4, and EOMES in trophoblast stem cell maintenance. Genome Research 2010; 20:458-472.

60. Ma GT, Roth ME, Groskopf JC, Tsai FY, Orkin SH, Grosveld F, Engel JD, Linzer DI. GATA-2 and GATA-3 regulate trophoblast-specific gene expression in vivo. Development 1997; 124:907-914.

61. Ralston A, Cox BJ, Nishioka N, Sasaki H, Chea E, Rugg-Gunn P, Guo G, Robson P, Draper JS, Rossant J. Gata3 regulates trophoblast development downstream of Tead4 and in parallel to Cdx2. Development 2010; 137:395-403.

62. Roberts RM, Fisher SJ. Trophoblast Stem Cells. Biology of Reproduction 2011; 84:412-421.

63. Barlow PW, Sherman MI. The biochemistry of differentiation of mouse trophoblast: studies on polyploidy. Journal of Embryology and Experimental Morphology 1972; 27:447-465.

64. Douglas GC, VandeVoort CA, Kumar P, Chang T-C, Golos TG. Trophoblast Stem Cells: Models for Investigating Trophectoderm Differentiation and Placental Development. Endocrine Reviews 2009; 30:228-240.

65. Vandevoort CA, Thirkill TL, Douglas GC. Blastocyst-derived trophoblast stem cells from the rhesus monkey. 2007.

66. Niwa H, Toyooka Y, Shimosato D, Strumpf D, Takahashi K, Yagi R, Rossant J. Interaction between Oct3/4 and Cdx2 Determines Trophectoderm Differentiation. Cell 2005; 123:917-929.

67. Niwa H, Miyazaki J-i, Smith AG. Quantitative expression of Oct-3/4 defines differentiation, dedifferentiation or self-renewal of ES cells. Nat Genet 2000; 24:372-376.

68. Harun R, Ruban L, Matin M, Draper J, Jenkins NM, Liew GC, Andrews PW, Li TC, Laird SM, Moore HDM. Cytotrophoblast stem cell lines derived from human embryonic stem cells and their capacity to mimic invasive implantation events. Human Reproduction 2006; 21:1349-1358.

69. Adjaye J, Huntriss J, Herwig R, BenKahla A, Brink TC, Wierling C, Hultschig C, Groth D, Yaspo M-L, Picton HM, Gosden RG, Lehrach H. Primary Differentiation in the Human Blastocyst: Comparative Molecular Portraits of Inner Cell Mass and Trophectoderm Cells. STEM CELLS 2005; 23:1514-1525.

70. Assou S, Boumela In, Haouzi D, Monzo Cc, Dechaud H, Kadoch I-J, Hamamah S. Transcriptome Analysis during Human Trophectoderm Specification Suggests New Roles of Metabolic and Epigenetic Genes. PLoS ONE 2012; 7:e39306.

71. Pijnenborg R, Bland JM, Robertson WB, Brosens I. Uteroplacental arterial changes related to interstitial trophoblast migration in early human pregnancy. Placenta; 4:397-413.

72. Vascular endothelium in human physiology and pathophysiology. Amsterdam: Harwood Academic; 2000.

73. Poston L. The control of blood flow to the placenta. Experimental Physiology 1997; 82:377-387.

74. Brosens I, Robertson W, Dixon H. The physiological response of the vessels of the placental bed to normal pregnancy. The Journal of Pathology and Bacteriology 1967; 93:569-579.

75. Moll W, Nienartowicz A, Hees H, Wrobel K, Lenz A. Blood flow regulation in the uteroplacental arteries. Trophoblast Res 1988; 3:83-96.

76. Martin D, Conrad KP. Expression of Endothelial Nitric Oxide Synthase by Extravillous Trophoblast Cells in the Human Placenta. Placenta 2000; 21:23-31.

77. Huppertz B, Kertschanska S, Demir AY, Frank H-G, Kaufmann P. Immunohistochemistry of matrix metalloproteinases (MMP), their substrates, and their inhibitors (TIMP) during trophoblast invasion in the human placenta. Cell and tissue research 1997; 291:133-148.

78. Genbacev O, Joslin R, Damsky CH, Polliotti BM, Fisher SJ. Hypoxia alters early gestation human cytotrophoblast differentiation/invasion in vitro and models the placental defects that occur in preeclampsia. Journal of Clinical Investigation 1996; 97:540.

79. Genbacev O, Zhou Y, Ludlow JW, Fisher SJ. Regulation of human placental development by oxygen tension. Science 1997; 277:1669-1672.

80. Zhou Y, Genbacev O, Damsky CH, Fisher SJ. Oxygen regulates human cytotrophoblast differentiation and invasion: implications for endovascular invasion in normal pregnancy and in pre-eclampsia. Journal of Reproductive Immunology 1998; 39:197-213.

81. Rodesch F, Simon P, Donner C, Jauniaux E. Oxygen measurements in endometrial and trophoblastic tissues during early pregnancy. Obstetrics and gynecology 1992; 80:283-285.

82. Burton GJ, Jauniaux E, Watson AL. Maternal arterial connections to the placental intervillous space during the first trimester of human pregnancy: the Boyd collection revisited. American Journal of Obstetrics and Gynecology 1999; 181:718-724.

83. Matijevic R, Meekins JW, Walkinshaw SA, Neilson JP, McFadyen IR. Spiral artery blood flow in the central and peripheral areas of the placental bed in the second trimester. Obstetrics & Gynecology 1995; 86:289-292.

84. Huppertz B, Gauster M. Trophoblast Fusion. In: Dittmar T, Zänker KS (eds.), Cell Fusion in Health and Disease, vol. 713: Springer Netherlands; 2011: 81-95.

85. Martin I, Pecheur E-I, Ruysschaert J-M, Hoekstra D. Membrane Fusion Induced by a Short Fusogenic Peptide Is Assessed by Its Insertion and Orientation into Target Bilayers. Biochemistry 1999; 38:9337-9347.

86. Decout A, Labeur C, Goethals M, Brasseur R, Vandekerckhove J, Rosseneu M. Enhanced efficiency of a targeted fusogenic peptide. Biochimica et Biophysica Acta (BBA) - Biomembranes 1998; 1372:102-116.

87. Blond J-L, Lavillette D, Cheynet V, Bouton O, Oriol G, Chapel-Fernandes S, Mandrand B, Mallet F, Cosset F-L. An Envelope Glycoprotein of the Human Endogenous Retrovirus HERV-W Is Expressed in the Human Placenta and

Fuses Cells Expressing the Type D Mammalian Retrovirus Receptor. J. Virol. 2000; 74:3321-3329.

88. Potgens AJG, Schmitz U, Bose P, Versmold A, Kaufmann P, Frank HG. Mechanisms of Syncytial Fusion: A Review. Placenta 2002; 23:S107-S113.

89. Chen YX, Allars M, Maiti K, Angeli GL, Abou-Seif C, Smith R, Nicholson RC. Factors affecting cytotrophoblast cell viability and differentiation: Evidence of a link between syncytialisation and apoptosis. The International Journal of Biochemistry & Cell Biology 2011; 43:821-828.

90. Muir A, Lever A, Moffett A. Expression and Functions of Human Endogenous Retroviruses in the Placenta: An Update. Placenta 2004; 25:S16-S25.

91. Black SG, Arnaud F, Palmarini M, Spencer TE. Endogenous Retroviruses in Trophoblast Differentiation and Placental Development. American Journal of Reproductive Immunology 2010; 64:255-264.

92. Blaise S, de Parseval N, B√©nit L, Heidmann T. Genomewide screening for fusogenic human endogenous retrovirus envelopes identifies syncytin 2, a gene conserved on primate evolution. Proceedings of the National Academy of Sciences 2003; 100:13013-13018.

93. Lin L, Xu B, Rote NS. Expression of Endogenous Retrovirus ERV-3 Induces Differentiation in BeWo, a Choriocarcinoma Model of Human Placental Trophoblast. Placenta 1999; 20:109-118.

94. Zhou X, Platt JL. Molecular and Cellular Mechanisms of Mammalian Cell Fusion. In: Dittmar T, Zänker KS (eds.), Cell Fusion in Health and Disease, vol. 713: Springer Netherlands; 2011: 33-64.

95. Lyden TW, Ah-Kau NG, Rote NS. Modulation of phosphatidylserine epitope expression by BeWo cells during forskolin treatment. Placenta; 14:177-186.

96. Huppertz B, Bartz C, Kokozidou M. Trophoblast fusion: Fusogenic proteins, syncytins and ADAMs, and other prerequisites for syncytial fusion. Micron 2006; 37:509-517.

97. Rote NS, Wei BR, Xu C, Luo L. Caspase 8 and Human Villous Cytotrophoblast Differentiation. Placenta 2010; 31:89-96.

98. Daleke DL. Phospholipid Flippases. Journal of Biological Chemistry 2007; 282:821-825.

99. Brasseur R, Vandenbranden M, Cornet B, Burny A, Ruysschaert J-M. Orientation into the lipid bilayer of an asymmetric amphipathic helical peptide located at the N-terminus of viral fusion proteins. Biochimica et Biophysica Acta (BBA) - Biomembranes 1990; 1029:267-273.

100. Rote NS, Chakrabarti S, Stetzer BP. The role of human endogenous retroviruses in trophoblast differentiation and placental development. Placenta; 25:673-683.

101. Lins L, Decaffmeyer M, Thomas A, Brasseur R. Relationships between the orientation and the structural properties of peptides and their membrane

interactions. Biochimica et Biophysica Acta (BBA) - Biomembranes; 1778:1537-1544.

102. Huppertz B, Frank H, Kingdom J, Reister F, Kaufmann P. Villous cytotrophoblast regulation of the syncytial apoptotic cascade in the human placenta. Histochem Cell Biol 1998; 110:495 - 508.

103. Fowden AL, Sferruzzi-Perri AN, Coan PM, Constancia M, Burton GJ. Placental efficiency and adaptation: endocrine regulation. The Journal of Physiology 2009; 587:3459-3472.

104. Chard T. Assessment of fetoplacental function by biochemical determinations. Journal of Clinical Pathology 1976; 3:18-26.

105. Kliman HJ. Trophoblast to human placenta. Encyclopedia of reproduction 1999; 4:834-846.

106. Csapo AI, Pulkkinen MO, Wiest W. Effects of luteectomy and progesterone replacement therapy in early pregnant patients. American Journal of Obstetrics and Gynecology 1973; 115:759.

107. Fomin VP, Cox BE, Word RA. Effect of progesterone on intracellular Ca2+ homeostasis in human myometrial smooth muscle cells. American Journal of Physiology - Cell Physiology 1999; 276:C379-C385.

108. Pepe G, Albrecht E. Central integrative role of oestrogen in the regulation of placental steroidogenic maturation and the development of the fetal pituitary-adrenocortical axis in the baboon. Human Reproduction Update 1998; 4:406-419.

109. SAMAAN N, YEN SCC, FRIESEN H, PEARSON OH. Serum Placental Lactogen Levels During Pregnancy and in Trophoblastic Disease. Journal of Clinical Endocrinology & Metabolism 1966; 26:1303-1308.

110. Handwerger S, Freemark M. The roles of placental growth hormone and placental lactogen in the regulation of human fetal growth and development. Journal of Pediatric Endocrinology and Metabolism 2000; 13:343-356.

111. Ryu KS, Ji I, Chang L, Ji TH. Molecular mechanism of LH/CG receptor activation. Molecular and Cellular Endocrinology 1996; 125:93-100.

112. Pierce JG, Parsons TF. GLYCOPROTEIN HORMONES - STRUCTURE AND FUNCTION. Annual Review of Biochemistry 1981; 50:465-495.

113. Fiddes JC, Goodman HM. The gene encoding the common alpha subunit of the four human glycoprotein hormones. Journal of molecular and applied genetics 1981; 1:3-18.

114. Policastro P, Ovitt CE, Hoshina M, Fukuoka H, Boothby MR, Boime I. The beta subunit of human chorionic gonadotropin is encoded by multiple genes. Journal of Biological Chemistry 1983; 258:11492-11499.

115. Talmadge K, Boorstein WR, Vamvakopoulos NC, Gething M-J, Fiddes JC. Only three of the seven human chorionic gonadotropin beta subunit genes can be expressed in the placenta. Nucleic Acids Research 1984; 12:8415-8436.

116. Henke A, Gromoll Jr. New insights into the evolution of chorionic gonadotrophin. Molecular and Cellular Endocrinology 2008; 291:11-19.

117. Maston GA, Ruvolo M. Chorionic Gonadotropin Has a Recent Origin Within Primates and an Evolutionary History of Selection. Molecular Biology and Evolution 2002; 19:320-335.

118. Birken S, Canfield RE. Isolation and amino acid sequence of COOH-terminal fragments from the beta subunit of human choriogonadotropin. Journal of Biological Chemistry 1977; 252:5386-5392.

119. Keutmann HT, Williams RM. Human chorionic gonadotropin. Amino acid sequence of the hormone-specific COOH-terminal region. Journal of Biological Chemistry 1977; 252:5393-5397.

120. Jablonka-Shariff A, Garcia-Campayo V, Boime I. Evolution of Lutropin to Chorionic Gonadotropin Generates a Specific Routing Signal for Apical Release in Vivo. Journal of Biological Chemistry 2002; 277:879-882.

121. Yoshida Y. Secretion of human chorionic gonadotropin in early pregnancy. Medical Molecular Morphology 2005; 38:104.

122. Cole LA. hCG, five independent molecules. Clinica Chimica Acta 2012; 413:48-65.

123. Minegishi T, Nakamura K, Ibuki Y. Structure and Regulation of LH/CG Receptor. Endocrine Journal 1993; 40:275-287.

124. Owen JA. Physiology of the menstrual cycle. The American Journal of Clinical Nutrition 1975; 28:333-338.

125. Lopata A, Oliva K, Stanton PG, Robertson DM. Analysis of chorionic gonadotrophin secreted by cultured human blastocysts. Molecular Human Reproduction 1997; 3:517-521.

126. JAMESON JL, HOLLENBERG AN. Regulation of Chorionic Gonadotropin Gene Expression. Endocrine Reviews 1993; 14:203-221.

127. Butler T, Elustondo P, Hannigan G, MacPhee D. Integrin-linked kinase can facilitate syncytialization and hormonal differentiation of the human trophoblast-derived BeWo cell line. Reproductive Biology and Endocrinology 2009; 7:51.

128. Leisser C, Saleh L, Haider S, Husslein H, Sonderegger S, Knofler M. Tumour necrosis factor-alpha impairs chorionic gonadotrophin beta-subunit expression and cell fusion of human villous cytotrophoblast. Molecular Human Reproduction 2006; 12:601-609.

129. Pittaway DE, Reish RL, Wentz AC. Doubling times of human chorionic gonadotropin increase in early viable intrauterine pregnancies. American Journal of Obstetrics and Gynecology 1985; 152:299-302.

130. Braunstein GD, Rasor J, Danzer H, Adler D, Wade ME. Serum human chorionic gonadotropin levels throughout normal pregnancy. American Journal of Obstetrics and Gynecology 1976; 126:678-681.

131. Sherwin JRA, Sharkey AM, Cameo P, Mavrogianis PM, Catalano RD, Edassery S, Fazleabas AT. Identification of Novel Genes Regulated by Chorionic

Gonadotropin in Baboon Endometrium during the Window of Implantation. Endocrinology 2007; 148:618-626.

132. Zygmunt M, Herr F, Keller-Schoenwetter S, Kunzi-Rapp K, Munstedt K, Rao CV, Lang U, Preissner KT. Characterization of Human Chorionic Gonadotropin as a Novel Angiogenic Factor. Journal of Clinical Endocrinology & Metabolism 2002; 87:5290-5296.

133. Kayisli UA, Selam B, Guzeloglu-Kayisli O, Demir R, Arici A. Human Chorionic Gonadotropin Contributes to Maternal Immunotolerance and Endometrial Apoptosis by Regulating Fas-Fas Ligand System. The Journal of Immunology 2003; 171:2305-2313.

134. ABRAMOVICH DR, BAKER TG, NEAL P. EFFECT OF HUMAN CHORIONIC GONADOTROPHIN ON TESTOSTERONE SECRETION BY THE FOETAL HUMAN TESTIS IN ORGAN CULTURE. Journal of Endocrinology 1974; 60:179-185.

135. HUHTANIEMI IT, KORENBROT CC, JAFFE RB. hCG Binding and Stimulation of Testosterone Biosynthesis in the Human Fetal Testis. Journal of Clinical Endocrinology & Metabolism 1977; 44:963-967.

136. Brizot ML, Jauniaux E, Mckie AT, Farzaneh F, Nicolaides KH. Molecular interactions during pregnancy: Placental mRNA expression of alpha and beta human chorionic gonadotrophin in early trisomy 18 pregnancies. Molecular Human Reproduction 1996; 2:463-465.

137. Massin N, Frendo JL, Guibourdenche J, Luton D, Giovangrandi Y, Muller F, Vidaud M, Evain-Brion D. Defect of Syncytiotrophoblast Formation and Human Chorionic Gonadotropin Expression in Down's Syndrome. Placenta 2001; 22:S93-S97.

138. Watson D. Urinary Chorionic Gonadotrophin Determination. Clinical Chemistry 1966; 12:577-585.

139. Yogo I. Biological Properties of Human Chorionic Gonadotropin. Endocrinologia Japonica 1969; 16:215-225.

140. Ambros V, Horvitz H. Heterochronic mutants of the nematode Caenorhabditis elegans. Science 1984; 226:409-416.

141. Moss EG, Tang L. Conservation of the heterochronic regulator Lin-28, its developmental expression and microRNA complementary sites. Developmental Biology 2003; 258:432-442.

142. Moss EG, Lee RC, Ambros V. The Cold Shock Domain Protein LIN-28 Controls Developmental Timing in C. elegans and Is Regulated by the lin-4 RNA. Cell 1997; 88:637-646.

143. Richards M, Tan S-P, Tan J-H, Chan W-K, Bongso A. The Transcriptome Profile of Human Embryonic Stem Cells as Defined by SAGE. STEM CELLS 2004; 22:51-64.

144. Vogt EJ, Meglicki M, Hartung KI, Borsuk E, Behr Rd. Importance of the pluripotency factor LIN28 in the mammalian nucleolus during early embryonic development. Development 2012; 139:4514-4523.

145. Zhu H, Shah S, Shyh-Chang N, Shinoda G, Einhorn WS, Viswanathan SR, Takeuchi A, Grasemann C, Rinn JL, Lopez MF, Hirschhorn JN, Palmert MR, et al. Lin28a transgenic mice manifest size and puberty phenotypes identified in human genetic association studies. Nat Genet 2010; 42:626-630.

146. Lettre G, Jackson AU, Gieger C, Schumacher FR, Berndt SI, Sanna S, Eyheramendy S, Voight BF, Butler JL, Guiducci C, Illig T, Hackett R, et al. Identification of ten loci associated with height highlights new biological pathways in human growth. Nat Genet 2008; 40:584-591.

147. Yu J, Vodyanik MA, Smuga-Otto K, Antosiewicz-Bourget J, Frane JL, Tian S, Nie J, Jonsdottir GA, Ruotti V, Stewart R, Slukvin II, Thomson JA. Induced Pluripotent Stem Cell Lines Derived from Human Somatic Cells. Science 2007; 318:1917-1920.

148. Xue D, Peng Y, Wang F, Allan RW, Cao D. RNA-binding protein LIN28 is a sensitive marker of ovarian primitive germ cell tumours. Histopathology 2011; 59:452-459.

149. Viswanathan SR, Powers JT, Einhorn W, Hoshida Y, Ng TL, Toffanin S, O'Sullivan M, Lu J, Phillips LA, Lockhart VL, Shah SP, Tanwar PS, et al. Lin28

promotes transformation and is associated with advanced human malignancies. Nat Genet 2009; 41:843-848.

150. King CE, Cuatrecasas M, Castells A, Sepulveda AR, Lee J-S, Rustgi AK. LIN28B Promotes Colon Cancer Progression and Metastasis. Cancer Research 2011; 71:4260-4268.

151. Hamano R, Miyata H, Yamasaki M, Sugimura K, Tanaka K, Kurokawa Y, Nakajima K, Takiguchi S, Fujiwara Y, Mori M, Doki Y. High expression of Lin28 is associated with tumour aggressiveness and poor prognosis of patients in oesophagus cancer. Br J Cancer 2012; 106:1415-1423.

152. Kumar MS, Lu J, Mercer KL, Golub TR, Jacks T. Impaired microRNA processing enhances cellular transformation and tumorigenesis. Nat Genet 2007; 39:673-677.

153. Kumar MS, Erkeland SJ, Pester RE, Chen CY, Ebert MS, Sharp PA, Jacks T. Suppression of non-small cell lung tumor development by the let-7 microRNA family. Proceedings of the National Academy of Sciences 2008; 105:3903-3908.

154. Feng C, Neumeister V, Ma W, Xu J, Lu L, Bordeaux J, Maihle NJ, Rimm DL, Huang Y. Lin28 regulates HER2 and promotes malignancy through multiple mechanisms. Cell Cycle 2012; 11:2486-2494.

155. Malik F, Korkaya H, Clouthier SG, Wicha MS. Lin28 and HER2: Two stem cell regulators conspire to drive aggressive breast cancer. Cell Cycle 2012; 11:2780-2781.

156. Guo Y, Chen Y, Ito H, Watanabe A, Ge X, Kodama T, Aburatani H. Identification and characterization of lin-28 homolog B (LIN28B) in human hepatocellular carcinoma. Gene 2006; 384:51-61.

157. Piskounova E, Polytarchou C, Thornton JE, LaPierre RJ, Pothoulakis C, Hagan JP, Iliopoulos D, Gregory RI. Lin28A and Lin28B Inhibit let-7 MicroRNA Biogenesis by Distinct Mechanisms. Cell 2011; 147:1066-1079.

158. Reinhart BJ, Slack FJ, Basson M, Pasquinelli AE, Bettinger JC, Rougvie AE, Horvitz HR, Ruvkun G. The 21-nucleotide let-7 RNA regulates developmental timing in Caenorhabditis elegans. Nature 2000; 403:901-906.

159. Abbott AL, Alvarez-Saavedra E, Miska EA, Lau NC, Bartel DP, Horvitz HR, Ambros V. The let-7 MicroRNA Family Members mir-48, mir-84, and mir-241 Function Together to Regulate Developmental Timing in Caenorhabditis elegans. Developmental Cell 2005; 9:403-414.

160. Cullen BR. Transcription and Processing of Human microRNA Precursors. Molecular Cell 2004; 16:861-865.

161. Nam Y, Chen C, Gregory RI, Chou JJ, Sliz P. Molecular Basis for Interaction of let-7 MicroRNAs with Lin28. Cell 2011; 147:1080-1091.

162. Mayr F, Sch√ºtz A, D√∂ge N, Heinemann U. The Lin28 cold-shock domain remodels pre-let-7 microRNA. Nucleic Acids Research 2012; 40:7492-7506.

163. Loughlin FE, Gebert LFR, Towbin H, Brunschweiger A, Hall J, Allain FdrHT. Structural basis of pre-let-7 miRNA recognition by the zinc knuckles of pluripotency factor Lin28. Nat Struct Mol Biol 2012; 19:84-89.

164. Thornton JE, Gregory RI. How does Lin28 let-7 control development and disease? Trends in Cell Biology 2012; 22:474-482.

165. Heo I, Joo C, Cho J, Ha M, Han J, Kim VN. Lin28 Mediates the Terminal Uridylation of let-7 Precursor MicroRNA. Molecular Cell 2008; 32:276-284.

166. Xu B, Zhang K, Huang Y. Lin28 modulates cell growth and associates with a subset of cell cycle regulator mRNAs in mouse embryonic stem cells. RNA 2009; 15:357-361.

167. Xu B, Huang Y. Histone H2a mRNA interacts with Lin28 and contains a Lin28-dependent posttranscriptional regulatory element. Nucleic Acids Research 2009; 37:4256-4263.

168. Balzer E, Moss EG. Localization of the Developmental Timing Regulator Lin28 to mRNP Complexes, P-bodies and Stress Granules. RNA Biology 2007; 4:16-25.

169. Peng S, Chen L-L, Lei X-X, Yang L, Lin H, Carmichael GG, Huang Y. Genome-Wide Studies Reveal That Lin28 Enhances the Translation of Genes Important for Growth and Survival of Human Embryonic Stem Cells. STEM CELLS 2011; 29:496-504.

170. Qiu C, Ma Y, Wang J, Peng S, Huang Y. Lin28-mediated post-transcriptional regulation of Oct4 expression in human embryonic stem cells. Nucleic Acids Research 2010; 38:1240-1248.

171. Polesskaya A, Cuvellier S, Naguibneva I, Duquet A, Moss EG, Harel-Bellan A. Lin-28 binds IGF-2 mRNA and participates in skeletal myogenesis by increasing translation efficiency. Genes & Development 2007; 21:1125-1138.

172. Cho J, Chang H, Kwon SC, Kim B, Kim Y, Choe J, Ha M, Kim YK, Kim VN. LIN28A Is a Suppressor of ER-Associated Translation in Embryonic Stem Cells. Cell 2012; 151:765-777.

173. Jin J, Jing W, Lei X-X, Feng C, Peng S, Boris-Lawrie K, Huang Y. Evidence that Lin28 stimulates translation by recruiting RNA helicase A to polysomes. Nucleic Acids Research 2011; 39:3724-3734.

174. Bleichert F, Baserga SJ. The Long Unwinding Road of RNA Helicases. Molecular Cell 2007; 27:339-352.

175. Lei X-X, Xu J, Ma W, Qiao C, Newman MA, Hammond SM, Huang Y. Determinants of mRNA recognition and translation regulation by Lin28. Nucleic Acids Research 2012; 40:3574-3584.

176. Qiao C, Ma J, Xu J, Xie M, Ma W, Huang Y. Drosha mediates destabilization of Lin28 mRNA targets. Cell Cycle 2012; 11:3590-3598.

177. Yang D-H, Moss EG. Temporally regulated expression of Lin-28 in diverse tissues of the developing mouse. Gene Expression Patterns 2003; 3:719-726.

178. Ilekis JV, Reddy UM, Roberts JM. Review Article: Preeclampsia, A Pressing Problem: An Executive Summary of a National Institute of Child Health and Human Development Workshop. Reproductive Sciences 2007; 14:508-523.

179. Chiswick ML. Intrauterine growth retardation. BMJ 1985; 291:845-848.

180. Hutchinson ES, Brownbill P, Jones NW, Abrahams VM, Baker PN, Sibley CP, Crocker IP. Utero-Placental Haemodynamics in the Pathogenesis of Pre-Eclampsia. Placenta 2009; 30:634-641.

181. Redman CW, Sargent IL. Latest Advances in Understanding Preeclampsia. Science 2005; 308:1592-1594.

182. Langbein M, Strick R, Strissel PL, Vogt N, Parsch H, Beckmann MW, Schild RL. Impaired cytotrophoblast cell–cell fusion is associated with reduced Syncytin and increased apoptosis in patients with placental dysfunction. Molecular Reproduction and Development 2008; 75:175-183.

183. Chaddha V, Viero S, Huppertz B, Kingdom J. Developmental biology of the placenta and the origins of placental insufficiency. Seminars in Fetal and Neonatal Medicine 2004; 9:357-369.

184. Krebs C, Macara LM, Leiser R, Bowman AW, Greer IA, Kingdom JCP. Intrauterine growth restriction with absent end-diastolic flow velocity in the umbilical artery is associated with maldevelopment of the placental terminal villous tree. American Journal of Obstetrics and Gynecology 1996; 175:1534-1542.

185. Simmons RA. Developmental origins of diabetes: The role of oxidative stress. Best Practice & Research Clinical Endocrinology & Metabolism 2012; 26:701-708.

186. Sarr O, Yang K, Regnault TRH. In Utero Programming of Later Adiposity: The Role of Fetal Growth Restriction. Journal of Pregnancy 2012; 2012:10.

187. Barker DJ, Bull AR, Osmond C, Simmonds SJ. Fetal and placental size and risk of hypertension in adult life. BMJ 1990; 301:259-262.

188. Darr H, Benvenisty N. Genetic Analysis of the Role of the Reprogramming Gene LIN-28 in Human Embryonic Stem Cells. STEM CELLS 2009; 27:352-362.

189. Viswanathan SR, Daley GQ. Lin28: A MicroRNA Regulator with a Macro Role. Cell 2010; 140:445-449.

190. Thornton JE, Chang H-M, Piskounova E, Gregory RI. Lin28-mediated control of let-7 microRNA expression by alternative TUTases Zcchc11 (TUT4) and Zcchc6 (TUT7). RNA 2012; 18:1875-1885.

191. Hagan JP, Piskounova E, Gregory RI. Lin28 recruits the TUTase Zcchc11 to inhibit let-7 maturation in mouse embryonic stem cells. Nat Struct Mol Biol 2009; 16:1021-1025.

192. Zhong X, Li N, Liang S, Huang Q, Coukos G, Zhang L. Identification of MicroRNAs Regulating Reprogramming Factor LIN28 in Embryonic Stem Cells and Cancer Cells. Journal of Biological Chemistry 2010; 285:41961-41971.

193. Bussing I, Slack FJ, Groflhans H. let-7 microRNAs in development, stem cells and cancer. Trends in molecular medicine 2008; 14:400-409.

194. Winger QA, Guttormsen J, Gavin H, Bhushan F. Heat Shock Protein 1 and the Mitogen-Activated Protein Kinase 14 Pathway Are Important for Mouse Trophoblast Stem Cell Differentiation. Biology of Reproduction 2007; 76:884-891.

195. Wice B, Menton D, Geuze H, Schwartz AL. Modulators of cyclic AMP metabolism induce syncytiotrophoblast formation in vitro. Experimental Cell Research 1990; 186:306-316.

196. Livak KJ, Schmittgen TD. Analysis of Relative Gene Expression Data Using Real-Time Quantitative PCR and the 2-[Delta][Delta]CT Method. Methods 2001; 25:402-408.

197. Kappes SM, Warren WC, Pratt SL, Liang R, Anthony RV. Quantification and cellular localization of ovine placental lactogen messenger ribonucleic acid expression during mid- and late gestation. Endocrinology 1992; 131:2829-2838.

198. Jeckel KM, Limesand SW, Anthony RV. Specificity protein-1 and -3 trans-activate the ovine placental lactogen gene promoter. Molecular and Cellular Endocrinology 2009; 307:118-124.

199. Bradford MM. A rapid and sensitive method for the quantitation of microgram quantities of protein utilizing the principle of protein-dye binding. Analytical Biochemistry 1976; 72:248-254.

200. Clay CE, Monjazeb A, Thorburn J, Chilton FH, High KP. 15-Deoxy-delta 12,14-prostaglandin J2-induced apoptosis does not require PPARgamma in breast cancer cells. Journal of Lipid Research 2002; 43:1818-1828.

201. Udayashankar R, Baker D, Tuckerman E, Laird S, Li TC, Moore HD. Characterization of invasive trophoblasts generated from human embryonic stem cells. Human Reproduction 2011; 26:398-406.

202. Schulz LC, Ezashi T, Das P, Westfall SD, Livingston KA, Roberts RM. Human Embryonic Stem Cells as Models for Trophoblast Differentiation. Placenta 2008; 29:10-16.

203. Marchand M, Horcajadas JA, Esteban FJ, McElroy SL, Fisher SJ, Giudice LC. Transcriptomic Signature of Trophoblast Differentiation in a Human Embryonic Stem Cell Model. Biology of Reproduction 2011; 84:1258-1271.

204. Simmons DG, Natale DRC, Begay V, Hughes M, Leutz A, Cross JC. Early patterning of the chorion leads to the trilaminar trophoblast cell structure in the placental labyrinth. Development 2008; 135:2083-2091.

205. Cross JC, Nakano H, Natale DRC, Simmons DG, Watson ED. Branching morphogenesis during development of placental villi. Differentiation 2006; 74:393-401.

206. Fernandes RA, Wenceslau CV, Reginato AL, Kerkis I, Miglino MA. Derivation and characterization of progenitor stem cells from canine allantois and amniotic fluids at the third trimester of gestation. Placenta 2012; 33:640-644.

207. Zeigler BM, Sugiyama D, Chen M, Guo Y, Downs KM, Speck NA. The allantois and chorion, when isolated before circulation or chorio-allantoic fusion, have hematopoietic potential. Development 2006; 133:4183-4192.

208. Müntener M, Hsu YC. Development of trophoblast and placenta of the mouse. Cells Tissues Organs 1977; 98:241-252.

209. Viswanathan SR, Daley GQ, Gregory RI. Selective Blockade of MicroRNA Processing by Lin28. Science 2008; 320:97-100.

210. Jozwik M, Pietrzycki B, Anthony RV. Expression of Enzymes Regulating Placental Ammonia Homeostasis in Human Fetal Growth Restricted Pregnancies. Placenta 2009; 30:607-612.

211. Gates KC. The role of proline rich 15 in trophoblast cell development. Colorado State University. Libraries; 2012.